



UNIVERSITÀ DEGLI STUDI DI CAMERINO

School of Advanced Studies

Doctoral course in

Life and Health Sciences – Molecular Biology and cellular Biotechnology

XXXV Cycle

**GUT MICROBIOTA MODULATION IN
ALZHEIMER'S DISEASE**

Doctoral Candidate:

Chunmei Gong

Supervisors:

Prof. Anna Maria Eleuteri

Dr. Laura Bonfili

Coordinator of the PhD curriculum

Prof. Anna Maria Eleuteri

Acknowledgements

My grateful acknowledgement goes first and foremost to my supervisor **Prof. Anna Maria Eleuteri** for her continuous guidance and scientific support of my PhD study and research, for her patience, motivation enthusiasm, immense knowledge and plentiful experience.

I would express my deep gratitude to my co-supervisor **Dr. Laura Bonfili** who gave me considerable help by means of constant support and availability, patient guidance, encouragement, technical knowledge, and scientific recommendations.

Special thanks to all my colleagues **Prof. Mauro Angeletti, Prof. Valentina Cecarini and Dr. Massimiliano Cuccioloni** for their valuable suggestions, friendship and encouragement.

Their encouragements and unwavering supports have sustained me through frustration and depression. Without their pushing me ahead, the completion of my thesis would be impossible.

I would like to thank my family for their unconditional love and support in all my decisions concerning my future over the years. I am also thankful to all my friends for their thoughtfulness and encouragement.

Contents

List of Tables	V
List of Figures	VI
Abstract	IX
Chapter 1: Introduction	1
1.1 Alzheimer's Disease	1
1.1.1 A brief overview of Alzheimer's Disease	1
1.1.2 Causes and risk factors of AD	2
1.1.3 Neuropathology	3
1.2 Metabolic impairment during AD: focus on lipid metabolism.....	6
1.3 The Role of Hypoxia in the Progression of AD pathology	13
1.4 Intracellular Proteolytic Pathways in neurodegeneration	17
1.4.1 Ubiquitin-proteasome system (UPS)	17
1.4.2 Autophagy	19
1.5 Gut microbiota.....	23
1.5.1 Gut microbiota dysbiosis and AD.....	24
1.6 The Gut microbiota-Brain Axis.....	27
1.7 Therapeutic approaches targeting microbiota	30
1.7.1 Faecal microbiota transplantation	31
1.7.2 Prebiotics.....	32
1.7.3 Probiotics.....	33
1.7.4 Polyphenols	35
Chapter 2: Gut microbiota modulation in Alzheimer's disease: Focus on lipid metabolism ...	39
2.1 Materials and methods	39
2.1.1 Reagents and chemicals	39
2.1.2 Animal model	40
2.1.3 Experimental design.....	41
2.1.4 Plasma lipid analysis.....	42
2.1.5 Preparation of brain and liver homogenates	42
2.1.6 Liver microsomes preparation	42

2.1.7 High performance liquid chromatography (HPLC) analysis.....	43
2.1.8 Western blotting	44
2.1.9 Plasma fatty acid profile.....	45
2.1.10 ELISA determination of 27-hydroxycholesterol	46
2.1.11 Statistical analysis.....	46
2.2 Results	48
2.2.1 Amelioration of blood lipid profile in AD mice upon probiotic administration.....	48
2.2.2 SLAB51 oral administration influences cholesterol biosynthesis and metabolism	49
2.2.3 Probiotic supplementation modifies plasma fatty acids composition	54
2.2.4 Decrease of 27-hydroxycholesterol upon probiotic treatment in AD mice.....	57
2.2.5 SLAB51 increased the brain expression of CYP46A1	58
2.3 Discussion.....	60
Chapter 3: Strategic Modification of Gut microbiota through Oral Bacteriotherapy Influences Hypoxia Inducible Factor-1 α : Therapeutic Implication in Alzheimer’s disease	67
3.1 Materials and Methods.....	67
3.1.1 Animal Studies	67
3.1.2 Preparation of Brain Homogenates	69
3.1.3 Western Blot Analysis	69
3.1.4 Nitrite Level Assay	69
3.1.5 Statistical Analysis.....	70
3.2 Results	71
3.2.1 SLAB51 Affected Nitric Oxide Related Pathways.....	71
3.2.2 SLAB51 Restored HIF-1 α Cerebral Expression in AD Mice	73
3.3 Discussion.....	76
Chapter 4: Flavan-3-ol Microbial Metabolites Modulate Proteolysis in Neuronal Cells Reducing Amyloid-beta (1-42) Levels.....	79
4.1 Materials and methods.....	79
4.1.1 Reagents and Chemicals	79
4.1.2 Molecular Docking	80
4.1.3 Measurements of Isolated 20S Proteasome Activity	81
4.1.4 Cell Culture and Transfections	81

4.1.5 Cell Treatment and Cytotoxicity Assay	82
4.1.6 Proteasome Activity.....	83
4.1.7 Cathepsin B Activity.....	83
4.1.8 Western Blotting Analysis.....	84
4.1.9 Monodansylcadaverine Assay	85
4.1.10 Quantification of A β (1-42).....	85
4.1.11 Statistical Analysis.....	85
4.2 Results	86
4.2.1 Effects of PVLs on Isolated Proteasomes Activity	86
4.2.2 Effects of PVLs on Neuronal Cells Proteasomes	87
4.2.3 Effects of PVLs on the Autophagic Pathway	97
4.2.4 PVLs Effect on Cathepsin B Activity	101
4.2.5 Amyloid- β (1-42) Levels Upon Exposure to PVLs	104
4.3 Discussion.....	106
Chapter 5: Role of Astrocytes' proteolytic systems in Alzheimer's disease	112
5.1 Materials and methods	112
5.1.1 Reagents and Chemicals	112
5.1.2 Cell lines.....	113
5.1.3 Cell treatment with 4-phenil-butirric-acid (4-PBA).....	113
5.1.4 Cell lysis.....	113
5.1.5 Proteasome activities	114
5.1.6 Cathepsins activities.....	115
5.1.7 Western blotting analysis	115
5.1.8 Monodansylcadaverine Assay	117
5.1.9 Statistical Analysis.....	117
5.2 Results	118
5.2.1 26S proteasome functionality is impaired in 3Tg-iAstro	118
5.2.2 20S proteasome activities are down-regulated in hippocampal murine AD astrocytes	119
5.2.3 Constitutive proteasome and immunoproteasome are differentially expressed in 3Tg-iAstro compared to WT-iAstro	121

5.2.4 The autophagic proteolytic pathway is altered in 3Tg-iAstro	123
5.2.5 4-PBA restores both proteasomal and autophagic deficits of 3Tg-iAstro cells....	127
5.3 Discussion.....	131
6. Conclusions.....	136
7. Reference	140

List of Tables

Table 1.	IC50 values obtained from in vitro activity assays on isolated proteasomes....	87
Table 2.	Computationally predicted affinities and energy contribution values for the complexes formed between human constitutive 20S proteasome catalytic subunits and C1, C2, and C3...	94
Table 3.	Predictive affinities and energy contribution values for the complexes formed between human cathepsin B and C1, C2, and C3	103

List of Figures

Figure 1.	Alzheimer's disease (AD) continuum.....	1
Figure 2.	AD risk factors.....	3
Figure 3.	Schematic representation of cerebral modifications in Alzheimer's disease.....	4
Figure 4.	Schematic representation of APP processing.....	6
Figure 5.	Schematic illustration of the proteolytic activation of SREBPs.	11
Figure 6.	Mechanism of liver X receptor activation.	12
Figure 7.	Schematic diagram describing HIF pathway.	16
Figure 8.	The 20S proteasome and immunoproteasome.	19
Figure 9.	Schematic diagram of autophagic pathway..	22
Figure 10.	Gut dysbiosis contributes to neurodegeneration and AD.	25
Figure 11.	Gut-brain axis.	30
Figure 12.	Strategies used to modulate gut microbiota composition.	31
Figure 13.	Outline of human flavan-3-ol metabolism and PVL formation..	37
Figure 14.	Blood lipid profile.....	49
Figure 15.	Inhibition of HMGR activity in 3xTg-AD mice treated with SLAB51.....	50
Figure 16.	Effect of SLAB51 on HMGR expression levels.	51
Figure 17.	SREBP1c and LXRs expression levels in wt and AD mice orally administered with SLAB51 for 4 and 12 months.	53
Figure 18.	IDOL expression levels in wt and AD mice orally administered with SLAB51 for 4 and 12 months.....	54
Figure 19.	Decreased omega6/omega 3 polyunsaturated fatty acids ratio in treated AD mice.....	55
Figure 20.	SLAB51 affects plasma lipid prolife.....	56
Figure 21.	27-Hydroxycholesterol plasma and brain levels.	58
Figure 22.	Brain CYP46 expression levels in wt and AD mice orally administered with SLAB51 for 4 and 12 months.	59
Figure 23.	SLAB51 decreased plasma nitrite and iNOS cerebral expression in AD mice.	72

Figure 24.	SLAB51 restored HIF-1 α cerebral expression in AD mice.	74
Figure 25.	Decreased cerebral expression of PDH2 in treated AD mice.	75
Figure 26.	Structure of the PVLs used in this study.	80
Figure 27.	ChT-L activity of the 26S proteasome measured in control and transfected SH-SY5Y cells upon 6 and 24 h exposure to the three tested PVLs (C1, C2, and C3).	89
Figure 28.	Proteasome ChT-L, T-L, PGPH and BrAAP activities measured in control and transfected SH-SY5Y cells upon 6 and 24 h exposure to C1.	90
Figure 29.	Proteasome ChT-L, T-L, PGPH and BrAAP activities measured in control and transfected SH-SY5Y cells upon 6 and 24 h exposure to C2.	91
Figure 30.	Proteasome ChT-L, T-L, PGPH and BrAAP activities measured in control and transfected SH-SY5Y cells upon 6 and 24 h exposure to C3.	91
Figure 31.	p27 and ubiquitin-conjugates detected in control and transfected SH-SY5Y cells upon 6 h exposure to PVLs.	92
Figure 32.	p27 and ubiquitin-conjugates detected in SH-SY5Y control and transfected cells upon 24 h exposure to PVLs.	93
Figure 33.	Comparative visualization of computed binding modes of PVLs C1, C2, and C3 to β 1, β 2, and β 5 subunits of human constitutive 20S proteasome (pdb ID: 6rgq).	96
Figure 34.	Comparative visualization of computed binding modes of PVLs C1, C2, and C3 to β 1i, β 2i, and β 5i subunits of human immunoproteasome (pdb ID: 6e5b).	96
Figure 35.	Binding models of C1, C2 and C3 bound to Thr-1 catalytic residue of constitutive 20S proteasome.	97
Figure 36.	LC3II and p62 detected in SH-SY5Y control and transfected cells upon 6 h exposure to PVLs.	99
Figure 37.	LC3II and p62 detected in SH-SY5Y control and transfected cells upon 24 h exposure to valerolactones.	100
Figure 38.	MDC staining of induced autophagic vacuoles in neuronal cells treated with C1, C2, and C3 (Control, 1 and 5 μ M).	101

Figure 39.	A) Cathepsin B activity measured in SH-SY5Y control and transfected cells upon 6 and 24-h exposure to PVLs. B) Comparative visualization of computed binding modes of valerolactones C1, C2, and C3 to human cathepsin B (pdb ID: 1csb).	103
Figure 40.	Binding models of C1, C2 and C3 bound to Cys-29 catalytic residue of cathepsin B.....	104
Figure 41.	Levels of A β (1-42) measured in cellular extracts and cell medium upon 24 h treatment with C1, C2, and C3 (5 μ M).....	105
Figure 42.	Deregulation of UPS in 3Tg-iAstro.....	119
Figure 43.	Decreased 20S proteasome activities in 3Tg-iAstro.	121
Figure 44.	20S proteasome subunits composition.	122
Figure 45.	Cathepsin B and Cathepsin L in immortalized astrocytes	124
Figure 46.	Autophagic markers.	127
Figure 47.	4-PBA restores the functionality of UPS in 3Tg-iAstro.....	129
Figure 48.	4-PBA restores the defective autophagy in 3Tg-iAstro.....	130

Abstract

Alzheimer's disease (AD) is a progressive neurodegenerative disease and the main cause of dementia in the elderly. It is a complex multifactorial disease involving cognitive dysfunctions, neuroinflammation, oxidative stress, impaired metabolic and proteolytic pathways. Recently, probiotics have emerged as a promising and safe strategy to manipulate gut microbiota composition affecting the gut-brain axis and increasing the host health status through a multi-level mechanism that is currently under investigation.

The present thesis describes specific mechanisms through which probiotics chronic supplementation exerted neuroprotective and anti-inflammatory effects in a murine model of AD, focusing on both cerebral hypoxia and lipid metabolism and contributes to unravel the neuroprotective properties of gut microbial metabolites in a cellular model of AD and in immortalized hippocampal AD astrocytes, focusing on proteolysis.

Specifically, upon SLAB51 multi-strain probiotic formulation, cholesterol biosynthesis was inhibited in 3xTg-AD mice and alternative pathways of bile acid synthesis were influenced. The plasmatic increase of arachidonic acid in treated AD mice reflected dynamic interactions among several actors of a complex inflammatory response, in which polyunsaturated fatty acids can compete each other and simultaneously cooperate in the resolution of inflammation. In addition, chronic supplementation with SLAB51 enhanced cerebral expression of hypoxia inducible factor 1 α and counteracted

the increase of inducible nitric oxide synthase brain expression and nitric oxide (NO) plasma levels in AD mice, supporting probiotics anti-inflammatory and antioxidant properties.

Considering that (poly)phenols and their derivatives/metabolites have been recognized as promising candidates for the prevention of AD due to their multiple beneficial effects, the ability of a selection of gut microbiota-derived metabolites of flavan-3-ols to modulate the functionality of cellular proteolytic pathways in a cellular model of AD has been investigated. *In vitro* and *in silico* studies demonstrated that the phenyl- γ -valerolactones modulated cellular proteolysis via proteasome inhibition and compensatory autophagy upregulation, consequently reducing the amount of intra- and extracellular amyloid-beta (1-42) peptides in SH-SY5Y neuroblastoma cells stably transfected with the 717 valine-to-glycine amyloid precursor protein mutated gene.

Furthermore, proteolytic pathways have been deeply studied and characterized in immortalized hippocampal astrocytes obtained from 3xTg-AD and wild-type mice (3Tg-iAstro and WT-iAstro, respectively), considering that astrocytes exert protective roles in the central nervous system and are implicated in the pathogenesis of neurodegenerative diseases such as AD with not completely unraveled mechanisms. Impaired proteostasis in AD astrocytes has been observed, with proteasome inhibition and autophagic compensatory activation. In addition, 4-phenylbutyric acid, a neuroprotective aromatic short chain fatty acid, restored proteolysis in 3Tg-iAstro cells

highlighting a new mechanism involved in the beneficial effect of this FDA approved compound in neurodegenerative disorders.

Collectively, *in silico*, *in vitro* and *in vivo* studies here reported contribute to deeply explain the molecular pathways affected by probiotics and/or their metabolites in AD, supporting their inclusion in future AD therapeutic/preventative protocols.

Chapter 1: Introduction

1.1 Alzheimer's Disease

1.1.1 A brief overview of Alzheimer's Disease

Alzheimer's disease (AD) is the main cause of dementia and the most common progressive neurodegenerative disease [1]. Dementia is characterized by a decline in memory, language, thinking, problem-solving and other cognitive skills that affects a person's ability to perform everyday activities. The progression of AD from unnoticeable brain changes to physical disability has been divided into three phases: preclinical AD, mild cognitive impairment (MCI) due to AD and dementia due to AD (see Fig. 1). The AD dementia phase could be further sub-divided into mild, moderate and severe stages [2]. As per the WHO update, on epidemiology of AD in 2013, the number of people suffering from dementia worldwide is likely to triple by 2050 which was approximately 35.6 million in 2010 [3], making it a global health and economical challenge [4]. At present there is no preventative or curative treatment that interferes with the development of the disease [5].

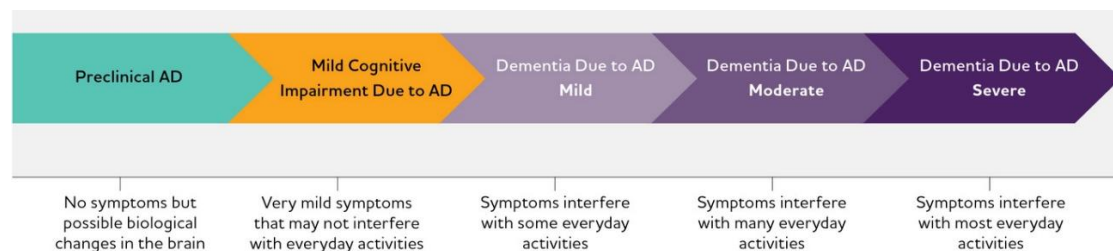


Figure 1. Alzheimer's disease (AD) continuum. The components of the AD continuum are not equal in duration [2].

1.1.2 Causes and risk factors of AD

AD has been considered a multifactorial disease associated with several modifiable and non-modifiable risk factors (Fig. 2) [6]. Incidence of AD is known to increase with age and age is the most important risk factor for the development of AD. AD can be classified by the age of onset of the first symptoms: early-onset AD affects individuals under 65 years of age, accounting for about 4–6% of cases of AD, while the most common late form AD affects individuals aged 65 years or older. Besides the age of onset of symptoms, the early and late forms of AD differ in other clinical, neuropsychological, neuropathological and neuroimaging variables [[1], [7]]. Meanwhile, according to Ballard *et al.* (2011) [8] about 70% of the risk of developing AD can be attributed to genetics. Early AD usually occurs due to mutations in the genes *APP*, *PSEN1* and *PSEN2* (genes of amyloid precursor protein, presenilin 1 and presenilin 2, respectively), whereas late-form AD is mainly associated with a polymorphism in *APOE* gene (apolipoprotein E gene), especially the presence of $\epsilon 4$ allele [[9], [10]]. ApoE is involved in lipid transport in the central and peripheral nervous system and brain injury repair. It has been estimated that between 40-65% of people diagnosed with AD have the APOE- $\epsilon 4$ haplotype. Among the three most common alleles of APOE (i.e., $\epsilon 2$, $\epsilon 3$, $\epsilon 4$), APOE- $\epsilon 4$ increases by three-fold the risk of developing AD in heterozygotes, while in homozygotes an approximately 13-fold increased risk can be estimated [11]. In addition to genetic factors, also environmental and lifestyle-related modifiable factors influence the risk of developing AD, primarily contributing to sporadic AD forms. These factors, such as dietary changes, antibiotic

exposure, infections, obesity, diabetes and hyperlipidemia, alter the gut homeostasis thus having potential influence on the central nervous system [[12], [13]]. For this reason, the growing excitement towards the recent understanding of the gut microbiota brain axis (GBA) may represent an important platform to be exploited to positively influence different neurodegenerative disorders.

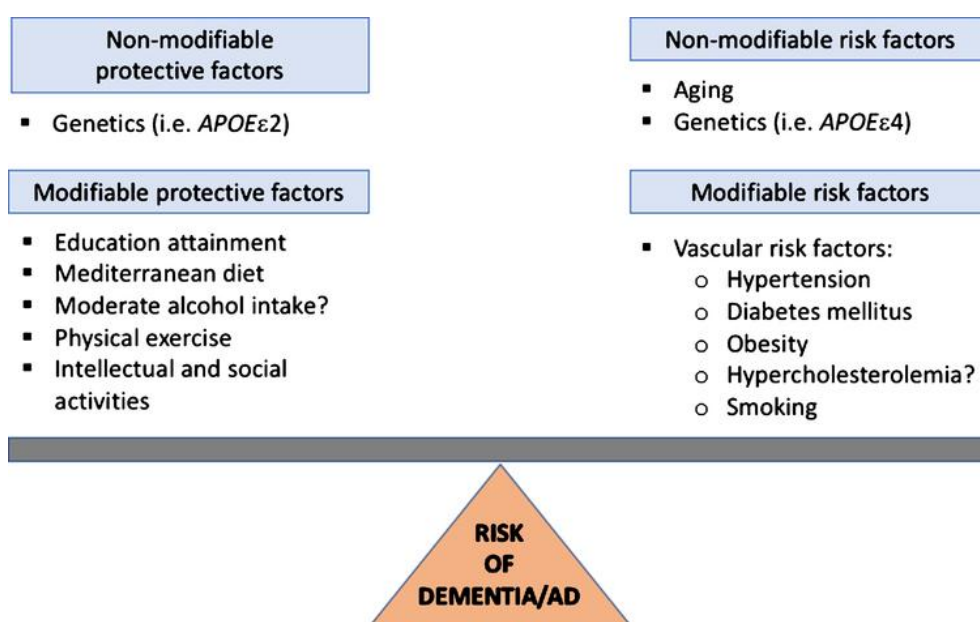


Figure 2. AD risk factors. Non-modifiable and modifiable factors that can counteract or promote AD onset are reported [6].

1.1.3 Neuropathology

The AD brain undergoes several key morphological changes such as loss of neurons in the hippocampus and cerebral cortex, shrinkage of the cortex and enlargement of ventricles [14]. Key molecular hallmarks of the disease are the extracellular amyloid beta ($A\beta$) plaques and the intraneuronal neurofibrillary tangles (NFT) composed of hyperphosphorylated tau protein (Fig. 3).

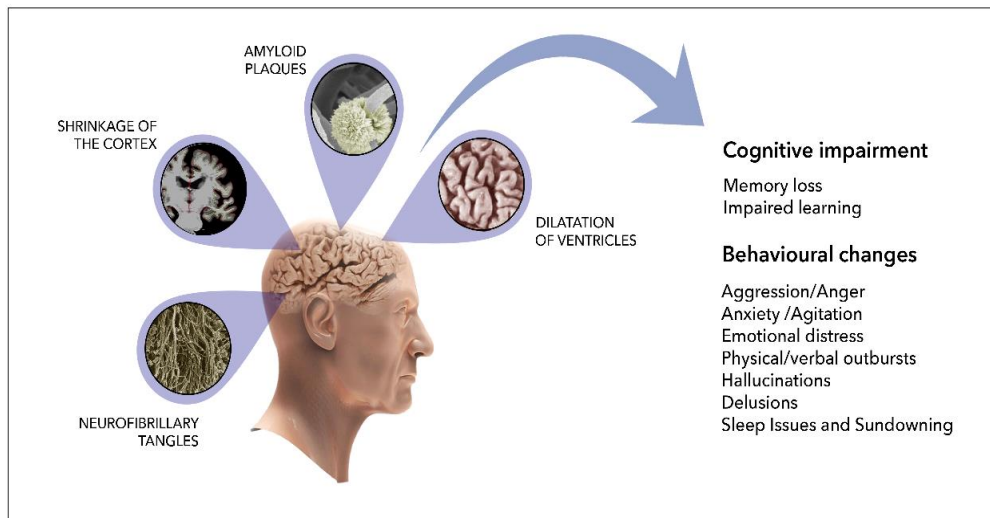


Figure 3. Schematic representation of cerebral modifications in Alzheimer's disease. SEM micrographs for neuronal deposition of amyloid plaques and neurofibrillary tangles are from Meyer *et al.* [15] and Itoh *et al.* [16], respectively. M.R.I. of the brain is from Ledig *et al.* [17].

In detail, NFT are abnormal filaments of the hyperphosphorylated tau protein that in some stages can be twisted around each other to form paired helical filament (PHF) and accumulate in the neural perikaryal cytoplasm, axons, and dendrites. The hyperphosphorylated tau protein is the major constituent of NFTs in AD brain, and its evolution can reflect NFTs morphological stages, which include: (1) pre-tangle phase, one type of NFT, where phosphorylated tau proteins are accumulated in the somatodendritic compartment without the formation of PHF, (2) mature NFTs, which are characterized by filament aggregation of tau protein with the displacement of the nucleus to the peripheral part of the soma, and (3) the extracellular tangles, or the ghost NFTs stage, that results from a neuronal loss due to large amounts of filamentous tau protein with partial resistance to proteolysis [[14], [18]]. The senile amyloid plaques

result from the extracellular accumulation of abnormal amyloid- β ($A\beta$) peptides deriving from the proteolytic cleavage of the transmembrane amyloid precursor protein (APP) [19]. APP was considered a good target for therapeutic interventions in the early treatment of AD. APP can undergo non-amyloidogenic cleavage processing mediated by α -secretase and γ -secretase that generates a soluble APP fragment ($sAPP\alpha$) and a membrane-bound C-terminal fragment of APP (α CTF). Alternatively, APP can be cleaved by β -secretase and γ -secretase releasing two major fragments, $sAPP\beta$ and a C-terminal fragment located in the membrane (β CTF). Further cleavage of β CTF results in the production of $A\beta$ peptides ranging from 37 to 43 amino acid in length, with $A\beta$ (1-40) and $A\beta$ (1-42) being the most dominant and neurotoxic (Fig.4) [[20]–[22]]. $A\beta$ monomers form oligomeric structures that can further aggregate into regular fibrils. According to the $A\beta$ oligomer hypothesis, small soluble $A\beta$ oligomers are considered more neurotoxic than insoluble fibers or amyloid plaques [23]. Recent research is moving towards the earlier phases of the disease, where $A\beta$ oligomers and synaptic tau are the most promising candidates [24].

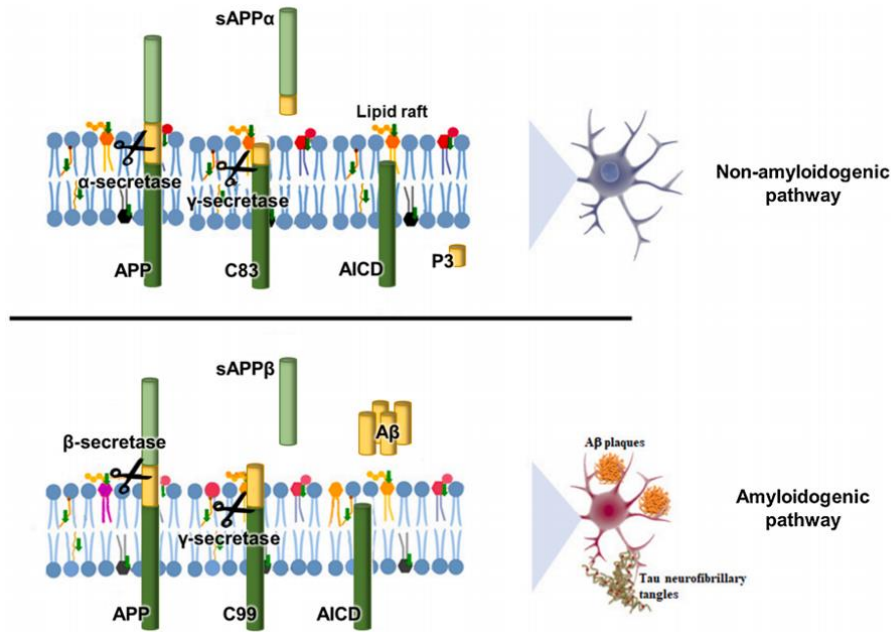


Figure 4. Schematic representation of APP processing. In the non-amyloidogenic pathway the concerted action of two transmembrane enzymes, α - and γ -secretases, produces the non-toxic soluble amino terminal ectodomain of APP (sAPP α), the carboxy-terminal fragment C83, the APP intracellular domain (AICD) and the short fragment p3. There is no production of beta amyloid peptide (A β) from this pathway. In the amyloidogenic pathway sequential cleavage of APP by β - and γ - secretases generates sAPP β , and the C-terminal domain of APP C99 which is further degraded in the two segments AICD and A β [22].

1.2 Metabolic impairment during AD: focus on lipid metabolism

Cerebral lipids account for at least 50% of dry brain weight and the central nervous system (CNS) has the second highest lipid content next to the adipose tissue in the body [25]. Lipids, as key components of cell membranes, have multiple functional roles in maintaining body health including regulation of energy storage and signal transduction, and also for the segregation of chemical reactions in discrete organelles. Various classes of lipids, including fatty acids (FA), phospholipids, sphingolipids, and sterol lipids, play

a crucial role in neuronal function [[25]–[27]]. These diverse and essential roles of lipids in cellular metabolism have been highlighted by the finding of abnormal lipid metabolism in various diseases including neurodegenerative disorders such as AD.

In the past, behavioral testing and neuroimaging were commonly used to diagnose AD. However, these methods may not only be invasive but also unaffordable to some patients. Recently, an interesting blood-based test for early AD diagnosis based on expression of signaling plasma proteins was reported [28]. In another study some lipids extracted from peripheral blood have been validated to predict phenotypic conversion to either amnesic mild cognitive impairment (aMCI) or AD with over 90% accuracy [29]. Kuo and colleagues showed that the plasma levels of total and low-density lipoprotein cholesterol (LDL-C) correlated with the amount of A β in AD brains [30]. Blood lipid profiles have potentially modifiable influencing factors, including age, sex, diet, exercise, medications, educational levels, and/or lifestyle, such as smoking, eating habits, and various other personal choices. Measures should be applied earlier to prevent the worsening of cognitive decline. Blood lipid parameters include high-density lipoprotein (HDL-C), low-density lipoprotein (LDL-C), total serum cholesterol, and triglycerides [31]. It is better to test this entire panel of biomarkers, as a single biomarker will not help to detect a complex condition, such as AD.

Fatty acids play a key role in brain function, both structurally and metabolically, of which the essential polyunsaturated fatty acids (PUFAs) such as arachidonic acid (AA),

α -linolenic acid (ALA), eicosapentaenoic acid (EPA) and docosahexaenoic acid (DHA) can exert pro/anti-inflammatory effects and neuronal protective functions [32]. The human lipidome showed changes during aging. A previous study demonstrated age-related reductions in total volume and relative levels of DHA and arachidonic (AA) acid in orbitofrontal cortex, a region in the brain that contributes significantly to cognitive function [33]. In a study involving lipids profiling and lipidomics in 396 cognitively-healthy and 67 cognitively-impaired patients spanning 100 years of human lifespan, Yu *et al.* (2018) reported that 682 lipids had significant age-dependent concentration changes in the grey matter of dorsolateral prefrontal cortex, a region of the brain important for cognitive control [34]. Indeed, the changes in the lipidome and how they relate to AD disease progression remain unclear. An in-depth lipidomic analysis has provided a global overview of changes in metabolites and lipids and their associated metabolic pathways [35].

Furthermore, the major sterol lipid in humans and animals is cholesterol [25]. The brain contains 25% of total body cholesterol [36], which is essential for its normal function, being a major component of neuronal cell membranes and a determinant of membrane fluidity [37]. A growing amount of epidemiological, as well as animal and cellular studies, supports the hypothesis that hypercholesterolemia is closely associated with AD [[38]–[41]]. However, the molecular events by which cholesterol causes A β accumulation and the real contribution of this steroid to the pathogenesis of AD are still poorly understood.

In the brain, cholesterol is mostly present in the free form and derives from the *de novo* biosynthesis from acetyl-coenzyme A mediated by 3-hydroxy-3-methyl-glutaryl-coenzyme A (HMG-CoA) reductase, which is the rate limiting enzyme in cholesterol biosynthesis and a target for pharmacological inhibitors (e.g. statins), but the exact mechanism of action of cholesterol lowering drugs and their implication in reducing susceptibility to AD is not exactly defined [[42]–[45]].

The synthesis and regulation of cholesterol are controlled by two distinct transcription factors, namely the sterol regulatory element-binding proteins (SREBPs) and the liver X receptors (LXRs). In detail, the sterol response element binding proteins (SREBPs) are a family of transcription factors known to regulate cholesterol and lipid metabolism, which include three isoforms, SREBP-1a, SREBP-1c and SREBP-2. The SREBPs are synthesized as large precursor proteins that are inserted into the endoplasmic reticulum (ER) membrane through two membrane-spanning domains. The membrane-associated proteins are transcriptionally inactive. In the ER, the C terminus of the SREBP interacts with a protein called Scap (SREBP-cleavage-activating protein), which functions as a sterol sensor. In sterol-depleted cells, Scap escorts the SREBPs from the ER to the Golgi, where they are processed by two membrane-associated proteases, the site 1 (S1P) and site 2 (S2P) proteases, which release the mature forms of the proteins. These transcriptionally active fragments of the SREBPs are translocated to the nucleus, where they bind to the promoters of SREBP target genes, including genes encoding the LDL

receptor, and the enzymes involved in the cholesterol biosynthesis, among them HMG-CoA synthase, HMG-CoA reductase (Fig. 5) [[46]–[48]]. Specifically, SREBP-1c expression is transcriptionally controlled by various nutritional and hormonal factors. It can be modulated in different tissues by LXR α/β in response to altered sterol and oxysterols levels, consequently regulating the expression of genes that coordinate cholesterol and fatty acids metabolism [49]. A previous study showed that the expression of SREBP-1c is abolished in LXR α/β -null mice and conversely, activation of LXR stimulates lipogenesis in hepatocytes mainly via SREBP-1c, which leads to liver steatosis and hypertriglyceridemia [50]. However, this LXR-SREBP-1c molecular mechanism is still not fully clarified in AD pathology.

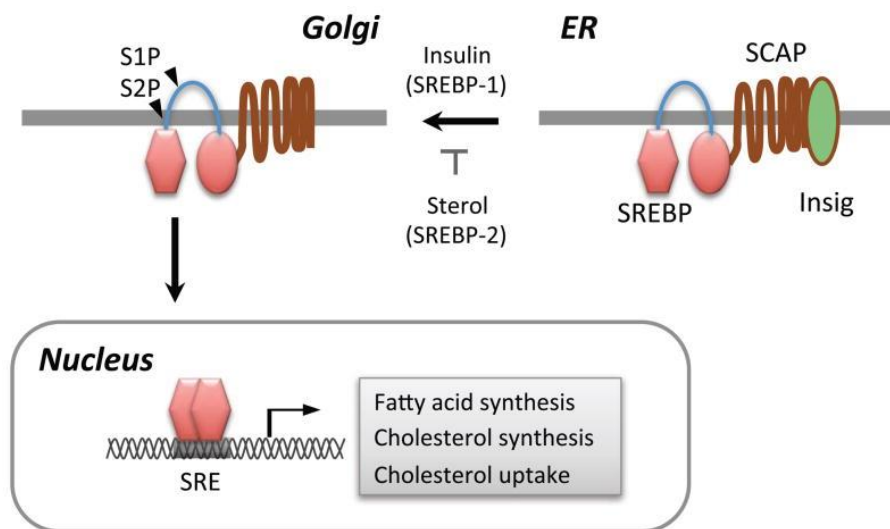


Figure 5. Schematic illustration of the proteolytic activation of SREBPs. SREBPs are synthesized as precursor forms containing two transmembrane helices that anchor the protein in the ER membrane. SREBPs are associated with the SREBP cleavage activating protein (SCAP) and ER retention protein called Insig. In order to be activated, SREBP-SCAP complex should be dissociated from Insig, associate with COPII-coated vesicles and then migrate to Golgi apparatus. SREBPs are sequentially cleaved by site 1 (S1P) and site 2 (S2P) proteases in the Golgi, which releases the N-terminal cytosolic portion of the protein which enters the nucleus to act as the active transcription factor. The processed SREBP enter the nucleus to activate the transcription of genes regulating fatty acid and cholesterol metabolism [48].

Secondly, the nuclear receptor superfamily members of LXRs ($LXR\alpha$ and $LXR\beta$) are DNA-binding transcription factors which respond to the excess of cholesterol through binding their physiological ligands, most of which are oxygenated metabolites of cholesterol (i.e. oxysterol). LXRs can regulate the expression of target genes through binding to target DNA sequences, termed LXR response elements (LXREs) as obligate heterodimeric complexes with the retinoid X receptor (RXR) (Fig.6) [[51], [52]]. The LXRs represent attractive therapeutic opportunities in AD because their activation controls the expression of genes involved in cholesterol uptake, efflux, transport, and excretion in multiple tissues, counteracts inflammation by modulating innate and adaptive immune responses, positively impacts glucose homeostasis, and decreases $A\beta$ production by modulating amyloid precursor protein processing [[50], [53]]. Interestingly, in response to increased cellular sterol levels, LXRs can enhance the expression of the inducible degrader of the LDL receptor (IDOL), an E3 ubiquitin ligase involved in the ubiquitin-proteasome mediated degradation of important substrates

including low-density lipoprotein receptor (LDLR) [54] thus regulating the structural and functional plasticity of synapses and neural circuits as well as the cholesterol uptake by the LDLR pathway [[55], [56]]. Structural studies have shown that IDOL interacts with the catalytically active ubiquitin conjugating enzyme E2D (UBE2D) group of ligases to accomplish both autoubiquitynation and LDLR ubiquitynation [57]. The contribution of the LXR–IDOL pathway to the control of lipid homeostasis could potentially be exploited for the pharmacologic modulation of lipid metabolism.

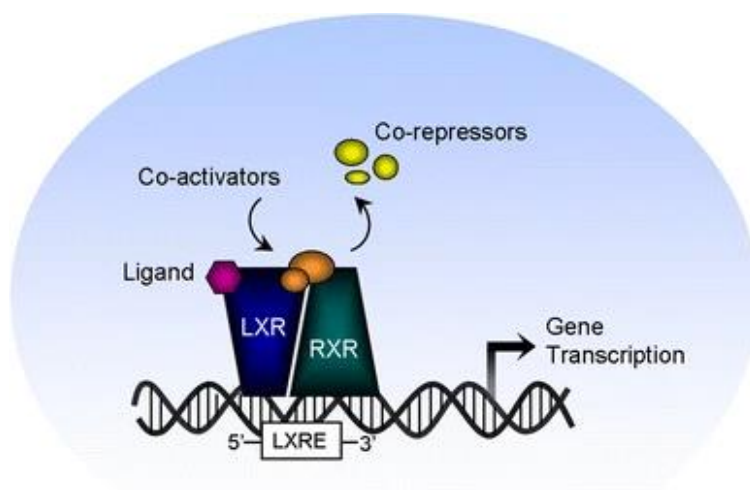


Figure 6. Mechanism of liver X receptor activation. In the nucleus, LXRs form an obligate heterodimer complex with the retinoid X receptor (RXR) that binds to an LXR response element (LXRE) in regulatory regions of target genes. Following ligand binding, the LXR/RXR complex undergoes a conformational change that leads to the release of co-repressors and the recruitment of co-activators, which activates target gene transcription [52].

Furthermore, the most important mechanism whereby the brain eliminates excess cholesterol is through the formation and excretion into the circulation of oxysterols, a

class of cholesterol oxidation products, the best studies and the most potent of which including 24(S)-hydroxycholesterol (24S-OHC) and 27-hydroxycholesterol (27-OHCE) [37]. The oxidized cholesterol products oxysterols are the ligands for LXR, as mentioned earlier. The brain-specific enzyme cholesterol 24-hydroxylase (CYP46A1), a cytochrome p450 enzyme, converts the excess of cholesterol into 24-hydroxycholesterol (24S-OHC), which may efflux across the blood-brain barrier (BBB) into the peripheral circulation, and as such plays a pivotal role in the brain cholesterol turnover [58]. Several works demonstrated that increased CYP46A1 activity improved memory [59], reduced A β plaques and restored spatial memory performances in mice [60]. There is also an inflow of 27-hydroxycholesterol (27-OHCE) to the brain, a product of peripheral metabolism of cholesterol generated by the enzyme sterol 27-hydroxylase (CYP27A1). A previously study demonstrated that increased levels of 27-hydroxycholesterol (27-OHCE) were observed in the brain of AD patients [61]. Evidently, abnormal levels of oxysterols in the brain can increase A β production [62] and worsen neuroinflammation [63]. However, the exact involvement of this mechanism needs to be further studied.

1.3 The Role of Hypoxia in the Progression of AD pathology

AD is also characterized by hypoxia, a state that is believed to exacerbate the disease progression. Hypoxia is a condition characterized by the deprivation of oxygen supply to maintain normal physiological function in cells [64]. The duration and extent of hypoxia determine its beneficial or detrimental effects; indeed, severe and/or chronic

hypoxia can impair oxygen delivery and affect cellular metabolism, ATP production, and Ca^{2+} homeostasis, and it can lead to ROS formation and neuroinflammation. Conversely, mild, moderate, or intermittent hypoxia has been shown to promote protective adaptations in the brain [[65], [66]]. However, the hypoxia and hypoxia-mediated molecular pathways in AD pathology are not well characterized.

Neuroinflammation is an inflammatory response secondary to infections or trauma or even micro-level insults, followed by overactivation of glial cells (microglia/astrocytes) [67]. Neuroinflammation is generally associated with high levels of pro-inflammatory cytokines, chemokines, and neurotoxic substances, such as matrix metalloproteinases, reactive oxygen species (ROS), and nitric oxide (NO) [66]. Specifically, the signaling molecule of NO is a diatomic, short-lived gas that regulates a wide range of homeostatic functions, mainly in the cardiovascular system and nervous system. NO can react with superoxide anions (O_2^-) to form the strong oxidant peroxynitrite (ONOO^-), that can trigger oxidative stress and then cause cell damage, contributing to dementia [68]. Specifically, NO is synthesized by three forms of nitric oxide synthase (NOS) enzymes counting neuronal NOS, endothelial NOS and inducible NOS (iNOS). Typically, the amount of NO produced by iNOS is substantially greater than that produced by the constitutive isoforms. iNOS is activated only in pathological conditions of AD in brain particularly in microglia [[69], [70]]. Previous studies have shown that inhibiting iNOS in microglia-neuron co-cultures [71], and glia-neuron co-cultures ameliorated neurotoxicity [72]. However, how NO synthesis by iNOS

contributes to oxidative stress-associated AD pathogenesis is still to be further explored. Interestingly, cells respond to hypoxia by stabilizing hypoxia-inducible factor (HIF), an important transcription, known to be a master regulator of oxygen homeostasis and glucose metabolism. The HIF family contains two different subunits: α and β . The α part includes HIF-1 α , HIF-2 α , and HIF-3 α ; the β part contains one protein (HIF-1 β). Specifically, HIF-1 α is ubiquitously expressed in all body tissues and is an oxygen regulated subunit. As depicted in Figure 7, under physioxia, HIF- α (HIF-1 α , HIF-2 α , and HIF-3 α) proteins undergo rapid ubiquitination and sequent degradation by proteasome through hydroxylation by the oxygen-dependent prolyl-4-hydroxylase domain enzyme (PHDs), including PHD1, PHD2, and PHD3 [[65], [73]]. Importantly, PHD2 is a negative regulator of HIF-1 α and leads to proteasomal degradation of HIF-1 α either in normoxia or following a short exposure to hypoxia [74]. However, under hypoxic conditions, the enzymatic activity of PHD2 is inhibited, preventing HIF-1 α hydroxylation and ubiquitin-mediated proteasome degradation (Fig.7). Subsequently, the HIF- α subunit interacts with HIF-1 β to form a transcriptional complex, inducing the expression of numerous downstream genes involved in glucose transport and metabolism, cell stress and survival, and the immune system[65]. It has been hypothesized that PHD inhibition may be part of a therapeutic strategy in AD because it can stabilize HIF with neuroprotective, anti-inflammatory and antioxidant consequences [75]. Recently hypoxic conditions have been described as a promising strategy to cure diseases of the central nervous system [[76], [77]].

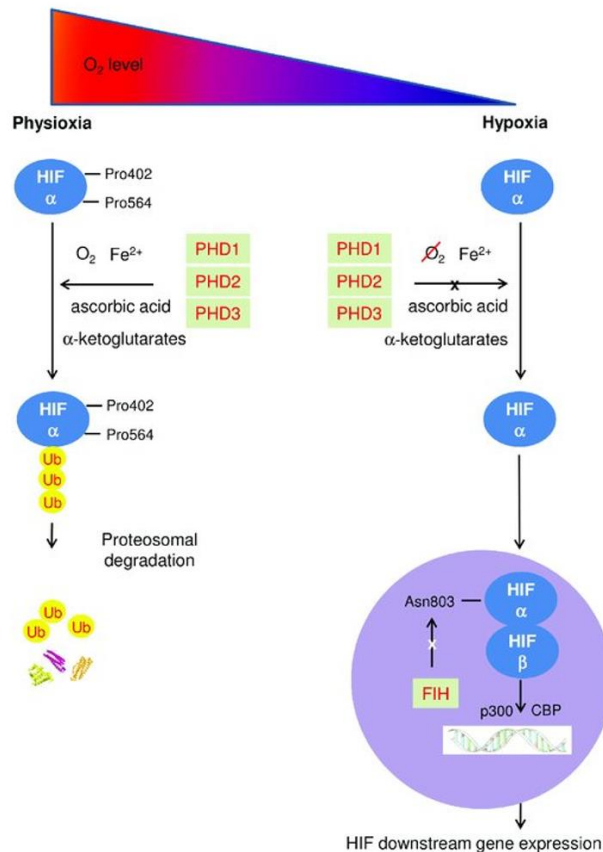


Figure 7. Schematic diagram describing HIF pathway. At physiological hypoxia, HIF α is continuously produced and constantly hydroxylated by prolylhydroxylases PHD1, PHD2 and PHD3 at prolyl residues 402 and 564 of C- and N-terminal oxygen dependent degradation domains (CDD and NODD). The hydroxylated HIF α is then poly-ubiquitinated and proteosome degradation by an E3 ubiquitin ligase – the von Hippel-Lindau protein (pVHL) complex. In addition, factor inhibiting HIF (FIH) hydroxylates an asparaginy residue in the C-terminal transcriptional domain of HIF α , inhibiting HIF mediated transcription; in hypoxia, activities of both PHD and FIH are reduced due to oxygen deficiency. HIF α accumulates in the cytoplasm, and enters the nucleus where HIF α dimerizes with HIF β to form the HIF molecule. The HIF complex is activated when interacting with the p300/CBP coactivators and then binds to hypoxia-responsive elements (HREs), leading to upregulating transcription of HIF downstream genes [73].

1.4 Intracellular Proteolytic Pathways in neurodegeneration

Disturbances in intracellular proteostasis trigger the accumulation of altered proteins and toxic aggregates that are widely recognized hallmarks of neurodegenerative diseases, including Alzheimer's disease (AD) [78]. As known cells possess two proteolytic machineries, namely the ubiquitin-proteasome system and autophagy, which regulate the majority of protein catabolism and are responsible for overall protein quality control and proteostasis.

1.4.1 Ubiquitin-proteasome system (UPS)

The ubiquitin-proteasome system (UPS) is the major degradation system used by cells to remove short-lived and misfolded or damaged proteins [79]. The eukaryotic proteasome (26S proteasome) is a large, multicatalytic protease complex in charge of the removal of intracellular misfolded, oxidized or aggregated ubiquitin-tagged-proteins, in an ATP-dependent manner. The main core of this system is the 20S proteasome, consisting of two rings made of seven α subunits, flanking two inner rings of composed seven β subunits. Three of these β -subunits β 1, β 2 and β 5, are catalytically active, and are responsible for different proteolytic activities: subunit β 1 is associated with the caspase-like activity or peptidylglutamyl-peptide hydrolysing (PGPH) activity whereas subunit β 2 exerts a trypsin-like (T-L) activity. Subunit β 5 accounts for the chymotrypsin-like (ChT-L) activity, but given its tendency to cleave after small neutral and branched side chains also the small neutral amino acid preferring (SNAAP) and branched-chain amino acid preferring (BrAAP) activities can be assigned to this subunit

(Figure 8A) [[80], [81]]. Numerous data have demonstrated that AD and other neurodegenerations are characterized by an impaired functionality of the UPS and that amyloid aggregates are able to further inhibit such complex [[82]–[84]]. However, in cells exposed to IFN- γ or tumor necrosis factor- α (TNF- α), the 20S proteasome is converted into the immunoproteasome with its constitutive catalytic subunits, β 1, β 2, and β 5, being replaced by the inducible subunits β 1i, β 2i, and β 5i (Figure 8B) [[80], [85]]. β 2i and β 5i show trypsin-like and chymotrypsin-like enzymatic activity as the constitutive β 2 and β 5. β 1i can exert chymotrypsin-like activity, differently from the constitutive β 1 which is associated to PGPH activity [85]. Due to distinct peptidase sites, inducible β subunits can cleave proteins in a distinct manner from constitutive particles and generate more peptides capable of binding to MHC class I molecules, thereby playing an important role in antigen presentation [86]. Depending on the tissue and specific cells types, different proteasome compositions are expressed and can coexist [87]. Previous works have shown that immunoproteasome expression was related not only to AD neuroinflammation but also to the ageing process in CNS [88].

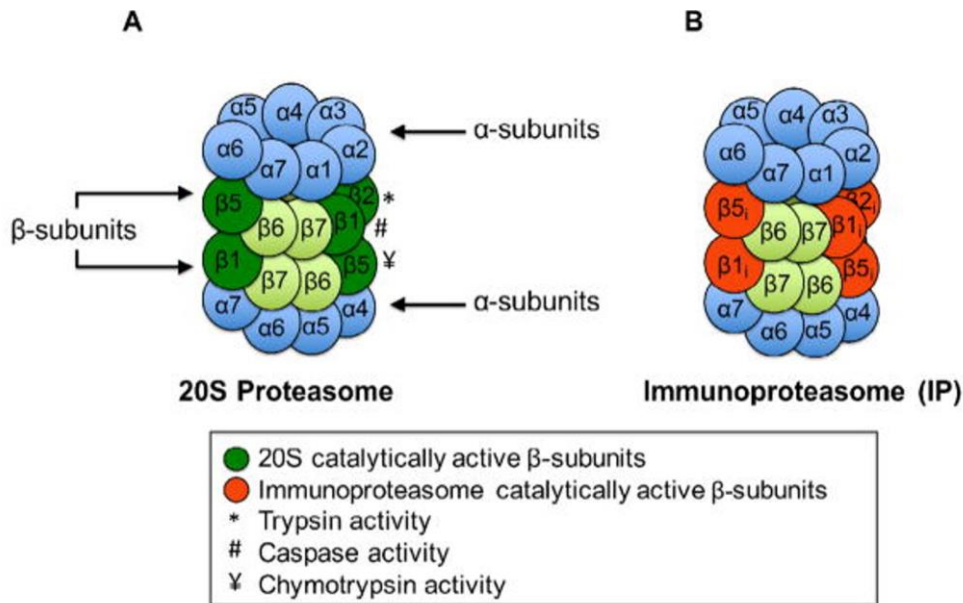


Figure 8. The 20S proteasome and immunoproteasome. (A) The 20S proteasome consists of four stacked rings: two rings composed of α -subunits and two rings composed of β -subunits. (B) The plasticity of the 20S proteasome allows for the synthesis of a subtly different form of the core 20S proteasome, called the immunoproteasome [80].

1.4.2 Autophagy

Another major intracellular degradation system reported to be activated in response to cellular stress is the autophagic pathway, which attempts to restore metabolic homeostasis through the degradation of aggregated proteins, unfolded/misfolded proteins or damaged subcellular organelles like ER, mitochondria or ribosomes [89]. As shown in Figure 9, the complex autophagic process consists of 4 sequential steps, including 1) induction and phagophore formation; 2) autophagosome formation; 3) autophagosome-lysosome fusion (autolysosome); and 4) degradation and recycling by acidic lysosomal hydrolase (Fig. 9) [90]. These steps are determined by the recruitment of specific Autophagy related (Atg) proteins or protein complexes. Disturbance at any

steps in this process causes autophagy dysfunction [91]. Although the study has reported that autophagic dysfunction may be involved in AD pathogenesis [92], the precise role of autophagy-initiating and autophagy-modulating protein complexes related to disease are unclear.

Importantly, Beclin-1/BECN1, also known as Atg6, is a scaffold/adaptor protein and execute multiple functions in autophagy. It interacts with autophagy-regulating class III PI3-kinase (PI3K-III), also known as VPS34 or PIK3C3 for nucleation of the phagophore. It potentially forms complexes with other proteins such as UVRAG, Atg14L, PIK3R4/Vps15, Ambra1, Rubicon, or Bif-1 involved in autophagosomal flux and degradation [[93], [94]]. Interestingly, recent papers suggest a role for Beclin-1 (BECN1) in AD and mild cognitive impairment [[94]–[96]]. Another molecule Microtubule-associated light chain protein 3 (LC3), a mammalian homologue of yeast Atg8, plays a key role in autophagosome biogenesis/maturation. During autophagy, a cytosolic form of LC3 (LC3I/LC3-I) is converted from a nonlipidated form (LC3I/LC3-I) to a phosphatidylethanolamine (PE)-conjugated form (LC3II/LC3-II), which is recruited to autophagosomal membranes. LC3-II specifically localizes in autophagosome membranes, and it is therefore considered a specific autophagy marker [97]. Interestingly, Sequestosome 1 (SQSTM1, also known as p62) is a multifunctional protein consisting of a N-terminal Phox-BEM1 domain (PB1), a ZZ-type zinc finger domain, a nuclear localization signal (NLS), an export motif (NES), an LC3-interacting region (LIR), a Keap1-interacting region (KIR), and a C-terminal

ubiquitin-associated domain (UBA). p62 interacts non-covalently with ubiquitin or polyubiquitin chains via the UBA domain, and then delivers polyubiquitinated cargoes to autophagy via the LIR domain by interacting with LC3. Therefore, p62 is a good indicator and can be used to monitor fluctuations in autophagy under certain conditions [98].

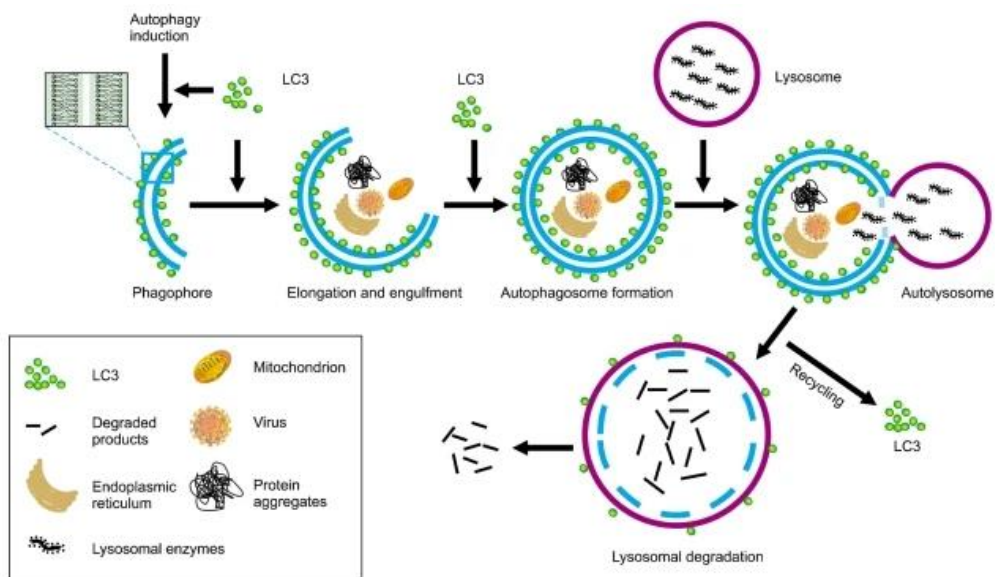


Figure 9. Schematic diagram of autophagic pathway. Autophagy induction signal leads to form a sequestering membrane called phagophore. Following a sequence of ubiquitination-like reactions, LC3 conjugates to the sequestering membrane and controls the elongation of phagophore. As the phagophore expands, cytoplasmic constituents, including organelles such as mitochondria and endoplasmic reticulum, aggregated proteins and foreign organisms (bacteria and virus) are enwrapped. At the end of elongation, sequestering membrane closes and results in the formation of a double-membrane vesicle, autophagosome. Once the autophagosome is formed, it is delivered to fuse with lysosome to form autolysosome for degradation. Lysosomal hydrolases degrade the cargo together with the inner membrane of autophagosome, and LC3 from the outer membrane as well as the autophagy-derived nutrients are recycled. Autophagic process can act as a mechanism to keep homeostatic balance and support cell survival. However, it can also cause cell death directly or indirectly [90].

Moreover, the progression and resolution of autophagy are dependent on lysosome function, as autophagic flux requires the fusion of the autophagosome with the lysosome, where the contents are degraded. Lysosomes are degradative organelles with a variety of hydrolytic enzymes containing cathepsins, which play important functions in the immune response, processing and activation of substrates, apoptosis, autophagy, and other processes [99]. Among the many enzymes, Cathepsin L and cathepsin B are strictly correlated to autophagy [100]. Cathepsin L is involved in degradation of the autolysosomal content and it is complemented by cathepsin D, which has been found increased in cathepsin L knockout cells [101]. Cathepsin B regulates lysosome and autophagosome populations through indirect suppression of the transcription factor TFEB which inhibits expression of autophagy related proteins [102]. These two enzymes are of particular importance for their relevance in AD pathogenesis. The role

of cathepsins in AD is not limited to their involvement in autophagosomes, representing the cell attempt to degrade protein aggregates, but they are also implicated in A β PP processing, thus contributing to A β plaque formation in AD [[103], [104]]. In details, cathepsin B is associated with amyloid plaques in AD brains and has been suggested to be responsible for the increase in A β production [105]. Conversely, cathepsin L activity increases α -secretase-mediated non-amyloidogenic pathway [[104], [106]]. Thus, regulating their activity is important to better understand the whole autophagic cascade during AD pathogenesis.

1.5 Gut microbiota

The human body hosts trillions of microorganisms (bacteria, archaea, fungi, and viruses) that colonize the skin surface, the respiratory tract, genitourinary organs and, most importantly, the gastrointestinal tract. Approximately 95% of the symbiotic organisms in the human body can be found in the gut (gut microbiota) [107]. The four main phyla in adults consist of Bacteroidetes (~48%) and Firmicutes (~51%), which make up the highest proportion, as well as Proteobacteria and Actinobacteria, which are found in relatively low amounts (1%) [108]. These diverse groups of microorganisms play multiple roles in human health, such as the synthesis of essential amino acids and vitamins, the fermentation of undigested carbohydrates, the production of short-chain fatty acids (SCFAs) and other metabolites, the metabolism of essential substances (bile acids, sterols and drugs), and the protection against exogenous pathogens. Intestinal microbiota is proposed as an essential “organ” which imparts substantial physiological

functions related to innate immunity, appetite, and energy metabolism locally and systematically [[109], [110]]. Its composition depends on an individual's age, genetic predisposition, nutrition, physical activity, environmental factors, stress, infection, presence of other diseases, and use of antibiotics [109]. Recently, the importance of gut microbiota has raised attention of researchers in the fields of neurochemistry, neurophysiology and neuropsychiatry, based on consistent pieces of evidence of the relationship between alteration in gut microbiota and brain homeostasis and subsequent implications of the disruption of gut microbiota to the pathogenesis of neurodegenerative diseases including AD.

1.5.1 Gut microbiota dysbiosis and AD

Abnormal changes in the composition of gut flora, a phenomenon known as dysbiosis, which is characterized by the unequivocal distribution of microorganisms, overpowering of beneficial effects of commensals/symbionts by pathogens, and resultant changes in their metabolic activity inducing local systematic inflammation [111]. Gut dysbiosis is strongly postulated as a factor increasing susceptibility to AD, influencing its development that is frequently reported in symptomatic patients [112]. It has been stated that dysbiosis contributes to the enhancement of pro-inflammatory bacteria (such as *Verrucomicrobia*, *Escherichia/Shigella*, *Proteobacteria*, and *Pseudomonas aeruginosa*) and decreases the abundance of anti-inflammatory bacteria (such as *Eubacterium hallii*, *Bacillus fragilis*, *Bacteroides fragilis*, *Eubacterium rectale*, *Faecalibacterium prausnitzii*, and *Bifidobacterium*). The

consequent increased secretion of lipopolysaccharides (LPS) and amyloid peptides can alter the intestinal permeability and the BBB, thus promoting neuroinflammation, oxidation and worsening the formation of amyloid beta plaques and neuronal degeneration (Fig. 10) [[113], [114]].

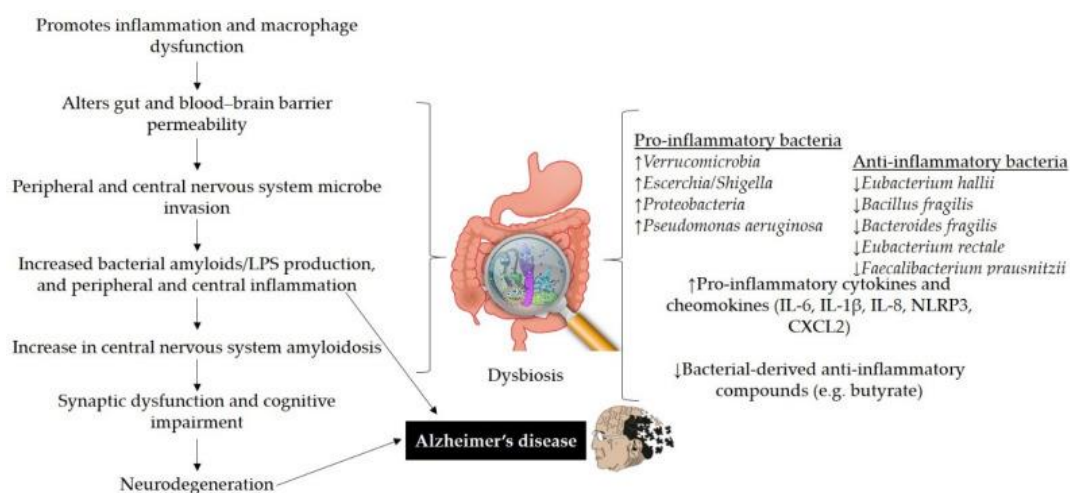


Figure 10. Gut dysbiosis contributes to neurodegeneration and AD. Disturbances in intestinal microbiota homeostasis impairs gut permeability due to pro-inflammatory bacteria that produce bacterial amyloids/lipopolysaccharide (LPS) and cause macrophage dysfunction. Amyloids and LPS can increase inflammatory cytokines. Impairment in gut and BBB may lead to cerebral A β deposition contributing to AD pathogenesis. NLRP3: nod-like receptor protein 3, CXCL2: C-X-C motif chemokine ligand 2 [[113], [114]].

Importantly, inflammation during gut dysbiosis stimulates the infiltration of immune cells into the brain and involves multiple processes at the cellular level including oxidative stress, neuroinflammation and hypoxia, thus strictly linked to the neurodegenerative disorders [115]. Specifically, NO, one of the key inflammatory mediators, produced in intestinal tissues, commensal anaerobes, and leukocytes, is

neuroprotective at minor concentration/optimum levels otherwise induce oxidative damages and activate the apoptotic pathway as described above. It is synthesized by iNOS and is upscaled during inflammation [116]. NO, the first of the gastrotransmitters to be studied in detail, acts in the CNS [117] triggering A β deposition, which in turn activates resident immune cells [118]. Interestingly, NO and oxidative stress characterize both early and late stages of neurodegenerative disorders [[119], [120]]. Moreover, in hypoxia, HIF-1 α binds to HIF-1 β subunit and forms a heterodimer with a role in glucose transport and metabolism, cell stress and survival, and the immune system as mentioned above [73]. In addition, the PHD2 is a negative regulator of HIF-1 α and leads to proteasomal degradation of HIF-1 α in an oxygen-dependent manner either in normoxia or following a short exposure to hypoxia [74]. It has been hypothesized that PHD inhibition may be part of a therapeutic strategy in AD because it can stabilize HIF with neuroprotective, anti-inflammatory and antioxidant consequences [75]. The targeting of gut microbiota and hypoxia have been described as a promising strategy to cure diseases of the central nervous system [[76], [109]].

Besides, the core functions of gut microbiota are the production of various bioactive metabolites that affect host health and disease. Dysregulated gut microbiota composition and its metabolites, which translocate from the gut across the disrupted intestinal barrier, affect various metabolic organs triggering metabolic deformities, such as insulin resistance, dyslipidemia, oxidative stress, hyperglycemia, and alteration in micronutrients, also find an adjacent connotation with AD pathogenesis and are

regarded as probable etiological factors for AD [121]. A growing body of studies have implicated alterations in lipid metabolism connected to AD pathogenesis. Cotillard *et al.* [122] noted that the reduced microbial richness commonly observed in obese patients was also linked with increased levels of total serum cholesterol (TC) and serum triglycerides (TG). Similarly, Le Chantelier noticed higher levels of TG in individuals with low microbial gene counts vs. those with high microbial gene counts [123]. Another study indicates that if the total cholesterol (TC) in the brain membrane increases, synapses are not performed normally and, therefore, affect cognitive degeneration in AD [124]. Another interesting study has demonstrated pro-inflammatory characteristics of cholesterol oxidation products, namely oxysterols, in human pathophysiology, especially side chain oxysterols with enzymatic origins. The major one 27-Hydroxycholesterol (27-OHCE), contributes to cognitive deficits in APP/PS1 transgenic mice through microbiota dysbiosis and intestinal barrier dysfunction [125]. Based on these data, gut dysbiosis involving lipid dysmetabolism contributes to the AD pathogenesis and it may provide insight into novel therapeutic strategies.

1.6 The Gut microbiota-Brain Axis

The gut microbiota communicates with the central nervous system (CNS) through the complex bidirectional gut-brain axis (GBA) involving multiple pathways: the neuroimmune system, sympathetic and parasympathetic branches of the autonomic nervous system, and neuroendocrine system (Fig. 11) [[109], [126]]. Gut to brain

signaling in the gut is accomplished by highly chemosensitive primary afferent neurons, immune cells and enteroendocrine cells, which contain over 30 different hormones and bioactive molecules. Immune pathways, such as cytokine signaling stimulated by microbial lipopolysaccharide (LPS) or peptidoglycan, also represent a communication link to the brain. Changes in gut barrier integrity may also lead to translocation of these microbial products in the periphery with downstream microglial activation and neuroinflammation [127]. In addition to enteric nerves, various hormones, immune mediators, and microbial metabolites represent pathways through which the brain receives information about environmental exposures such as diet and the gut ecosystem functioning. The importance of the gut-brain axis is highlighted by the fact that psychiatric symptoms are related with co-morbidity at gastrointestinal level, including inflammatory bowel disorder (IBD) and irritable bowel disorder (IBS) [128]. Mounting evidence reported that the gut microbiome dysbiosis significantly impacts on this axis associated with neuroinflammation and metabolic syndrome [[129], [130]], thus contributing to the development of neurodegenerative disease such as AD [[131], [132]]. There is pioneering evidence supporting the existence of a microbiota-gut-inflammasome-brain axis, in which enteric bacteria modulate, via the nucleotide-binding oligomerization domain leucine rich repeat and pyrin domain-containing protein 3 (NLRP3) signaling, inflammatory pathways that, in turn, contribute to influence brain homeostasis [133]. One interesting study demonstrated that changes in diet can cause rapid alteration of gut microbiome composition affecting insulin sensitivity and glycemic control [134]. Remarkably, a novel formulation of lactic acid

bacteria and bifidobacteria (namely SLAB51) chronically administered to a triple-transgenic mouse model of AD, B6; 129-Psen1tm1Mpm Tg (APP^{Swe}, tau^{P301L})1Lfa/J (named 3xTg-AD). 3xTg-AD mice were previously characterized and represent a reliable model of human AD. A β intracellular immunoreactivity can be detected in some brain regions as early as 3 to 4 months of age in 3xTg-AD mice [135]. Interestingly, gut microbiome and mycobiome alterations have been observed in 3xTg-AD mice compared to a wild type counterpart [136]. Consequently, upon SLAB51 probiotic treatment produced a decreased cognitive decline, reduced A β aggregates and brain damages influencing key systemic metabolic functions in this model [[106], [135]]. The novel therapeutic approach such as psychobiotics (microbiota, which supports good mental health) targeting this axis for the treatment of neurological disorders related to cognitive function has become hot point, but still fully unclear.

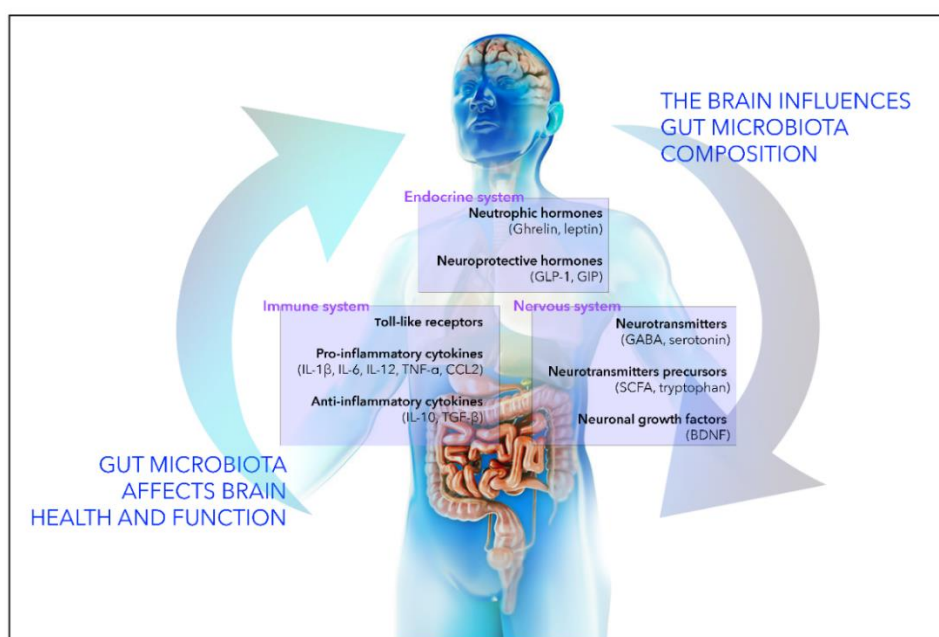


Figure 11. Gut-brain axis. Schematic illustration of the bidirectional communication network between the gut microbiota and the brain. Principal molecular mediators are reported.

1.7 Therapeutic approaches targeting microbiota

Most therapies for AD simply delay the loss of cognition and memory as there is no definitive treatment for AD. A growing body of evidence has focused on the role of the human microbiome in regulating multiple neuro-chemical pathways through the gut-brain axis [[137], [138]]. As previously discussed dysbiosis is strongly correlated with the development of neurodegenerative diseases including AD, thus gut microbiota modulation targeting the gut-brain axis can play a key role in combating AD [[112], [113]]. Studies have reported that nutritional interventions might be helpful to mitigate or delay the risk of cognitive impairment, AD and other non-psychiatric comorbidities. Fieldhouse *et al.* [139] stated that a suboptimal diet is related to severely impaired cognition, attributed to low vegetable consumption and is pronounced in AD and dementia. Oral bacteriotherapy has been identified as an accepted practice for the prevention and treatment of gastrointestinal infections [140] and inflammatory conditions [[141], [142]]. Moreover, manipulating microorganisms through fecal transplants to treat various conditions, the most well studied demonstrated that effective therapy for recurrent *Clostridioides difficile* (*C. difficile*) infections[143]. Diet-based strategies (such as foods rich in prebiotics, probiotics or probiotics enriched foods, and polyphenols) and faecal microbiota transplantation (FMT) could be represented promising approaches to regulate function and composition of gut microbial population,

favoring the abundance of beneficial bacterial groups [113] (Fig.12). The clearly molecular pathways remain to be further explored.

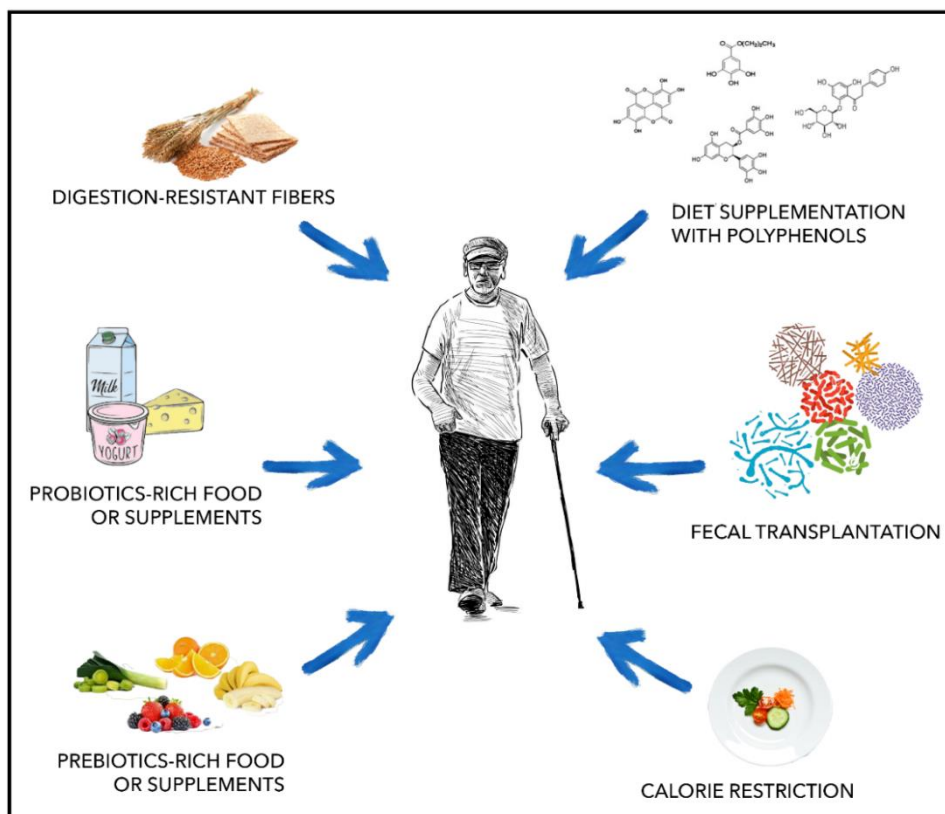


Figure 12. Strategies used to modulate gut microbiota composition. Diet-based strategies and faecal transplantation are considered promising approaches to regulate function and composition of gut microbial population, favoring the abundance of beneficial bacterial groups.

1.7.1 Faecal microbiota transplantation

Faecal microbiota transplantation (FMT) is the transfer of stool from a healthy donor into the gastrointestinal tract of patients with the aim of increasing overall diversity and restoring the function of gut microbiota [109]. At present, FMT is widely used for the treatment of *Clostridium difficile* infections[143], however, trials related to human

diseases ranging from inflammatory bowel disease to metabolic diseases, cancer and neurodegenerative diseases including AD are still ongoing worldwide. Emerging evidences have demonstrated that FMT could be beneficial for cognitive impairment, decreasing phosphorylation of tau protein and the levels of amyloid peptides, and also ameliorating synaptic plasticity in AD brains [[144], [145]]. The fecal material is expected to be sourced from a highly organized stool bank and various routes of administration such as enema, capsule, or colonoscopy [146]. However, studies suggest that patient acceptance, and tolerability must be assessed before recommending this method because of the inherent limitations of rodent models of human brain disorder. Technical standardization, stool bank services and management, safety assessment, etc., still need to be further studied, causing complex challenges for both regulators and clinicians. Stool availability, adverse effects, and poorly or undefined mechanisms of action are the major concerns related to FMT [113]. The FMT methodology is gaining considerable attention in both preclinical and clinical research and is likely to develop rapidly over the next decade.

1.7.2 Prebiotics

Numerous studies also highlighted that dietary interventions with specific nutrients or combination of nutrients may act on gut microbes and their metabolites to ameliorate AD neuropathology. Diet supplementation with prebiotics was demonstrated to be a possible strategy to attenuate AD symptoms modulating the microbiota. Prebiotics are non-digestible substances that act as substrate selectively utilized by host micro-

organisms and confer a health benefit. There are many kinds of prebiotics, among which inulin, resistant starch (RS), fructooligosaccharides (FOS), galactooligosaccharides, and xylooligosaccharides are most frequently highlighted [[109], [110], [147]]. Treatment of APP/PS1 transgenic mice with FOS, commonly found in natural fruits and vegetables, changed microbiota composition and activated the GLP-1 pathway with consequent amelioration of cognitive deficits and pathological changes [148]. RS is known to exert a powerful influence on metabolic and systemic health and has been shown to modify the abundance of gut microbiome [149]. Research on dietary inulin has been demonstrated that it enhanced systemic metabolism and decreased inflammatory gene expression in hippocampus and altered gut microbiome composition in an APOE4 mice model [150]. In addition, supplementation of prebiotics in humans alters the expression level of cytokines genes, which may be beneficial for the elderly [151]. Although the prebiotics exert effect on gut microbiota, which may provide major benefits, basic knowledge on the delicate interactions between the host, gut microbiota, and prebiotics are still fully unclear. Many technical and pragmatic difficulties, such as ensuring it reaches the location where it can exert its potential therapeutic effect, remain to be solved. Randomized controlled studies with larger cohorts are needed to evaluate the effect of prebiotics and to provide clinical evidence [147].

1.7.3 Probiotics

Probiotics are living microorganisms that promote health benefits when consumed in

adequate quantity. The most commonly used probiotic microorganisms belong to the genera *Lactobacillus* and *Bifidobacterium* since members of both groups have been used extensively in promoting human health [152].

Our lab has recently reported on the beneficial properties of SLAB51, a formulation of lactic acid bacteria and bifidobacteria able to modulate microbiota in 3xTg-AD mice increasing the relative abundance of *Bifidobacterium spp.* and decreasing *Campylobacterales*, bacterial groups differently involved in the regulation of inflammatory pathways. These changes in microflora composition, together with enriched gut concentration of SCFAs and increased plasma levels of neuroprotective gut peptide hormones, contributed to counteract cognitive decline through a reduction in A β aggregates and brain damages, and a partial restoration of impaired neuronal proteolytic pathways [106]. SLAB51-mediated microbiota modulation also mitigated oxidative stress by activating SIRT1-dependent mechanisms and restored glucose homeostasis in 3xTg-AD mouse brain [[19], [153]].

Another probiotic formulation, ProBiotic-4, containing *B. lactis*, *L. casei*, *B. bifidum* and *L. acidophilus*, significantly improved cognitive functions and attenuated intestinal and BBB injury in aged SAMP8 mice through inhibition of both TLR4 and RIG-I-mediated NF-kB signaling pathways and inflammatory responses [154]. Abraham *et al.* showed that probiotics were sufficient to improve cognitive performance in mice with AD compared to mice not treated with probiotics [155]. Interestingly, AD patients

administered with probiotics showed cognitive function improvement and favorable changes in related plasma biomarkers such as malondialdehyde and serum triglyceride [156]. These findings suggest that probiotic supplementation may have the therapeutic potentials to block or reverse the progression of AD. However, clinical evidence is insufficient to reach conclusions regarding the recommendation of probiotics for patients with AD. The exact mechanism by which probiotics display effects on AD remains to be further elucidated.

1.7.4 Polyphenols

Dietary polyphenols are a group of natural compounds present in foodstuffs such as vegetables, fruits, cereals, tea, coffee, dark chocolate, cocoa powder, and wine [157]. The neuroprotective as well as antioxidant properties of the dietary polyphenols are associated with the modulation of AD related pathologies, suggesting a new approach for research and clinical interventions to treat neurodegenerative diseases. Structurally, polyphenolic compounds consist of phenolic rings and are generally classified as flavonoids, including flavonols, flavan-3-ols, flavones, flavanones, isoflavones and anthocyanins; and nonflavonoids such as phenolic acids, hydroxycinnamic acids, lignans, stilbenes and tannins [158]. Specifically, flavan-3-ols, a common subclass of flavonoids, and their consumption was associated with healthy brain aging, neuronal protection against disorders, and amelioration of cognitive function [[159], [160]]. Flavan-3-ols exist either as simple monomers called catechins or as oligomeric and complex polymeric structures known as proanthocyanidins. Importantly, the phenyl- γ -

valerolactones (PVLs) and their related phenylvaleric acids (PVAs), a major group of low-molecular phenolic compounds, are the main microbial metabolites of flavan-3-ols in humans [[161], [162]]. As illustrated in Figure 13, PVLs can originate from (–)-epicatechin but also from condensed epicatechins such as the dimeric procyanidin B2, through 5-carbon side-chain ring fission catalyzed by gut, mainly colonic, microbial enzymes, and subsequent phase II metabolic conversion by the hepatic enzymes [[161], [163]].

It has been reported that PVLs, particularly (R)-5-(3',4'-dihydroxyphenyl)- γ -valerolactone, and their sulfated forms, protect brown adipocytes from increased production of reactive oxygen species [162]. 5-(3',5'-dihydroxyphenyl)- γ -valerolactone, an epigallocatechin gallate-derived microbial metabolite, significantly induced neurites outgrowth and elongation in human neuroblastoma SH-SY5Y cells [164]. In addition, given the neuroprotective role of flavonoids, several studies investigated also the ability of these molecules and their derivatives to cross the BBB. The metabolite 5-(3',5'-dihydroxyphenyl)- γ -valerolactone showed a slightly higher BBB permeability than its parental compound epigallocatechin-3-gallate (EGCG) [164]. Similarly, Angelino *et al.* recently evidenced that the 5-(hydroxyphenyl)- γ -valerolactone-sulfate (3',4' isomer), another key microbial metabolite of flavan-3-ols, is able to reach the brain [165]. Although increasing attention has been directed to the possible biological effects exerted by this class of molecules, being them one of the most abundant phenolic metabolites in the circulation upon consumption of a (poly)phenol-rich diet, still much

less data are available in the literature [[161], [163]].

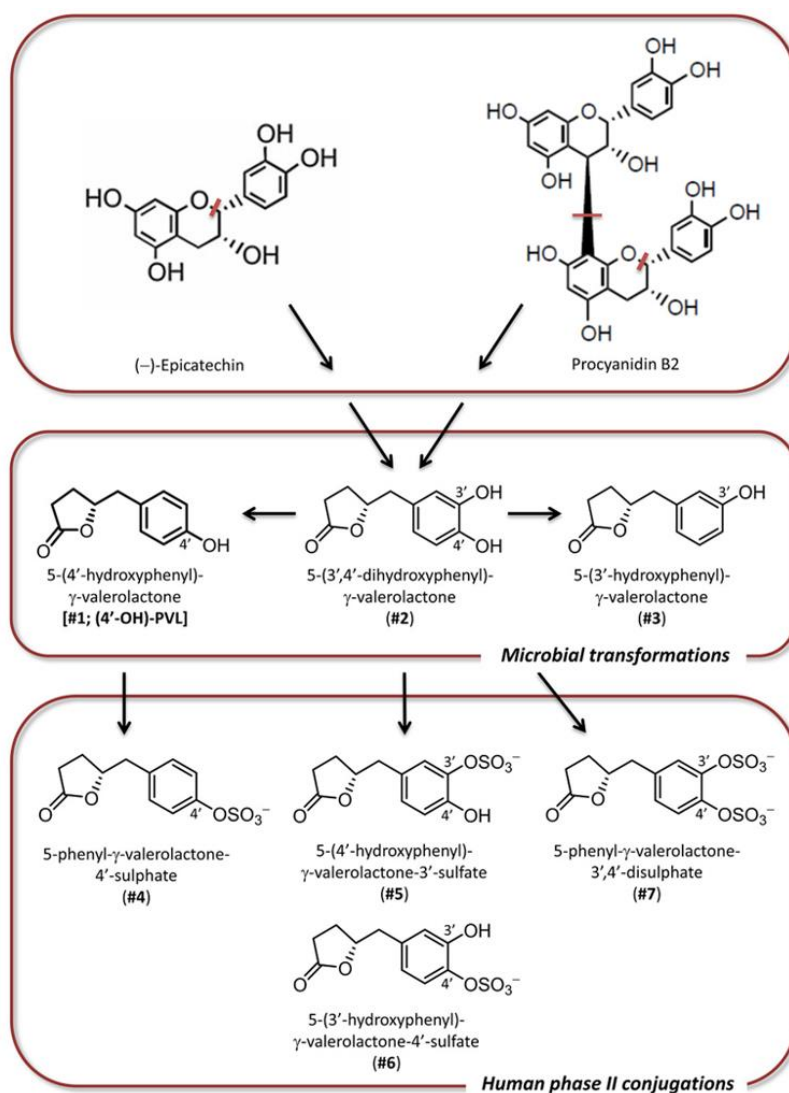


Figure 13. Outline of human flavan-3-ol metabolism and PVL formation. Starting from (-)-epicatechin and procyanidin B2, chosen as representative plant polyphenol precursors, after 5-carbon side-chain ring fission and initial transformation catalyzed by gut microbial enzymes, compounds #1-2 serve as precursors for subsequent phase II metabolism as indicated. The latter is catalyzed by host colonic and hepatic enzymes and generates the indicated sulfated PVL derivatives (compounds #4-7) as major products (collectively designated as “phase II metabolites”) that are then released into the circulation [166].

To date, there is no definitive cure to control the onset and progression of AD. Altered components of the gut could represent a key role in gut-brain axis, which is a bidirectional system between the CNS and the enteric nervous system. Diet can alter the microbiota composition, affecting the gut-brain axis function. Gut microbiome restoration is able to counteract the AD progression and this effect could be exerted by food-based therapy or by probiotic supplementation. More recently, our lab has demonstrated that a novel probiotic formulation (SLAB51) was able to counteract cognitive decline and neuronal injury, to reduce β -amyloid plaques through a SIRT1-mediated mechanism, to restore glucose metabolism in AD transgenic mice model. Regarding this context, we have explored the role of the dietary supplementation SLAB51 probiotic formulation on the impaired lipid metabolism and hypoxia-inducible factor-1 α (HIF-1 α), a key molecule regulating host-microbial crosstalk in the same mice model. Further, we have also investigated the ability of a selection of phenyl- γ -valerolactones, gut microbiota-derived metabolites of flavan-3-ols, to modulate the functionality of the two cellular proteolytic pathways in a cellular model of AD. Specifically, human SH-SY5Y neuroblastoma cells stably transfected with either wild-type A β PP gene (APPwt) or 717 valine-to-glycine A β PP-mutated gene (APPmut) were used. Additionally, the intracellular proteolytic systems of immortalized Alzheimer's disease astrocytes from the hippocampus of 3xTg-AD and wild-type mice (3Tg-iAstro and WT-iAstro, respectively) were also dissected, and the ability of 4-phenil butyric acid to restore proteolysis in AD has been explored, providing a not previously explores mechanism of action of this neuroprotective compound.

Chapter 2: Gut microbiota modulation in Alzheimer's disease:

Focus on lipid metabolism

2.1 Materials and methods

2.1.1 Reagents and chemicals

SLAB51 multi-strain probiotic formulation was provided by Ormendes SA (Jouxten-Mézery, Switzerland, <https://agimixx.net>). SLAB51 contains eight different live bacterial strains: *Streptococcus thermophilus* DSM 32245, *Bifidobacterium lactis* DSM 32246, *Bifidobacterium lactis* DSM 32247, *Lactobacillus acidophilus* DSM 32241, *Lactobacillus helveticus* DSM 32242, *Lactobacillus paracasei* DSM 32243, *Lactobacillus plantarum* DSM 32244, *Lactobacillus brevis* DSM 27961.

Enzymatic colorimetric kits for total cholesterol, high-density lipoprotein cholesterol (HDL-C) and low-density lipoprotein cholesterol (LDL-C) determination were kindly provided by Chema Diagnostica (Monsano, AN, Italy). HMGCR, HMG-CoA, NADPH, NADP⁺, CoA, potassium phosphate, sodium phosphate, magnesium sulfate, phenylmethanesulfonyl-fluoride, tosyl-phenyl-alanyl-chloromethyl-ketone, ethylenediaminetetraacetic acid (EDTA), dithiothreitol (DTT), and dimethyl sulfoxide (DMSO) were all purchased from Sigma–Aldrich. HPLC grade methanol was obtained from JT Baker. All solvents and reagents were of the highest purity available. The reverse phase Luna C18 column (5 µm particle size, 250 × 4.6 mm, equipped with a 5 mm guard column) was purchased from Phenomenex S.r.l. (Bologna, Italy).

Membranes and reagents for western blotting analyses were purchased from Merck KGaA, (Darmstadt, Germany). The rabbit polyclonal anti IDOL (ab-74562) and the rabbit monoclonal anti-HMGCR [EPR1685(N)] (ab174830) antibodies were from AbCam (Milano, Italy). The mouse monoclonal antibodies anti-glyceraldehyde-3-phosphate dehydrogenase (GAPDH), anti CYP461A antibody, anti-LXR α/β antibody and anti-SREBP-1c were from Santa Cruz Biotechnology, Inc. (Heidelberg, Germany).

2.1.2 Animal model

AD triple-transgenic mice, B6;129-Psen1^{tm1Mpm} Tg (APPSwe, tauP301L)1Lfa/J (named 3xTg-AD) and the wild type B6129SF2 mice, were purchased from the Jackson Laboratory (Bar Harbor, ME, USA). 3xTg-AD mice contain three mutations associated with frontotemporal dementia or familial AD (amyloid precursor protein [APP]Swe, tau MAPT P301L, and presenilin-1 M146V). This reliable model of human AD displays both plaque and tangle pathology, with A β intracellular immunoreactivity detectable at three months of age and hyperphosphorylation of tau protein occurring by 12–15 months of age [135]. Consequently, in 12–15 months it is possible to reliably reproduce traits similar to those observed in the entire life of Alzheimer's disease patients. Moreover, we have observed gut microbiome and mycobiome alteration in 3xTg-AD mice compared to a wild type counterpart [136] and the ability of SLAB51 probiotic formulation to strategically shift gut microbiota in these animals has been demonstrated [106].

Experiments complied with the ARRIVE guidelines, in accordance with the EU Directive 2010/63/EU for animal experiments and with a protocol approved by the Italian Ministry of Health (518/2018-PR). Mice were housed in plastic cages (Makrolon, Covestro A.G., Filago, Italy) in a temperature-controlled room (21 ± 5 °C) and 60% humidity on 12-h light/dark reversed cycle (light was switched on at 8:00 p.m.) and maintained on standard laboratory diet (Mucedola, Italy) and water ad libitum. Appropriate measures minimized pain and discomfort in experimental animals.

2.1.3 Experimental design

Eight-week-old AD male mice ($n = 48$) were organized in two groups and were treated with SLAB51 dissolved in water ($n = 24$) or with water (control group, $n = 24$). At the same time, 48 age-matched wild type (wt) mice were organized into wt control ($n = 24$) and wt-treated ($n = 24$) groups. Based on the body surface area principle the dosage of SLAB51 2×10^{11} bacteria/kg/day was calculated. The body weight was monitored during the treatment to ensure single-housed animals received the proper intake of the probiotic. Preliminary studies were performed to evaluate both viability and stability of the probiotic formulation as previously described [153] and probiotic drinking solution was freshly prepared every day. With the aim to start treatment before the deposition of protein aggregates, and based on preliminary experiments, 8, 24 and 56 weeks of age were selected as timepoints, in order to evaluate the preventative and therapeutic properties of chronic supplementation with probiotics. Eight mice per group were euthanized by CO₂ overdose at 8, 24 and 56 weeks of age, and the tissues were properly

collected for biochemical analyses. In detail, murine brains and livers were quickly removed and placed on an ice-cold glass plate. Plasma samples and tissue homogenates were promptly supplemented with protease inhibitors (1 mM tosyl phenylalanyl chloromethyl ketone (TPCK) and Pefabloc).

2.1.4 Plasma lipid analysis

Plasma total cholesterol, high-density lipoprotein cholesterol (HDL-C) and low-density lipoprotein cholesterol (LDL-C) were determined enzymatically, using commercially available colorimetric kits (Chema Diagnostica, Italy) according to the manufacturer's instructions. Data are expressed as mg/dL \pm SE.

2.1.5 Preparation of brain and liver homogenates

Upon sacrifice, tissues were homogenized in 50 mM Tris-buffer, 150 mM KCl, 2 mM EDTA, pH 7.5 (1:5 weight/volume of buffer). Homogenates were immediately centrifuged at 13,000 \times g for 20 min at 4 °C and the supernatants were used. Protein concentration was measured with the Bradford protein assay [167].

2.1.6 Liver microsomes preparation

Liver microsomes were prepared as previously reported [168]. In detail, liver tissue samples (0,1 g) were added to 1 mL of cold homogenization buffer (50 mM Tris-HCl buffer, 0,3 M sucrose, 10 mM EDTA, 10 mM DTT and 50 mM NaCl at pH 7.4 in the presence of protease inhibitors and homogenized using a bench-top Ultra-Turrax TP

18/10 homogenizer (Janke and Kunkel; Staufen, Germany). The homogenate was centrifuged at 20,000 × g for 15 min at 4 °C. Supernatant was collected and (ultra)centrifuged at 100,000 × g for 60 min at 4 °C. Microsomal pellet was finally resuspended in the activity buffer (100 mM phosphate buffer, 10 mM DTT, 1 mM EDTA, 2% DMSO at pH 6.8). Total protein concentration was determined with the Bradford assay [169].

2.1.7 High performance liquid chromatography (HPLC) analysis

The Amersham Biosciences AKTA basic HPLC system equipped with a UV/VIS detector was used for the analysis. Reaction mixture consisting of ultracentrifuged liver homogenates, NADPH and HMG-CoA was incubated at 37 °C (aliquots were withdrawn at indicated times and separated by HPLC). Each species was injected and separated with Phenomenex Luna C18 reverse-phase-HPLC column (5 µm particle size, 250 × 4.6 mm) with the following linear gradient of 100 mM potassium phosphate (solvent A) and methanol (solvent B): 10%–30% B in 3 column volumes, 30%–30% B in 1 column volume and 30%–10% B in 1 column volume at flow rate of 0.6 mL/min, UV/VIS detector set at 260 nm. After each chromatographic elution, column was regenerated with two column volumes of 60% methanol. HMG-CoA, NADPH, and NADP⁺ were directly monitored, whereas mevalonate was determined by monitoring CoA production (mevalonate/CoA 1:1 stoichiometric ratio) [170].

Liver microsomes dissolved in the activity buffer (100 mM sodium phosphate buffer

containing 1 mM EDTA, 10 mM DTT, 2% DMSO, and 1 mM magnesium sulfate, pH 6.8) were incubated with substrate and NADPH for 60 min at 37 °C. The resulting mixture (10 µL) was separated with the above-described Luna C18 column thermostatted at 26 ± 0.1 °C.

2.1.8 Western blotting

The expression levels of liver microsomal HMGCR were analyzed through Western blot assay with the aim to verify a possible change upon probiotics treatment. In detail, for each time point (8-week-old, 24-week-old and 56-week-old) microsomes (20 µg of total proteins) were resolved on a 10% sodium dodecyl sulphate-polyacrylamide gel electrophoresis (SDS-PAGE) then transferred on polyvinylidene fluoride (PVDF) membranes. Successively, upon incubation with specific antibodies, the immunoblot detection was carried out with an enhanced chemiluminescence (ECL) Western Blotting ChemiDoc™ System (Biorad, Milano, Italy). Molecular weight markers were included in the gel. With the same approach LXRs (α/β) and SREBP1c expression levels were measured.

GAPDH was used to check equal protein loading and to normalize Western blot data. The densitometric analysis was conducted as previously described [171]. Briefly, ChemiDoc acquired images or scanned autoradiographs (16-bit gray scale) were processed through Image J (NIH) to calculate the background mean value and its standard deviation. The background-free image was then obtained subtracting the

background intensity mean value from the original digital data. The integrated densitometric value associated with each band was then calculated as the sum of the density values over all the pixels belonging to the considered band having a density value higher than the background standard deviation. The band densitometric value was then normalized to the relative GAPDH signal intensity. The ratios of band intensities were calculated within the same Western blot. All the calculations were carried out using the Matlab environment (The MathWorks Inc., Natick, MA, USA).

2.1.9 Plasma fatty acid profile

The determination of the fatty acid composition of plasma glycerophospholipids was obtained using a previously described method [172], with the aim to verify the ability of the treatment to shift the lipid metabolic pathway exerting a neuroprotective effect. Briefly, 100 μ L of plasma and 0.6 mL methanol (precooled at 5 °C) were combined in glass tubes and shaken for 30 s. The precipitated proteins were separated from the methanolic phase by centrifugation at 900 \times g for 5 min. The methanolic supernatant was transferred into another glass tube. 25 μ L of sodium methoxide solution were added to the supernatant, then the tubes were shaken at room temperature during selective synthesis of methyl esters. The reaction was stopped after 3 min with 75 μ L of methanolic HCl. Fatty acid methyl esters (FAME) were extracted by adding 300 μ L hexane and shaking the tubes for 30 s. The upper hexane phase was transferred into a 2 mL vial. The extraction was repeated, and combined extracts were dried under nitrogen flow at RT. The dry residue was taken up in 50 μ L hexane (containing 2 g/L

tert-butyl-hydroxy-toluene) for GC analysis.

FAME were quantified using gas chromatography by a standard procedure using a capillary column ZB-FAME, 30 m × 0.25 mm, film thickness 0.20 μm (Phenomenex, USA) in a 7820 A GC System (Agilent Technologies, Santa Clara, California, EUA). The FAME was evaluated by calculating each FA as a percentage over the total FA cluster (relative %). GC peaks were identified as 97% of the total peaks present in the GC analysis by comparison with commercially available standards. Results were interpreted using the post hoc Tukey's test and are expressed as percent abundance.

2.1.10 ELISA determination of 27-hydroxycholesterol

27-Hydroxycholesterol (27-OHCE) was measured in the plasma and the brain of control and treated 56-week-old AD mice using the mouse 27-hydroxycholesterol solid-phase ELISA kit (My BioSource, San Diego, California, USA) following the manufacturer's instructions. Data are expressed as ng/mL ±SE.

2.1.11 Statistical analysis

Biochemical data are expressed as mean values ± SE. Statistical analysis was performed with one-way ANOVA, followed by the Bonferroni and Tukey test using Sigma-Stat 3.1 software (SPSS, Chicago, IL, USA). Statistical significance of treated mice compared to untreated 8-week-old mice of the same genotype is indicated with asterisks (* $p < 0.05$). To describe the effect of SLAB51 treatment, statistical

significance of treated mice compared to age-matched untreated mice of the same genotype is indicated with hashtags ($\#p < 0.05$).

2.2 Results

2.2.1 Amelioration of blood lipid profile in AD mice upon probiotic administration

Cholesterol is involved in APP processing and high levels of cholesterol correlate with increased risk of AD [173]. Considering that cholesterol lowering therapies improve cognitive performance in AD subjects, the ability of SLAB51 to ameliorate blood lipid profile was investigated. As expected, cholesterol plasma concentration in 3xTg-AD mice was significantly higher than that of age matched wt mice (Fig. 14). Interestingly, upon probiotic administration, a significant decrease of total cholesterol concentration was detected in the plasma of 56-week-old AD mice (Fig. 14). Conversely, no significant variations were observed in wt animals.

Moreover, AD mice showed decreased levels of high-density lipoprotein cholesterol (HDL-C) and increased levels of low-density lipoprotein cholesterol (LDL-C) with respect to age matched wt mice. Probiotics oral administration induced a significant increase of HDL-C and a significant decrease of LDL-C plasma concentrations. Altogether, these data indicate a positive effect on blood lipid profile and suggesting an amelioration of AD pathology.

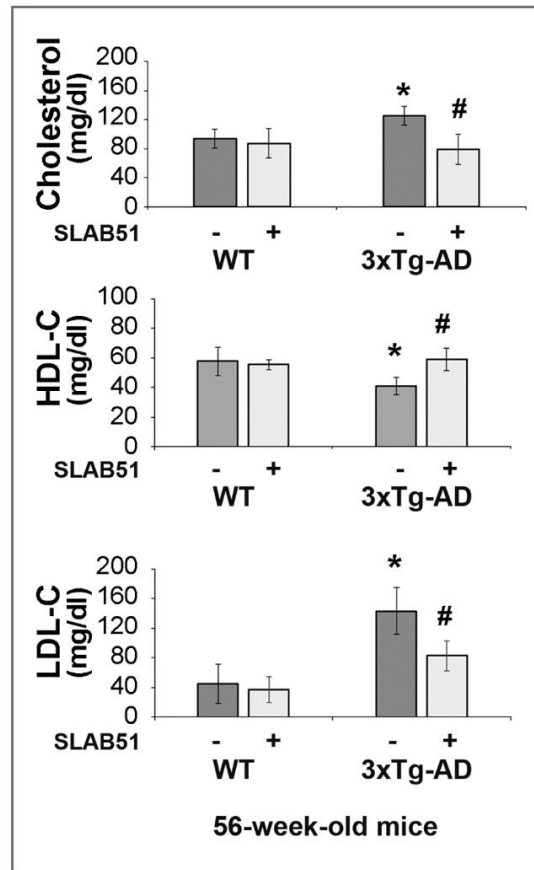


Figure 14. Blood lipid profile. Plasma concentrations (mg/dl) of total cholesterol, HDL-C and LDL-C in 56-week-old wild type and AD mice treated (light grey) or not (dark grey) with SLAB51 probiotic formulation (* $p > 0.05$ compared with untreated wild type mice; # $p > 0.05$ compared with untreated age-matched mice of the same group).

2.2.2 SLAB51 oral administration influences cholesterol biosynthesis and metabolism

Then we explored the ability of probiotics to modulate the functionality of HMGCR, the rate-limiting step of cholesterol biosynthesis. In detail, the activity of HMGCR was measured in liver microsomes of mice administered with SLAB51 or water using a previously described HPLC based method [170].

HMGCR activity was significantly lower in 56-week-old AD mice orally administered with SLAB51 for 12 months, as indicated by the decreased area of the CoA peak (Fig. 15). No significant differences were observed in wt mice (data not shown).

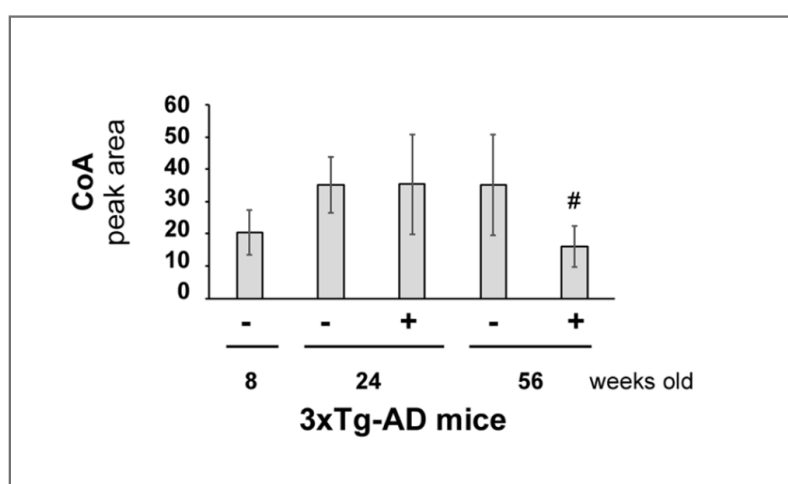


Figure 15. Inhibition of HMGR activity in 3xTg-AD mice treated with SLAB51. Mevalonate production calculated from changes in CoA peak area (mevalonate/CoA 1:1 stoichiometric ratio) in 8, 24 and 56-week-old mice orally administered with SLAB51. Data points marked with a hashtag are statistically significant compared to age-matched untreated mice ($\#p < 0.05$).

Liver homogenates were analyzed through western blotting in order to evaluate the expression levels of HMGR enzyme. 56-week-old untreated AD mice showed a significant increased expression of HMGR with respect to young animals (Fig. 16). Interestingly, HMGR expression significantly decreased in the liver of 56-week-old 3xTg-AD mice treated with probiotics, indicating that cholesterol lowering effect (Fig. 14) was due to both decreased HMGR activity (Fig. 15) and reduced expression of

the protein (Fig. 16). These data suggest that SLAB51 play positive role in regulating cholesterol metabolism.

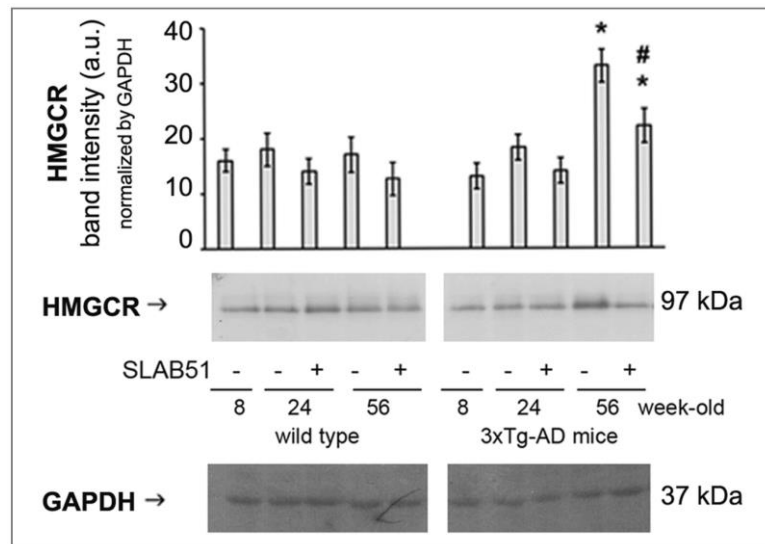


Figure 16. Effect of SLAB51 on HMGR expression levels. HMGR expression levels were detected in 8-week-old mice treated for 4 and 12 months with SLAB51 probiotic formulation. Representative immunoblots of both wt (right) and 3xTg-AD (left) mice is reported and corresponding densitometric analyses are shown. Equal protein loading was verified by using an anti-GAPDH antibody. Data points marked with an asterisk are statistically significant compared to 8-week-old untreated control mice of the same genotype ($*p < 0.05$). Data points marked with a hashtag are statistically significant compared to age-matched untreated mice ($#p < 0.05$).

Amelioration of blood lipid profile can also be explained by the modulated expression of SREBP1c and LXRs in probiotic-treated 3xTg-AD mice. In detail, increased levels of SREBP1c were observed in both liver and brain of untreated AD mice (Fig. 17, upper panels) indicating an increased cholesterol synthesis and in agreement with the

enhanced expression and activity of HMGCR (Figures 15 and 16). Interestingly, cerebral and hepatic protein expression of SREBP1c significantly decreased upon 12 months treatment with probiotics (Fig. 17, upper panels), suggesting that HMGCR inhibition can be also modulated through SREBP1c dependent pathways.

Additionally, SLAB51 oral administration significantly upregulated LXRs expression in the brain and the liver of 3xTg-AD mice, at 24- and 56- weeks of age (Fig. 17, lower panels), in line with the previously documented anti-inflammatory effects [19] and cognitive improvement [106], and consistently with the ameliorated blood lipid profile (Fig. 14). This is of significant importance considering that LXRs also regulate the expression of genes involved in cholesterol absorption, transport, efflux, excretion and conversion to bile acids, finally affecting the reverse cholesterol transport [174].

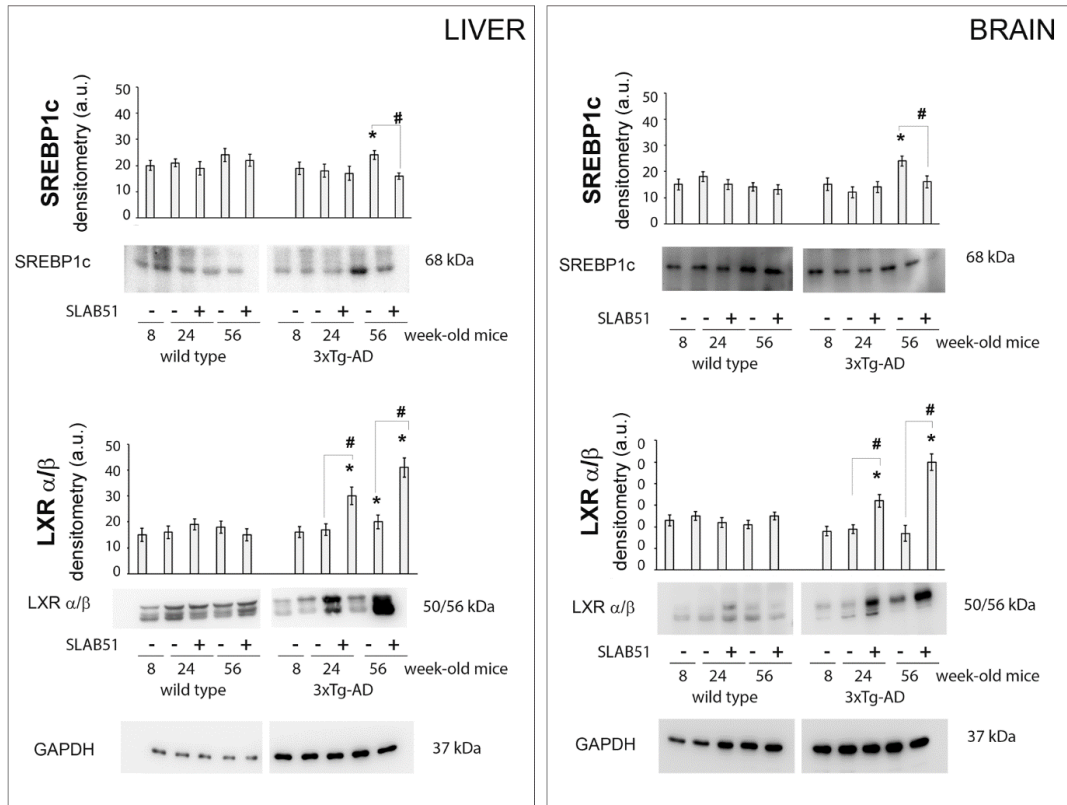


Figure 17. SREBP1c and LXRs expression levels in wt and AD mice orally administered with SLAB51 for 4 and 12 months. Representative immunoblots and corresponding densitometric analyses derived from six separate blots are shown. Equal protein loading was verified by using an anti-GAPDH antibody and normalized expression of the target protein is reported as arbitrary units (a.u.). Data points marked with an asterisk are statistically significant compared to 8-week-old untreated control mice of the same genotype ($*p < 0.05$). Data points marked with a hashtag are statistically significant compared to age-matched untreated mice ($\#p < 0.05$).

In turn, LXRs can induce the expression of the inducible degrader of LDL receptor (IDOL) which is a E3 ubiquitin ligase that targets lipoprotein receptors for proteasome-mediated degradation and with a key role in metabolism and AD. Figure 18 shows that IDOL increased in the brain of SLAB51-treated mice, in agreement with the ability of probiotics to improve neuronal proteolysis in AD mice [106].

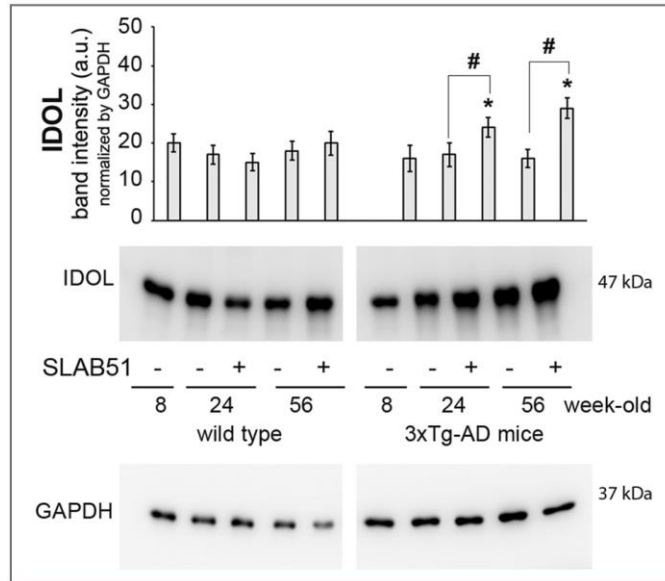


Figure 18. IDOL expression levels in wt and AD mice orally administered with SLAB51 for 4 and 12 months. Representative immunoblots and corresponding densitometric analyses derived from six separate blots are shown. Equal protein loading was verified by using an anti-GAPDH antibody and normalized expression of the target protein is reported as arbitrary units (a.u.). Data points marked with an asterisk are statistically significant compared to 8-week-old untreated control mice of the same genotype ($*p < 0.05$). Data points marked with a hashtag are statistically significant compared to age-matched untreated mice ($#p < 0.05$).

2.2.3 Probiotic supplementation modifies plasma fatty acids composition

The determination of the fatty acid composition of plasma glycerophospholipids was performed to investigate the neuroprotective effects of chronic SLAB51 treatment attributable to the modulation of lipid metabolic pathway.

Plasma lipidomic analyses confirmed the probiotics anti-inflammatory effects as indicated by the significant decrease of cis-linoleic acid (Fig. 20) and the decreased ratio of cis-linoleic acid/(EPA + DHA) in 3xTg-AD mice supplemented with SLAB51

for 12 months (Fig.19). In fact, the ratio of omega-6 to omega-3 is a recognized indicator of the health status and a lower ratio of n-6 to n-3 fatty acids is associated with reduction in inflammation [[175], [176]].

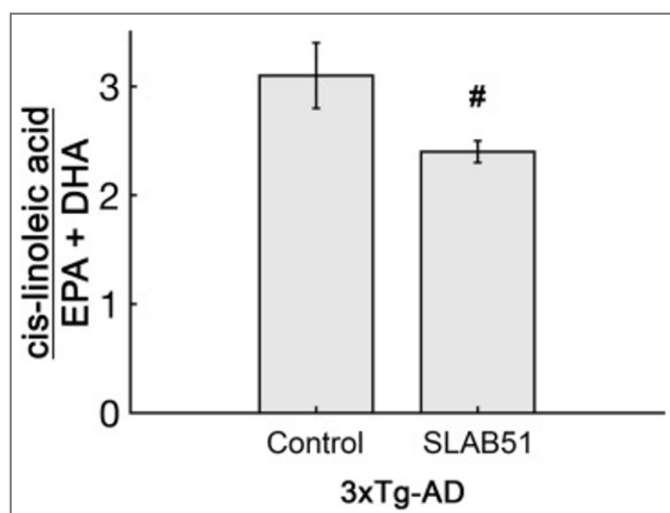


Figure 19. Decreased omega6/omega 3 polyunsaturated fatty acids ratio in treated AD mice. cis-linoleic acid/(EPA + DHA) ratio in the plasma of 56-week-old AD mice chronically administered with water (control) or with SLAB51 for 12 months. Data points marked with an asterisk are statistically significant compared to control ($\#p < 0.05$).

Data reported in Fig. 20 reveal that SLAB51-modified intestinal microbial status can affect plasma fatty acids composition. Although a slight but significant decrease of the omega-3 fatty acids α -linolenic acid and eicosapentaenoic acid was observed in 56-week-old AD mice upon SLAB51 supplementation (Fig. 20), the important reduction of the omega-6 cis-linoleic acid definitively determine the anti-inflammatory effect, by decreasing the omega6/omega-3 ratio (Fig. 19).

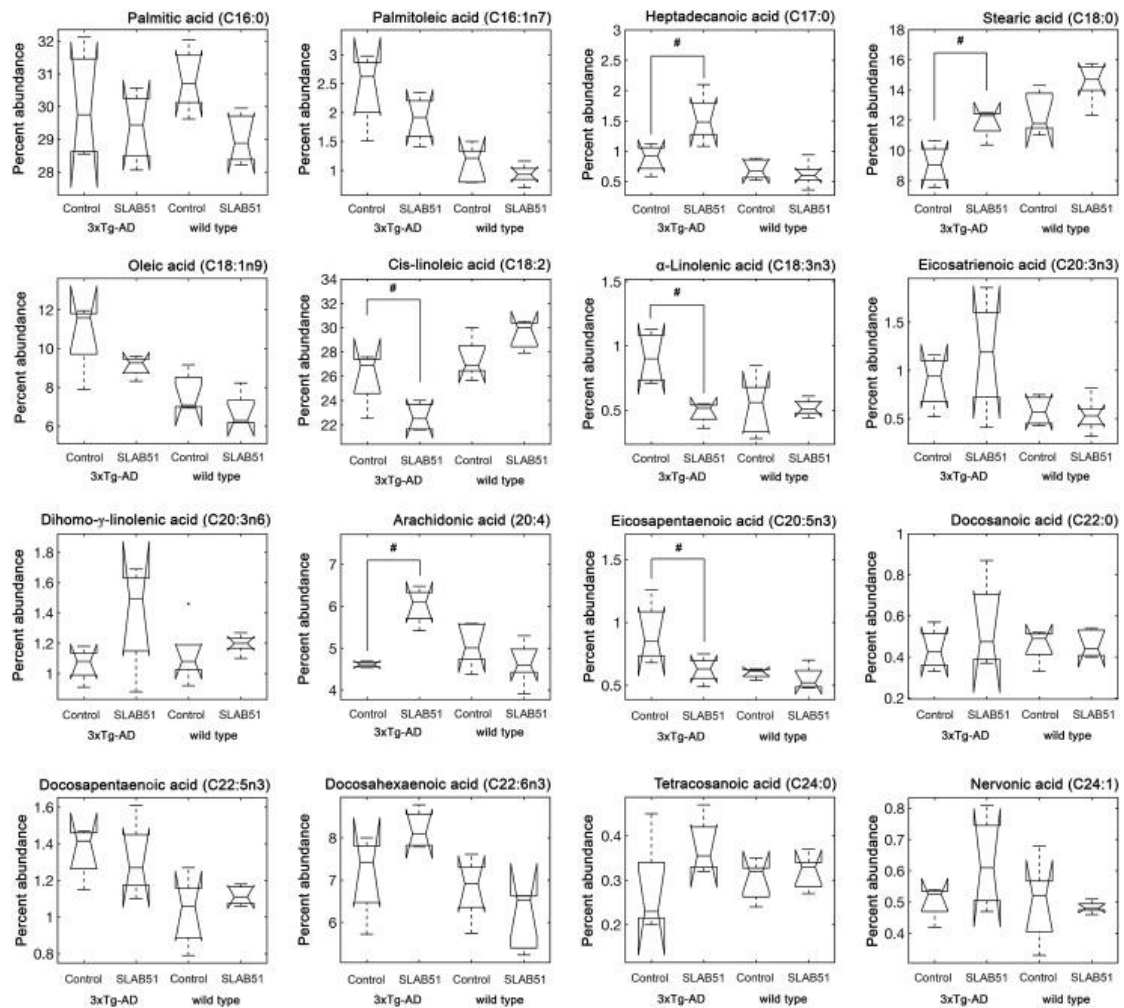


Figure 20. SLAB51 affects plasma lipid profile. Fatty acid composition of plasma glycerophospholipids in 56-week-old wt and 3xTg-AD mice treated with water (control) or SLAB51 for 12 months. Results were analyzed using the post hoc Tukey's test and are expressed as percent abundance. Data points marked with an asterisk are statistically significant compared to age-matched control mice of the same genotype ($\#p < 0.05$).

Interestingly, SLAB51 treated AD mice displayed increased plasma levels of stearic acid, which was previously demonstrated to exert hypocholesterolemic effects [177]. Moreover, probiotic treated AD mice showed higher levels of heptadecanoic acid, which is inversely associated with insulin resistance and type 2 diabetes [178], in line

with a correlation with the amelioration of glucose metabolism in the same mice upon SLAB51 chronic administration [153].

Altered composition of plasma fatty acids observed in AD mice was significantly modulated by probiotics (Fig. 20), indicating dynamic effects of the shifted gut microbiota on the plasma lipid profile of AD mice. In fact, gut microbiota of AD mice has a significantly different structure with respect to wild type mice, causing disequilibrium in energy homeostasis. No significant differences were observed in SLAB51-treated wt mice, confirming the safety of the probiotic-based approach, most likely due to the higher stability of wt gut microbiota [106].

2.2.4 Decrease of 27-hydroxycholesterol upon probiotic treatment in AD mice

The neurotoxic oxysterol 27-hydroxycholesterol (27-OHCE) can pass from the circulation across the BBB thus mediating the effects of hypercholesterolemia on the brain [61]. Interestingly, upon SLAB51 chronic administration, 27-OHCE concentration significantly decreased in both the plasma and the brain of 56-week-old AD mice compared to age-matched controls (Fig. 21).

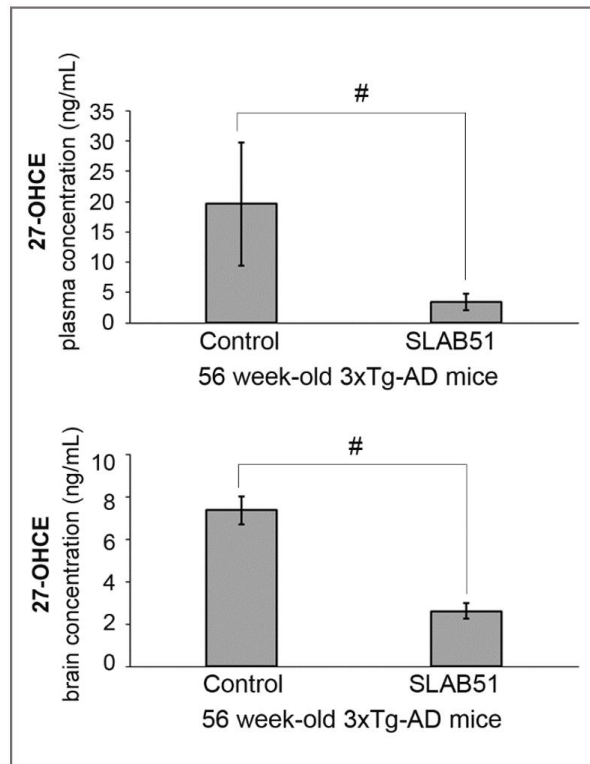


Figure 21. 27-Hydroxycholesterol plasma and brain levels. ELISA determination of 27-Hydroxycholesterol (27-OHCE) in the plasma (upper panel) and the brain (lower panel) of control and treated 56-week-old 3xTg-AD mice. 27-OHCE concentrations are expressed as ng/mL \pm SE. Data marked with a hashtag are significantly different with respect to age-matched controls ($\#p < 0.05$).

2.2.5 SLAB51 increased the brain expression of CYP46A1

CYP46A1 is the rate limiting enzyme in cholesterol degradation and its cerebral restoration implicates neuroprotective effects. The increased expression of CYP46A1 enzyme in the brain of 24- and 56- week-old AD mice chronically administered with SLAB51 suggested the probiotic-dependent induction of cerebral cholesterol turnover [179]. No significant differences were observed in wild type animals (Fig. 22).

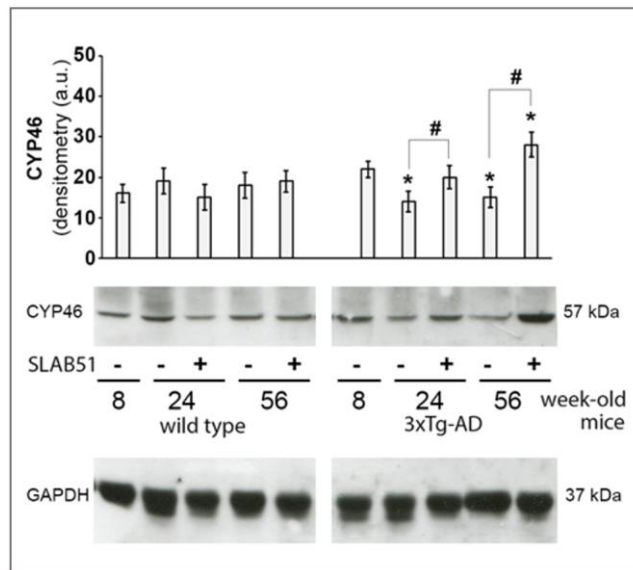


Figure 22. Brain CYP46 expression levels in wt and AD mice orally administered with SLAB51 for 4 and 12 months. Representative immunoblots and corresponding densitometric analyses derived from six separate blots are shown. Equal protein loading was verified by using an anti-GAPDH antibody. Data points marked with an asterisk are statistically significant compared to 8-week-old untreated control mice of the same genotype ($*p < 0.05$). Data points marked with a hashtag are statistically significant compared to age-matched untreated mice ($\# p < 0.05$).

2.3 Discussion

Current established treatments for AD are only able to counterbalance the symptoms but they cannot prevent or stop the disorder. One of the main global challenges for health and social care is to identify new strategies aimed at preventing or delaying AD onset and development. Potentially modifiable risk factors received increasing attention, with gut microbiota representing an attractive preventative/therapeutic target because of its role in regulating multiple neurochemical pathways through the gut–brain axis [[137], [138]]. Deregulation of lipid homeostasis substantially contributes to AD onset and progression and cholesterol lowering compounds (like statins), were demonstrated to reduce the risk of dementia. However, mechanistic insights into the link between abnormal lipid metabolism and A β aggregation and clearance are still unavailable. The ability of statins to improve metabolism can be explained through gut microbiota altered composition [180]. In this context, dietary interventions, including probiotics, which are able to modulate microbiota composition, have been studied for their ability to improve energy homeostasis and immune system in neurodegenerative diseases [[121], [181]].

Recently in Bonfili, L., *et al.*, 2017, our lab has demonstrated that chronically dietary supplementation with SLAB51 probiotic formulation administration of SLAB51 probiotic formulation modified gut microbiota in 3xTg- AD mice, where the treatment induced larger microbial shifts particularly increase in *Bifidobacterium spp.* and reduction in *Campylobacterales*; that favored several metabolic pathways associated

with energy metabolism, amino acid metabolism, nucleotide metabolism and glucose metabolism. *Bifidobacterium strains* possess anti-inflammatory properties while *Campylobacter jejuni* is known to increase the expression of pro-inflammatory cytokines and this was observed as reduced plasma concentrations of pro-inflammatory cytokines in SLAB51 treated AD mice. Improvement of cognitive performances observed in these mice was supported by increased plasma concentrations of neuroprotective gut hormones and correlated with decreased A β load and partially recovery of neuronal proteolytic pathways, with consequent delay of AD progression [[19], [106], [153]].

Considering the contradictory data on the role of deregulated lipid homeostasis in AD and in light of the promising effects of probiotics on energy metabolism, 3xTg-AD mice and their wild type counterpart were chronically treated with SLAB51 with the aim of deeply dissecting the role of microbiota modulation in ameliorating AD pathology by affecting lipid homeostasis. High levels of total cholesterol and LDL-C and low levels of HDL-C are associated with vascular dementia and, indirectly, with AD [182]. As expected, dyslipidemia was observed in older 3xTg-AD mice but not in wild type animals (Fig. 14). Interestingly, the probiotic mixture exerted hypocholesterolemic effects in AD mice, qualitatively ameliorating plasma lipid composition (Fig. 14), with a consequent reduction of total cholesterol/HDL-C and LDL-C/HDL-C ratios. These results can be partially explained with the significant decrease in HMGCR concentration and activity observed in hepatic microsomes,

indicating that this multi-strain probiotic mixture can inhibit cholesterol biosynthesis, consistently with other studies [[183], [184]]. The present data are in agreement with the increased fecal content of short chain fatty acids induced by SLAB51 in the same animal model [106], particularly for the ability of propionate to inhibit hepatic lipogenesis and cholesterol synthesis, finally alleviating metabolic disorders [185].

Additionally, the increased hepatic expression of the lipogenic SREBP1c in untreated AD mice (Fig. 17, upper panels) indicates an age-dependent increase in cholesterol synthesis, in line with the enhanced expression and activity of HMGCR (Figures 15 and 16). Interestingly, cerebral and hepatic protein expression of SREBP1c significantly decreased upon 12 months treatment with probiotics (Fig. 17, upper panels), suggesting a probiotic-dependent effect on fatty acid and triglyceride synthesis [[49], [50]] and indicating that HMGCR levels/activity can be regulated through SREBP1c dependent pathways. Moreover, SREBP1c decreased expression in both the brain and the liver of treated AD mice is in agreement with the ability of SLAB51 to counteract insulin resistance in the same animal model [153], since SREBP1c emerged as a metabolic mediator between insulin/glucose signaling and lipogenesis [186]. In fact, other studies indicated that hyperinsulinemia could mediate the induction of SREBP-1c that, in turn, triggers lipogenesis, suggesting inhibition of SREBP-1c as a therapeutic approach in dyslipidemia-associated disorders [[48], [187]].

In parallel, SLAB51 improved blood lipid profile and cholesterol homeostasis also by

triggering LXRs-mediated pathways. In fact, these receptors can induce genes that positively regulate bile acid synthesis and apolipoprotein metabolism, and that decrease A β production, exerting neuroprotection [188], as previously reported [106]. Considering the recognized anti-inflammatory effects of LXRs [19], enhancement levels upon treatment (Fig. 17, lower panels) better explain the ameliorated inflammatory status in SLAB51 treated AD mice [106]. Additionally, SLAB51 anti-inflammatory properties were confirmed by the decreased ratio of cis-linoleic/(EPA + DHA) in the plasma of 3xTg-AD mice (Fig. 19). This is a crucial information, because the ratio of omega-6 to omega-3 has been previously described as a fundamental indicator of human health and a lower ratio of omega-6 to omega-3 fatty acids is associated with reduction in inflammation [176]. Inflammation-associated diseases, such as diabetes, obesity, mental disorders, cardiovascular and autoimmune diseases are associated to an increased omega-6/omega-3 ratio leading to the production of pro-inflammatory molecules [[175], [189]]. Consequently, the ameliorated omega6/omega 3 balance in AD mice chronically supplemented with SLAB51 can represent one possible mechanism through which oral bacteriotherapy can modulate inflammatory processes.

Interestingly, the augmented expression of LXRs in the brain of treated mice contribute to elucidate the partial restored functionality of the ubiquitin-proteasome system (UPS) observed in the same mice upon SLAB51 treatment [106]. In fact, LXRs can trigger the expression of the E3 ubiquitin ligase IDOL, promoting the lipoprotein receptors

proteolysis, affecting the structural and functional plasticity of synapses and neural circuits with effects on memory and behavior [55]. Moreover, they can also limit cholesterol uptake, complementary to SREBP mediated effects [56]. Improved cognitive abilities are also confirmed by the significant decrease of EPA plasma concentrations in treated AD mice, in line with a recent study suggesting that this n-3 polyunsaturated fatty acid contributed to impair memory and learning in animal models [190]. Other significant variations in plasma fatty acid composition were detected upon SLAB51 chronic supplementation. For example, heptadecanoic acid increased in probiotic-treated AD mice, suggesting a correlation with the improved glucose homeostasis and decreased insulin resistance in the same animal model chronically supplemented with SLAB51 for 12 months [153], since heptadecanoic acid is inversely associated with insulin resistance and type 2 diabetes mellitus [178].

On the other hand, the slight but significant reduction of α -linolenic acid and the increase of arachidonic acid detected in the plasma of 56-week-old treated AD mice are apparently in contrast with the previously documented decrease of pro-inflammatory cytokines in the plasma of SLAB51 treated mice at 24 weeks of age [106]. Actually, these variations highlight the dynamic interactions among numerous actors of a complex inflammatory response, in which polyunsaturated fatty acids can compete each other [191] and simultaneously co-operate in resolution of inflammation. In particular, the role of arachidonic acid in neurodegenerative conditions is controversial [192]; importantly, it is essential for the development of the brain, as it regulates cell

membrane fluidity and ion channels activity and guarantees optimal cognitive functions, in agreement with the ameliorated behavioral performances observed in 3xTgAD mice chronically administered with SLAB51 [106]. Additionally, it stimulates type 2 immune response [193] and possesses anti-diabetic properties [194] in agreement with the previously documented effects of SLAB51 on glucose uptake and metabolism in 3xTgAD mice [153]. Consequently, arachidonic acid represents one of the key mediators in the interactions among probiotic-induced lipid profile changes, insulin sensitivity and inflammation.

An important linker among hypercholesterolemia, oxidative stress and neuropathology of AD in the brain is the cholesterol oxidation product 27-hydroxycholesterol [61], which is an intermediate of the alternative pathway of bile acids biosynthesis [195] and a recognized biomarker for impaired glucose homeostasis [196]. As expected, 27-OHCE was significantly increased in both the plasma and the brain of AD mice (Fig. 21, upper panel), confirming a correlation between circulating 27-OHCE and cholesterol [63] and in agreement with the altered BBB permeability, enhanced oxidative status and reduced glucose uptake in the brain of 3xTg-AD mice with respect to wild type animals [[19], [153]]. Upon SLAB51 supplementation, decreased concentrations of the oxysterol were measured both in the plasma and the brain of transgenic mice confirming the probiotics antioxidant efficacy [19] and the ability to restore glucose homeostasis [153]. Decreased 27-OHCE, together with the increased levels of CYP46A1 enzyme in the brain of SLAB51 treated AD mice (Figures 21 and 22) indicated an effect on

alternative pathways of bile acid production and confirm the activation of LXRs dependent pathways that maintain cholesterol turnover and homeostasis and support neuronal function [[60], [195]]. Considering the role of CYP46A1 in regulating memory functions [59] and A β deposition [60], its increase in SLAB51 treated AD mice contribute to elucidate the restored cognitive abilities and the reduced number of A β plaques previously observed in younger animals [106]. Collectively, these data contribute to address the unclear microbiota-influenced changes in the plasma lipids and demonstrate that probiotics can significantly affect the gut microbial composition with positive impact on the host lipid profile.

Chapter 3: Strategic Modification of Gut microbiota through Oral Bacteriotherapy Influences Hypoxia Inducible Factor-1 α : Therapeutic Implication in Alzheimer's disease

3.1 Materials and Methods

3.1.1 Animal Studies

AD triple-transgenic mice, B6;129-Psen1tm1Mpm Tg (APP^{Swe}, tau^{P301L})1Lfa/J (named 3xTg-AD), and their respective wild-type animals were purchased from the Jackson Laboratory (Bar Harbor, ME, USA). 3xTg-AD mice contain three mutations associated with familial Alzheimer's disease (APP, Tau MAPT P301L, and Presenilin-1 M146V). This reliable model of human AD displays both plaque and tangle pathology, with A β intracellular immunoreactivity detectable at three months of age and hyperphosphorylation of tau protein occurring by 12 to 15 months of age [135]. Experiments were in accordance with the guidelines laid down by the European Communities Council (86/609/ECC) for the care and use of laboratory animals and with a protocol approved by the Italian Ministry of Health (518/2018-PR). Mice were housed in Makrolon[®] cages (4 animals per cage) in a temperature-controlled room (21 \pm 5 °C) and 60% humidity on a 12 h light/dark inverted cycle (light was switched on at 8:00 p.m.) and maintained on laboratory diet (Mucedola Srl, Milano, Italy) with water ad libitum. Appropriate measures minimized pain and discomfort in experimental animals.

SLAB51 probiotic formulation was kindly provided by Prof. Claudio De Simone, MD

(Ormendes SA, Jouxkens-Mézery, Switzerland, <https://agimixx.net>). SLAB51 contains eight different live bacterial strains: *Streptococcus thermophilus* DSM 32245, *Bifidobacterium lactis* DSM 32246, *Bifidobacterium lactis* DSM 32247, *Lactobacillus acidophilus* DSM 32241, *Lactobacillus helveticus* DSM 32242, *Lactobacillus paracasei* DSM 32243, *Lactobacillus plantarum* DSM 32244, and *Lactobacillus brevis* DSM 27961.

Eight-week-old AD male mice ($n = 48$) were divided in two groups: one administered with SLAB51 dissolved in water ($n = 24$), and the control group administered with water ($n = 24$). Simultaneously, 48 age-matched wild type (wt) mice were organized into wt control ($n = 24$) and wt-treated ($n = 24$) groups. The dosage of SLAB51 (200 bn bacteria/Kg/day) was determined by application of the body surface area principle [197]. The body weight was monitored during the treatment to ensure single-housed animals received the proper intake of treatment. Preliminary studies were performed to evaluate both viability and stability of the probiotic formulation upon solubilization in water at 21 ± 5 °C. The percentage of vital bacteria was determined by fluorescence microscopy, which revealed that 88% of the strains survived after 30 h under the above-mentioned conditions. Thus, probiotic drinking solution was freshly prepared every day. Eight mice per group were euthanized at 8, 24, and 56 weeks of age, and the tissues were properly collected and stored at -80 °C.

3.1.2 Preparation of Brain Homogenates

Upon sacrifice, mice brains were homogenized (1:5 weight/volume of buffer) in 50 mM Tris-buffer, 150 mM KCl, 2 mM EDTA, pH 7.5. Homogenates were immediately centrifuged at 13,000× g for 20 min at 4 °C, and the supernatant was used. Protein concentration was measured through the Bradford protein assay [167].

3.1.3 Western Blot Analysis

Mice brain homogenates were analyzed through western blotting to measure the levels of inducible nitric oxide synthase (iNOS), hypoxia-inducible factor 1- α (HIF-1 α), and prolyl hydroxylase 2 (PHD2). In detail, for each time point, brain homogenates (30- μ g total protein) were resolved on a 10–12% sodium dodecyl sulphate-polyacrylamide gel electrophoresis (SDS-PAGE) and electroblotted onto polyvinylidene fluoride membranes for chemiluminescent western blotting. Molecular weight markers (6.5 to 205 kDa) were included in each gel. Glyceraldehyde-3-phosphate dehydrogenase (GAPDH) was used to check equal protein loading and to normalize the target proteins signal. The densitometric analysis has been conducted using Image J software as previously described [153].

3.1.4 Nitrite Level Assay

Nitrite quantitation in the plasma of treated and untreated AD and wt mice was performed with the Griess Reagent kit for nitrite determination (Molecular Probes, Leiden, The Netherlands) according to the manufacturer instruction.

3.1.5 Statistical Analysis

Statistical analysis of data was performed using Sigma-stat 3.1 software (SPSS, Chicago, IL, USA). For comparison between two means, Student's unpaired test was used. For comparison of the mean values among the groups, upon Shapiro–Wilk normality test, a two-way ANOVA, followed by a Bonferroni post hoc test, was used. The results were expressed as mean values \pm SD, as specified in figure legends. *p* values less than 0.05 were considered to be statistically significant and are indicated by one asterisk (*); two asterisks (**) indicates a *p* value of less than 0.01; three asterisks (***) indicates a *p* value of less than 0.001.

3.2 Results

3.2.1 SLAB51 Affected Nitric Oxide Related Pathways

Nitric oxide (NO) production and oxidation are increased in the brains of AD subjects, contributing to neuronal cell loss and neurodegeneration [198]. As expected, nitrite plasma concentration and iNOS cerebral levels significantly increased in 56-week-old 3xTg-AD untreated animals with respect to younger transgenic mice. Interestingly, treatment with SLAB51 restored the plasmatic nitrite concentration and iNOS protein expression in the brain of these animals (Fig. 23), indicating downstream positive effects of these changes on the compromised inflammatory and oxidative status in AD. Additionally, these results are in line with previously published evidence on the antioxidant effects of the probiotic formulation. Specifically, significantly decreased levels of 3-nitrotyrosine were detected in the brain of SLAB51-treated 3xTg-AD mice [19].

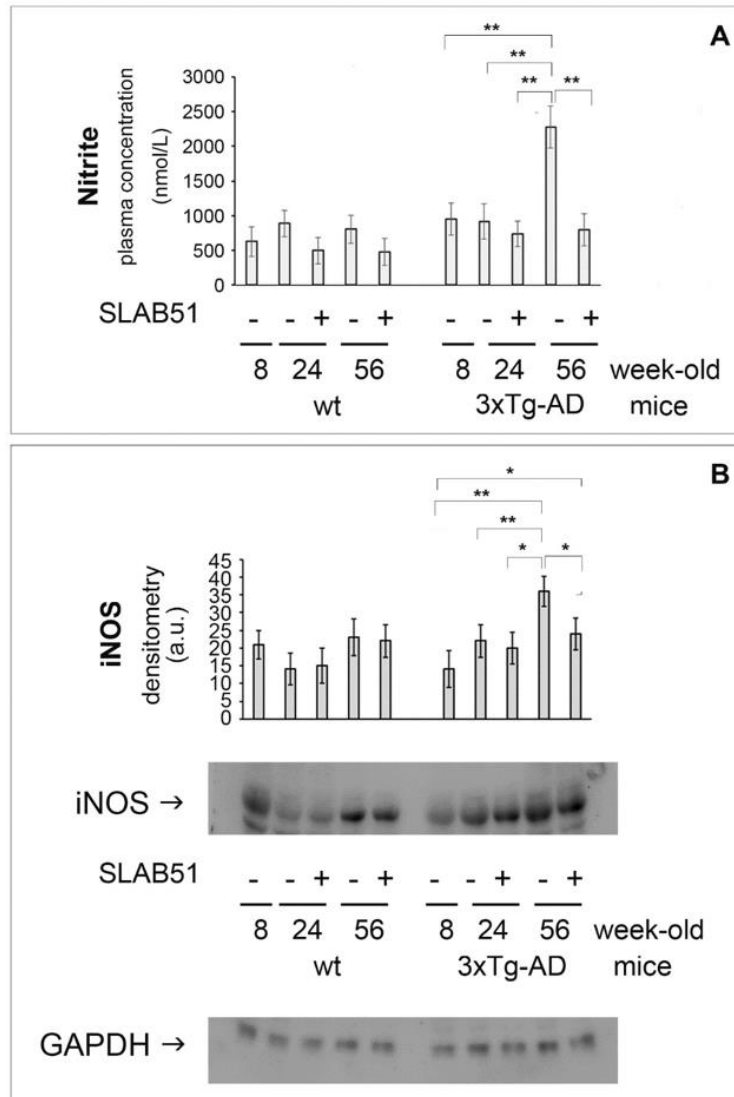


Figure 23. SLAB51 decreased plasma nitrite and iNOS cerebral expression in AD mice. (A): Nitrite plasma concentration (nmol/L) in 8-, 24-, and 56-week-old wt (left) and AD (right) mice administered with water or SLAB51. (B): Cerebral iNOS expression levels normalized by GAPDH measured in SLAB51-treated (+) and SLAB51-untreated (-) wt (left) and AD (right) mice. The densitometric analyses obtained from three separate blots and representative immunoblots are shown. Equal protein loading was verified by using an anti-GAPDH antibody. The detection was performed with an ECL Western blotting analysis system. Statistical significance compared to untreated 8-week-old mice and age-matched mice is indicated with asterisks (* $p < 0.05$, ** $p < 0.01$).

3.2.2 SLAB51 Restored HIF-1 α Cerebral Expression in AD Mice

Hypoxic responses are regulated by hypoxia-inducible transcription factor-1, with HIF-1 α being the oxygen-regulated subunit. A decreased expression of HIF-1 α in untreated 3xTg-AD mice compared to age-matched untreated wild type animals was observed. Chronic treatment with probiotics restored HIF-1 α cerebral expression (Fig. 24), suggesting a positive effect on oxygen homeostasis and glucose metabolism. In fact, HIF-1 α regulates the activity of glucose transporters 1 and 3 (GLUT1 and GLUT3) that are crucial for brain glucose uptake [75]. These data are in agreement with a study demonstrating that HIF-1 levels are reduced in AD brains compared to age-matched controls, [199] resulting in decreased GLUT1 and GLUT3 levels and with abnormal tau hyperphosphorylation [64]. Interestingly, the increased brain expression of HIF-1 α in SLAB51-treated 3xTg-AD mice is in agreement with previously published data demonstrating that these probiotics can ameliorate cerebral glucose uptake in AD mice by increasing the brain expression of GLUT1 and GLUT3 [153].

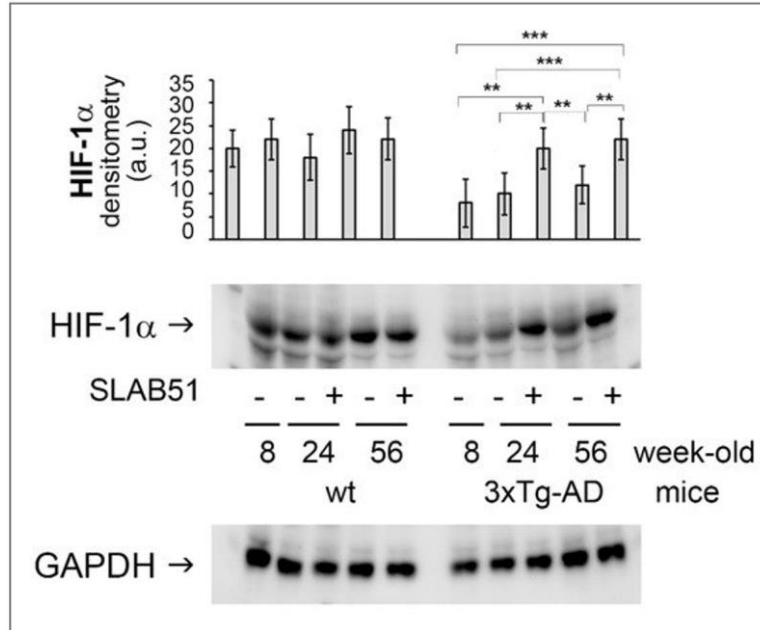


Figure 24. SLAB51 restored HIF-1 α cerebral expression in AD mice. HIF-1 α expression levels normalized by GAPDH measured in brain homogenates of SLAB51-treated and SLAB51-untreated wt (left) and AD (right) mice. The densitometric analyses obtained from three separate blots and representative immunoblots are shown. Equal protein loading was verified by using an anti-GAPDH antibody. The detection was performed with an ECL Western blotting analysis system. Statistical significance compared to untreated 8-week-old mice and age-matched mice is indicated with asterisks (** $p < 0.01$, *** $p < 0.001$).

HIF-1 α restored levels in treated mice correlated to the decreased brain expression levels of PHD2 upon SLAB51 chronic supplementation (Fig. 25). In fact, PHD2 is known to regulate HIF-1 α degradation, and the HIF/PHD2 pathway has been studied as a pharmaceutical target to promote the endogenous HIF transcriptional response for treatment of hypoxic human diseases [200].

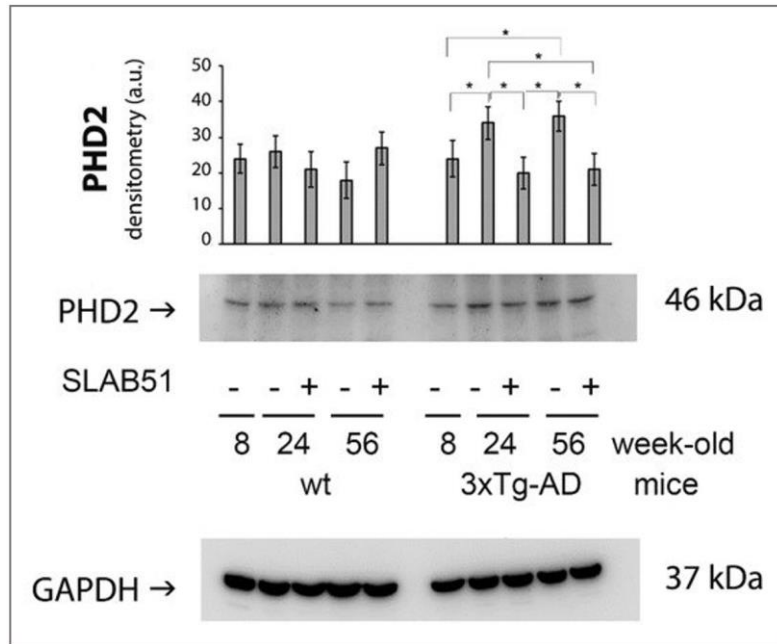


Figure 25. Decreased cerebral expression of PDH2 in treated AD mice. PHD2 expression levels normalized by GAPDH, measured in brain homogenates of SLAB51-treated and SLAB51-untreated wt (left) and AD (right) mice. The densitometric analyses obtained from three separate blots and representative immunoblots are shown. Equal protein loading was verified by using an anti-GAPDH antibody. The detection was performed with an ECL Western blotting analysis system. Statistical significance compared to untreated 8-week-old mice and age-matched mice is indicated with asterisks ($*p < 0.05$).

3.3 Discussion

Gastrointestinal-tract microbiota-derived LPS is an important contributor to inflammatory neurodegeneration in the brain of AD patients [113], causing neuronal loss and memory impairment. Considering that, in AD subjects, specific cerebral regions are more susceptible to damages due to BBB dysfunction, impaired vascularization, and hypoxic insult [201], it is crucial to identify new strategies to improve neuronal function by modulating the expression level of key molecular agents that can finely modulate the gut–brain axis, reduce nitric oxide and ROS production, and counteract neuronal cell loss. In particular, during hypoxia the oxygen-regulated subunit HIF-1 α forms a heterodimer with the constitutively expressed HIF-1 β , influencing the transcription of important regulators of glucose homeostasis, cellular stress, inflammation, and apoptosis [[65], [73]]. Moreover, HIF can induce genes involved in anaerobic metabolism, such as GLUT1 and GLUT3, and genes encoding glycolytic enzymes [73]. Additionally, HIF-1 α is degraded in an oxygen dependent manner under regular oxygenated conditions through the hydroxylation of proline residues by prolyl hydroxylases, particularly PHD2. Several factors, such as ROS [202] and NO [203], can interfere with PHD activity finally influencing HIF-stability. In particular, HIF-1 α and PHDs are directly regulated by S-nitrosylation, leading to stabilization of HIF-1 α . Normoxic HIF-1 activity can be up-regulated through NO-mediated S-nitrosylation and stabilization of HIF-1 α ; however, during hypoxia, NO is inactivated by superoxide to form deleterious peroxynitrite, known to destabilize HIF-1 α [203]. SLAB51 multi-strain probiotic formulation is able to shift microbiota

composition and counteract AD progression in transgenic mice [106], and a recent clinical study reported the effect of oral bacteriotherapy to increase nitric oxide synthesis in intestinal cells, with positive consequences in vital organs like the brain [204]. In the present work, the ability of the same probiotic formulation to positively interfere with the HIF-1 α /PHD2 pathway in 3xTg-AD mice was explored in order to clarify the incompletely understood mechanisms of action of SLAB51.

The brain expression of HIF-1 α was reduced in AD mice with respect to age-matched wild type animals, indicating compromised inflammatory status [65] and immune response [205]. Interestingly, upon SLAB51 oral administration, restored HIF-1 α brain levels suggest a positive effect on oxidative status and immune functionality, but also indicate a beneficial effect on glucose metabolism (Fig.24). In fact, HIF-1 α regulates the activity of glucose transporters 1 and 3 (GLUT1 and GLUT3) that are crucial for brain glucose uptake [206]. These data are in agreement with a study demonstrating that HIF-1 levels are reduced in AD brains compared to age-matched controls [199], resulting in decreased GLUT1 and GLUT3 levels and with abnormal tau hyperphosphorylation [64]. The increase of HIF-1 α in 24- and 56-week-old AD mice administered with SLAB51 probiotics corroborates previously published data showing that chronic treatment with the same probiotic formulation ameliorated glucose uptake in 3xTg-AD mice by increasing the brain expression of GLUT1 and GLUT3 [153]. Moreover, PHD2 is a negative regulator of HIF-1 α which causes its hydroxylation, followed by polyubiquitination and proteasomal degradation [73]. Inhibition of PHD2

is a promising therapeutic approach because not only has pleiotropic neuroprotective effect as a consequence of HIF-1 α . induction, but also exerts both antioxidant and anti-inflammatory actions [75]. Interestingly, the decreased expression of PHD2 reflects the upregulation of HIF-1 α in treated animals (Fig. 25). Furthermore, SLAB51 chronic administration counteracted the increase of nitrite plasma concentration and iNOS cerebral levels (Fig. 23), indicating both an antioxidant and anti-inflammatory effect of SLAB51, in agreement with previously published data on the increased gut concentration of anti-inflammatory bacterial metabolites in 3xTg-AD mice treated with the same probiotic formulation [106] and with the ameliorated oxidative status in this animal model [19]. Specifically, we have previously observed decreased nitrotyrosine accumulations in the brains of 3xTg-AD mice treated with probiotics [19], and other authors demonstrated that iNOS is aberrantly increased in both neurons and glial cells of AD subjects [207] being structurally related to nitrotyrosine formation [208].

Potentially negative side effects of microbiome alterations [209] should be carefully evaluated [210] in future pre-clinical and clinical studies. In fact, microbiome structure and genetic and epigenetic factors can influence the final effect [211]. SLAB51 beneficially impacts gut microbiota in 3xTg-AD mice with multi-level mechanisms, and these data contribute to describe another molecular mechanism through which this specific probiotic formulation can counteract oxidation and inflammation and can improve energy metabolism in AD.

Chapter 4: Flavan-3-ol Microbial Metabolites Modulate Proteolysis in Neuronal Cells Reducing Amyloid-beta (1-42) Levels

4.1 Materials and methods

4.1.1 Reagents and Chemicals

5-(4'-hydroxyphenyl)- γ -valerolactone (C1), 5-(3',4'-dihydroxyphenyl)- γ -valerolactone (C2) and 5-(3'-hydroxyphenyl)- γ -valerolactone-4'-sulfate (C3) (Fig. 26) were synthesized and kindly provided by Prof. C. Curti (University of Parma, Italy) [[212], [213]]. The substrates Suc-Leu-Leu-Val-Tyr-AMC, Z-Leu-Ser-Thr-Arg-AMC, Z-Leu-Leu-Glu-AMC for assaying the chymotrypsin-like (ChT-L), trypsin-like (T-L), and peptidyl glutamyl-peptide hydrolyzing (PGPH) activities of the proteasomal complex were purchased from Sigma-Aldrich S.r.L. (Milano, Italy). The substrate Z-Gly-Pro-Ala-Leu-Ala-MCA to test the branched chain amino acids preferring (BrAAP) activity was obtained from Biomatik (Cambridge, Ontario). Aminopeptidase N (EC 3.4.11.2) for the coupled assay utilized to detect BrAAP activity was purified from pig kidney as reported elsewhere [214]. Membranes for western blot analyses were purchased from Millipore (Milan, Italy). Proteins immobilized on films were detected with the enhanced chemiluminescence (ECL) system (Amersham Pharmacia Biotech, Milan, Italy). All chemicals and solvents were of the highest analytical grade available.

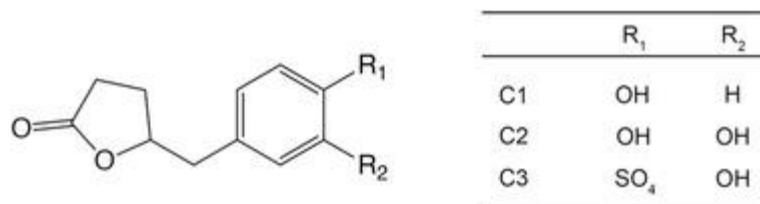


Figure 26. Structure of the PVLs used in this study. C1, 5-(4'-hydroxyphenyl)- γ -valerolactone; C2, 5-(3',4'-dihydroxyphenyl)- γ -valerolactone; C3, 5-(3'-hydroxyphenyl)- γ -valerolactone-4'-sulfate.

4.1.2 Molecular Docking

The molecular models of complexes between the PVLs and the catalytic subunits of human proteasomes were obtained according to flexible ligand-receptor docking using Autodock 4 [215]. 3D structures of the molecules of interest were built and optimized with Avogadro [216] and docked onto crystallographic structures of human constitutive (PDB ID: 6rgq [217]) and immuno- proteasomes (PDB ID: 6e5b) retrieved from the RCSB Protein Data Bank [218]. Specifically, a grid box (20 \times 20 \times 20 Å) was individually placed around the accessible internal portions of catalytic subunits β 1, β 2 and β 5 and β 1i, β 2i and β 5i immune counterparts, respectively, each box being centered on the catalytic Thr-1 residues and covering the entire surface extending 10 Å in each direction. Likewise, the valerolactones-cathepsin B models were obtained. The grid box was placed around the catalytic site of 3D structure of human cathepsin B (PDB ID: 1csb [219]), spanning 10 Å in each direction around the catalytic Cys-29. Unless stated differently, default settings were used throughout. Resulting models were rendered with PyMOL (The PyMOL Molecular Graphics System, Version 2.4 Schrödinger, LLC).

4.1.3 Measurements of Isolated 20S Proteasome Activity

PVLs effects on the 20S constitutive and immunoproteasome peptidase activities were measured through *in vitro* assays performed with fluorogenic peptides as substrates. Isolation and purification of the 20S proteasome from bovine brain and thymus were performed as previously reported [220]. The incubation mixture contained the compound at concentrations ranging from 0.0 to 10 μM , 1 μg of the isolated 20S proteasome, the appropriate substrate (5 μM final concentration), and 50 mM Tris/HCl (pH 8.0), up to a final volume of 100 μL . Purified proteasomes were always preincubated with each compound at 37°C for 30 min before the fluorogenic peptide substrates were added to the reaction mixture. Final incubation was performed at 37°C, and after 60 min the fluorescence of the hydrolyzed 7-amino-4-methyl-coumarin (AMC) and 4-aminobenzoic acid (pAB) was detected (AMC, $\lambda_{\text{exc}} = 365$ nm, $\lambda_{\text{em}} = 449$ nm; pAB, $\lambda_{\text{exc}} = 304$ nm, $\lambda_{\text{em}} = 664$ nm) on a SpectraMax Gemini XPS microplate reader.

4.1.4 Cell Culture and Transfections

SH-SY5Y cells were cultured in 1:1 Dulbecco's modified Eagle's medium and Nutrient Mixture F12 containing 10% fetal bovine serum (FBS), 2 mM glutamine, 100 units mL^{-1} penicillin, and 100 $\mu\text{g mL}^{-1}$ streptomycin at 37°C in a 5% CO_2 -containing atmosphere. The SH-SY5Y cells stable transfection with wild type A β PP 751 (APPwt) and A β PP (Val717Gly) mutations (APPmut), was prepared as described elsewhere [82]. These cells were a kind gift of Prof. Daniela Uberti from the University of Brescia.

Stably transfected cells expressing either the APPwt or the APPmut construct were

maintained in SH-SY5Y medium added with G418 at a final concentration of 600 $\mu\text{g mL}^{-1}$.

4.1.5 Cell Treatment and Cytotoxicity Assay

Cell viability was evaluated with the 3-(4,5-dimethylthiazol-2-yl)-2,5-diphenyltetrazolium bromide assay (MTT) [221]. Upon 6 h and 24 h treatment with increasing concentrations (0-10 μM) of C1, C2, and C3 dissolved in DMSO, cells were washed in PBS, pH 7.5, and then MTT (final concentration 0.5 mg mL^{-1}) was added to the culture medium without FBS and incubated for 2 h at 37 °C. The medium was then removed and replaced with 100 μL of DMSO. The optical density was measured at 550 nm in a microtiter plate reader. At least six cultures were utilized for each time point. Neuroblastoma cells, control and transfected cells, were then treated with C1, C2, and C3 for 6 and 24 h at the concentrations 0–1–5 μM . Compounds were dissolved in DMSO and then added to cell culture media. Control cells were included in each time point. After removing the medium and washing with cold phosphate buffered saline (PBS), cells were harvested in 4 mL of PBS and centrifuged at 1600 $\times g$ for 5 min. The pellet was resuspended in lysis buffer (20 mM Tris, pH 7.4, 250 mM sucrose, 1 mM EDTA, and 5 mM β -mercaptoethanol) and passed through a 29-gauge needle at least ten times. Lysates were centrifuged at 12 000 $\times g$ for 15 min and the supernatants were stored at -80°C until use. Protein concentration was determined by the method of Bradford using bovine serum albumin (BSA) as standard [167].

4.1.6 Proteasome Activity

The effects on the proteasome system were evaluated through fluorimetric assays, as previously reported [222], using the following synthetic substrates: Leu-Leu-Val-Tyr-AMC for ChT-L, Leu-Ser-Thr-Arg-AMC for T-L, Leu-Leu-Glu-AMC for PGPH, and Gly-Pro-Ala-Leu-Ala-AMC for BrAAP, whose test is performed with the addition of the aminopeptidase-N (AP-N). The incubation mixture contained 1 μ g of cell lysate, the appropriate substrate, and 50 mM Tris/HCl pH 8.0, up to a final volume of 100 μ L. Incubation was performed at 37 °C, and after 60 min, the fluorescence of the hydrolyzed 7-amino-4-methyl-coumarin (AMC) was recorded (AMC, λ_{exc} = 365 nm, λ_{em} = 449 nm) on a SpectraMax Gemini XPS microplate reader. The 26S proteasome ChT-L activity was tested using Suc-Leu-Leu-Val-Tyr-AMC as substrate and 50 mM Tris/HCl pH 8.0 buffer containing 10 mM MgCl₂, 1 mM dithiothreitol, and 2 mM ATP. The effective 20S proteasome contribution to short peptide cleavage was evaluated with control experiments performed using specific proteasome inhibitors, Z-Gly-Pro-Phe-Leu-CHO and lactacystin (5 μ M in the reaction mixture). The fluorescence values of lysates were subtracted of the values of control assays in the presence of the two inhibitors.

4.1.7 Cathepsin B Activity

Cathepsin B proteolytic activity was measured using the fluorogenic peptide Z-Arg-Arg-AMC at a final concentration of 50 μ M, as previously described [82]. The mixture for cathepsin B, containing 1 μ g of cell lysate, was pre-incubated in 100 mM phosphate

buffer pH 6.0, 1 mM EDTA, and 2 mM dithiothreitol for 5 min at 30°C. Upon the addition of the substrate, the mixture was incubated for 15 min at 30°C. The fluorescent signal released by the hydrolyzed 7-amino-4-methyl-coumarin (AMC, $\lambda_{exc} = 365$ nm, $\lambda_{em} = 449$ nm) was detected on a SpectraMax Gemini XPS microplate reader.

4.1.8 Western Blotting Analysis

Proteins were resolved on SDS-PAGE and electroblotted onto PVDF membranes. Membranes with transferred proteins were incubated with the primary monoclonal antibody and successively with the specific peroxidase conjugated secondary antibody. Monoclonal antibodies against Ub and p27 were obtained from Santa Cruz Biotechnology, Inc. (Heidelberg, Germany). SQSTM1/p62 (sequestosome 1, herein p62) mouse monoclonal antibody was from Sigma-Aldrich S.r.L. (Milano, Italy) and the anti-LC3B antibody was purchased from Cell Signaling Technology, Inc. The immunoblot detection was performed with ECL Western blotting detection reagents using a ChemiDoc MP system. Each gel was loaded with molecular weight markers in the range of 12 to 225 kDa (GE Healthcare). Glyceraldehyde-3-phosphate dehydrogenase (GAPDH) was utilized as a control for equal protein loading: membranes were stripped and re-probed with anti-GAPDH monoclonal antibody (Santa Cruz Biotechnology, Heidelberg, Germany). Stripping buffer contained 200 mM glycine, 0.1% SDS, and 1% Tween 20. Immunoblot images were quantified using ImageJ 1.52p software (NIH, USA).

4.1.9 Monodansylcadaverine Assay

Upon treatment with PVLs, the formation of autophagic vacuoles was monitored with monodansylcadaverine assay (MDC, Sigma-Aldrich S.r.L. Milano, Italy). In detail, 1 μ M MDC was added to cell medium. After 10 min incubation at 37 °C, cells were washed three times with phosphate buffered solution (PBS) and immediately analyzed with a fluorescence microscope (Olympus IX71).

4.1.10 Quantification of A β (1-42)

Levels of A β (1-42) secreted into the medium and present in cellular extracts were determined after PVLs treatment using the Human A β 42 solid-phase sandwich ELISA Kit from Invitrogen, following the manufacturer's instructions. For A β quantification in cell medium, culture medium was collected after neuronal cells treatment, centrifuged at 300 \times g for 10 min to remove non adherent cells and debris and then treated with protease inhibitors.

4.1.11 Statistical Analysis

Data are expressed as mean values \pm S.D. Statistical analysis was performed with one way ANOVA, followed by the Bonferroni post hoc test using Sigma-stat 3.1 software (SPSS, Chicago, IL, USA) and $p < 0.05$ was considered statistically significant.

4.2 Results

4.2.1 Effects of PVLs on Isolated Proteasomes Activity

PVLs were first tested on isolated constitutive and immunoproteasomes purified from bovine brain and thymus, respectively. The constitutive 20S proteasome is a barrel-shaped complex of four stacked rings, made of seven α subunits in the two outer rings and seven β subunits in the two inner rings, the latter bearing the catalytically active sites in the $\beta 1$, $\beta 2$, and $\beta 5$ subunits. Treatment with inflammatory cytokines induces the transcription of three additional active subunits, known as $\beta 1i$, $\beta 2i$, and $\beta 5i$, that replace constitutive homologues during proteasome assembly [80]. Proteasome proteolytic activities depend on the hydroxyl group of the N-terminal threonine (Thr-1) residue, responsible for cleaving peptides through a nucleophilic attack [223].

Increasing concentrations of the PVLs (0-10 μM in DMSO) were used in the fluorescent assays, as described in materials and methods. An evident inhibitory effect on the catalytic components of the two enzymes, namely the ChT-L (associated with the $\beta 5$ subunit), T-L ($\beta 2$ subunit), PGPH ($\beta 1$ subunit), and BrAAP ($\beta 5$ subunit), was observed, with the highest tested concentration inducing an almost complete inhibition. As reported in Table 1, the three PVLs showed a subunit-dependent specificity of inhibition. Considering the constitutive proteasome, C1 and C3 were particularly effective in inhibiting the T-L component whereas C2 showed the highest inhibitory effect toward the ChT-L. Globally, the catalytic components of the constitutive proteasome were more susceptible to the action of the three PVLs, showing lower

IC₅₀ values (down the nanomolar range) compared to the values obtained for the components of the immunoproteasome. The only exception was the BrAAP activity, whose inhibition was more evident in the immunoproteasome (see Table 1).

Table 1. IC₅₀ values obtained from in vitro activity assays on isolated proteasomes

	IC ₅₀ [μM]		IC ₅₀ [μM]	
	ChT-L		T-L	
	Constitutive proteasome	Immunoproteasome	Constitutive proteasome	Immunoproteasome
C1	0.1196 ± 0.0121	0.1258 ± 0.0113	0.0130 ± 0.0021	0.2272 ± 0.0132 ^{##}
C2	0.0162 ± 0.0012 ^{**}	0.2379 ± 0.0167 ^{*,##}	0.0874 ± 0.0079 ^{**}	0.3344 ± 0.0289 ^{*,#}
C3	0.1090 ± 0.0110	1.4520 ± 0.1530 ^{**,##}	0.0568 ± 0.0023 [*]	0.5876 ± 0.0476 ^{*,##}

	PGPH		BrAAP	
	Constitutive proteasome	Immunoproteasome	Constitutive proteasome	Immunoproteasome
	C1	0.0628 ± 0.0587	0.0418 ± 0.0038	0.2427 ± 0.0201
C2	0.0858 ± 0.0078	0.1136 ± 0.0197 ^{*,#}	0.2558 ± 0.0144	0.0613 ± 0.0057 ^{*,#}
C3	0.1044 ± 0.0110	0.0727 ± 0.0057 ^{*,#}	0.3024 ± 0.0278 [*]	0.0884 ± 0.0070 ^{*,#}

Asterisks refer to statistically significant differences obtained comparing C1 effects with C2/C3 effects on constitutive proteasomes or immunoproteasomes, respectively. Hashtags refer to statistically significant differences obtained comparing the effects of a single metabolite on the constitutive and immunoproteasome. ^{*},[#]*p* < 0.05, ^{**},^{##}*p* < 0.01.

4.2.2 Effects of PVLs on Neuronal Cells Proteasomes

Next, SH-SY5Y control and transfected cells were exposed to increasing concentration of PVLs (0-10 μM) and viability was checked with the MTT assay. No cytotoxic effect was detected, with only a minor reduction in the number of APPmut viable cells upon 24 h exposure to 10 μM C2 (data not shown). Neuronal cells were then treated with 1 and 5 μM of each PVLs for 6 and 24 h.

The effects of the three compounds on the functionality of the proteasomal system, both the 20S core and the 26S proteasome, the latter consisting of a 20S core and one or two 19S regulatory particles, were then evaluated with fluorometric tests and immunoassays (Fig. 27). The inhibitory activity previously observed on isolated complexes was confirmed in the assays on cellular lysates. In detail, the metabolites induced the most remarkable effect upon 24h exposure displaying a concentration- and subunit-dependent pattern of proteasome inhibition, with the BrAAP activity being the least affected (Figures 28, 29, and 30). Among the three tested compounds, the dihydroxylated metabolite C2 was the least efficient whereas C1 and C3 displayed a similar behavior strongly altering the functionality of the enzymatic complex, mainly the ChT-L component of both the 20S and 26S proteasome (C1: 30% ChT-L residual activity for both enzymes, C3: 50 and 60% ChT-L residual activity for the 20S and 26S proteasome, respectively). Interestingly, the presence of the wt or mut APP sequence influenced the results and APPmut cells showed the highest extent of proteasomal inhibition. The inhibitory effect of the PVLs was confirmed by immunodetection of two proteasome cellular substrates, ubiquitin-protein conjugates and p27. As shown in Figures 31 and 32, no particular effect was observed upon 6 h exposure to C1, C2 and C3 whereas an evident increase in the levels of both Ub-conjugates and p27 was obtained upon 24 h treatment, mainly in APPmut cells exposed to C1, confirming the data observed in the fluorescent assays. Together, these data show that these metabolites strongly affect proteasome functionality, selectively inhibiting its catalytic

activity and favoring the accumulation of its related substrates.

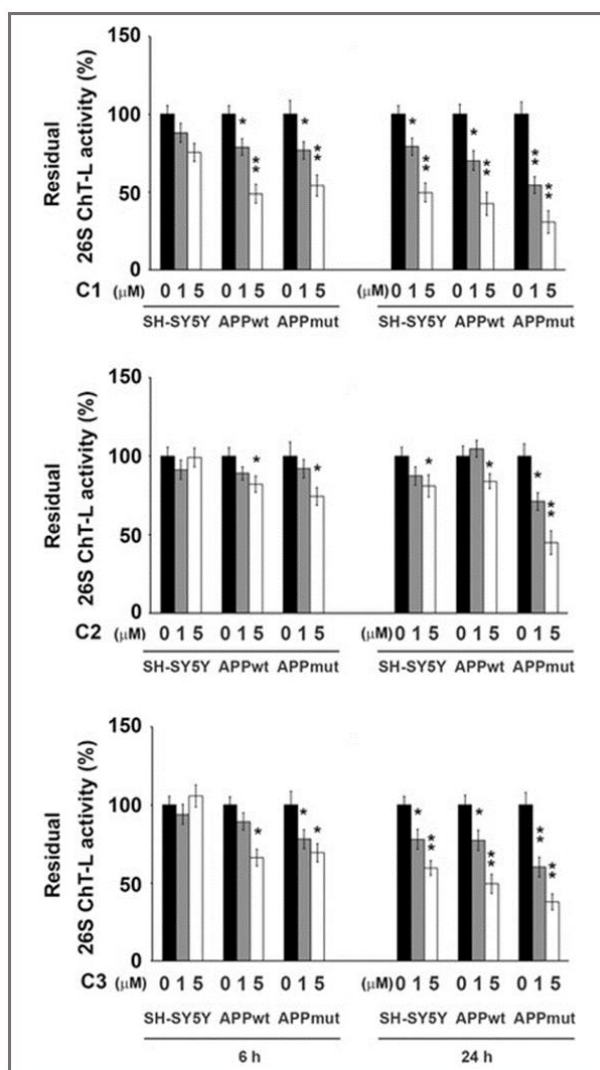


Figure 27. ChT-L activity of the 26S proteasome measured in control and transfected SH-SY5Y cells upon 6 and 24 h exposure to the three tested PVLs (C1, C2, and C3). Activities were measured using a fluorogenic peptide as a substrate as described in the Materials and methods section. Data are indicated as percentage versus untreated control/transfected cells (* $p < 0.05$, ** $p < 0.01$).

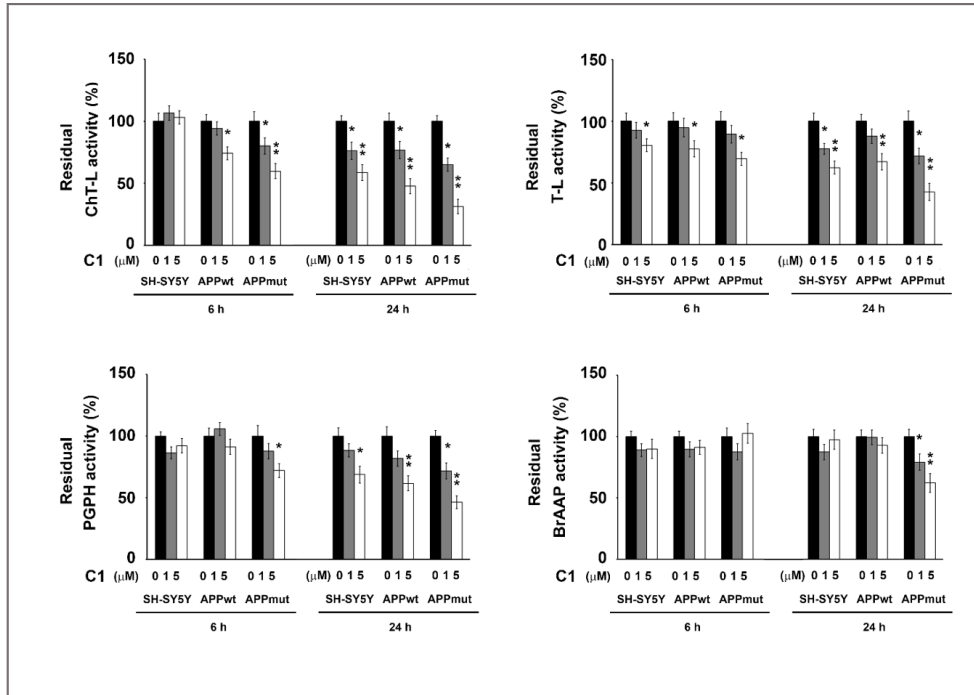


Figure 28. Proteasome ChT-L, T-L, PGPH and BrAAP activities measured in control and transfected SH-SY5Y cells upon 6 and 24 h exposure to C1. Activities were measured using a fluorogenic peptide as a substrate as described in the Materials and methods section. Data are indicated as percentage vs. untreated control/transfected cells (* $p < 0.05$, ** $p < 0.01$).

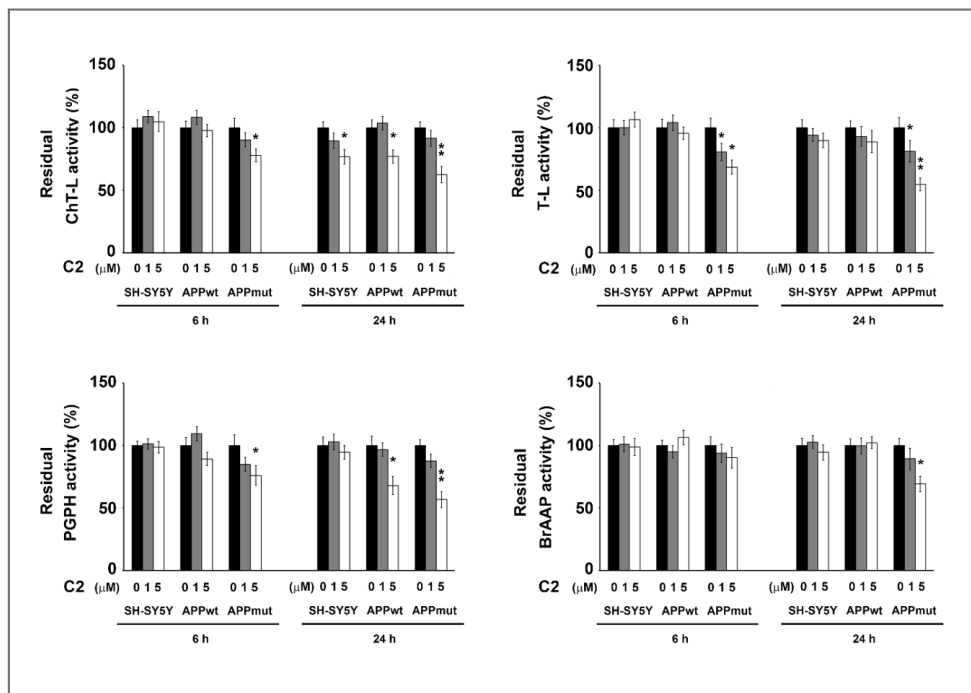


Figure 29. Proteasome ChT-L, T-L, PGPH and BrAAP activities measured in control and transfected SH-SY5Y cells upon 6 and 24 h exposure to C2. Activities were measured using a fluorogenic peptide as a substrate as described in the Materials and methods section. Data are indicated as percentage vs. untreated control/transfected cells ($*p < 0.05$, $**p < 0.01$).

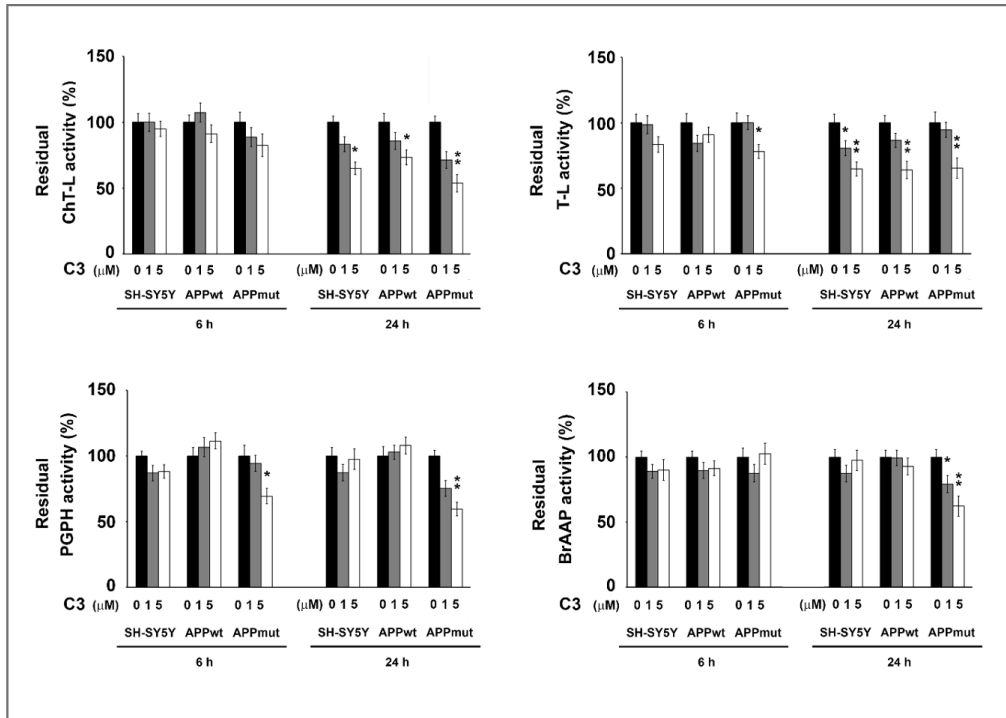


Figure 30. Proteasome ChT-L, T-L, PGPH and BrAAP activities measured in control and transfected SH-SY5Y cells upon 6 and 24 h exposure to C3. Activities were measured using a fluorogenic peptide as a substrate as described in the Materials and methods section. Data are indicated as percentage vs. untreated control/transfected cells ($*p < 0.05$, $**p < 0.01$).

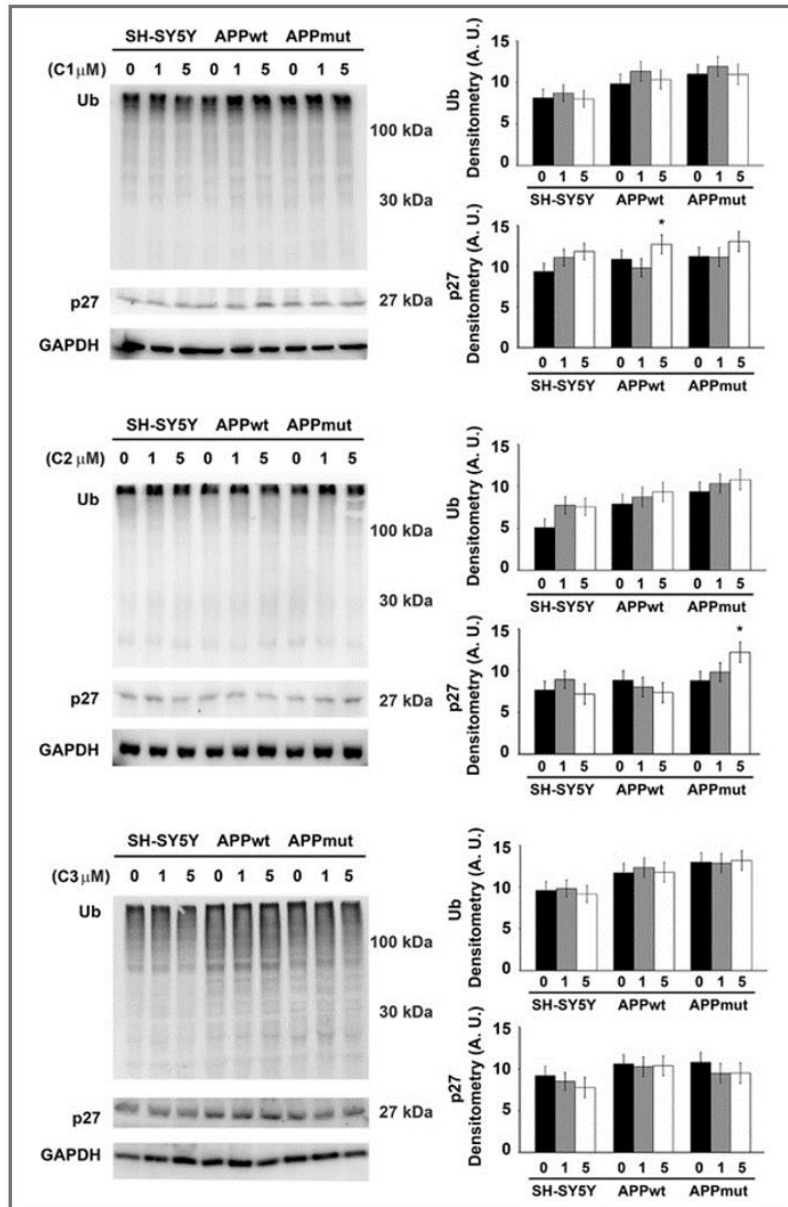


Figure 31. p27 and ubiquitin-conjugates detected in control and transfected SH-SY5Y cells upon 6 h exposure to PVLs. Representative immunoblots and densitometric analyses obtained from five separate experiments are shown (A.U. arbitrary units). Equal protein loading was verified by using an anti-GAPDH antibody. Data points marked with an asterisk are statistically significant compared to the respective untreated cell line (* $p < 0.05$).

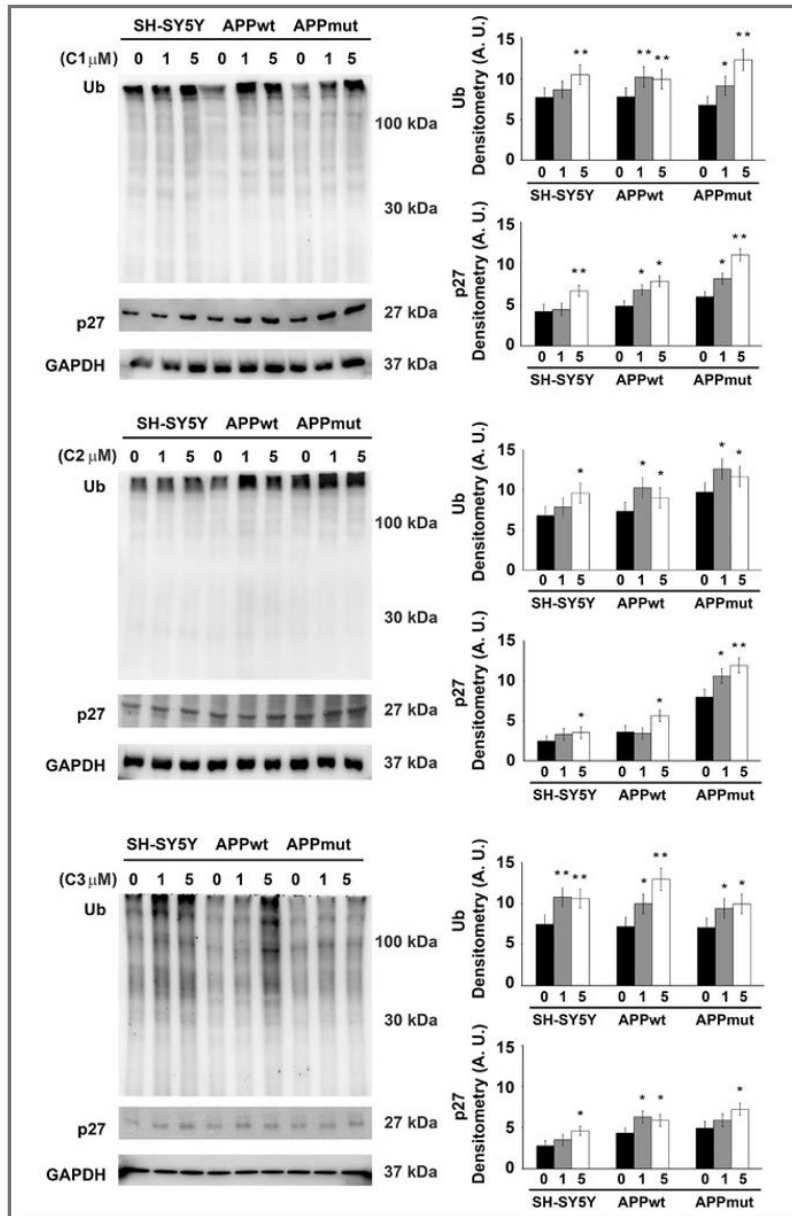


Figure 32. p27 and ubiquitin-conjugates detected in SH-SY5Y control and transfected cells upon 24 h exposure to PVLs. Representative immunoblots and densitometric analyses obtained from five separate experiments are shown (A.U. arbitrary units). Equal protein loading was verified by using an anti-GAPDH antibody. Data points marked with an asterisk are statistically significant compared to the respective untreated cell line (* $p < 0.05$, ** $p < 0.01$).

In silico analyses were also conducted to dissect the mechanisms that mediate the interaction between the active site of the enzyme and the metabolites and to explain the

observed inhibitory trend. The compounds of interest showed moderate binding affinities for proteasome catalytic subunits, with predicted equilibrium constants in the range 3–23 μM and a general conserved trend ($\text{C1} > \text{C2} > \text{C3}$). K_{D} values and energy contributions are summarized in Table 2A and 2B.

Table 2. Computationally predicted affinities and energy contribution values for the complexes formed between human constitutive 20S proteasome catalytic subunits and C1, C2, and C3

A	Compound	$K_{\text{D,pred}}$ [μM]	ΔG [kcal mol^{-1}]	T. Energy [kcal mol^{-1}]	I. Energy [kcal mol^{-1}]	vdW Energy [kcal mol^{-1}]	Electrostatic Energy [kcal mol^{-1}]	Thr-1-Lactone distance [\AA]
$\beta 1$	C1	3.3	-7.475	-7.22	-23.971	-15.386	-8.585	6.8
	C2	19.09	-6.435	-6.754	-23.422	-10.742	-14.044	7.3
	C3	22.87	-6.328	-6.213	-26.784	-3.132	-24.939	6.9
$\beta 2$	C1	7.12	-7.019	-19.119	-26.17	-13.22	-12.95	3.9
	C2	9.02	-6.879	-6.001	-24.086	-10.042	-14.044	4.5
	C3	12.86	-6.669	-6.931	-28.253	-3.314	-24.939	6.9
$\beta 5$	C1	8.9	-6.887	-23.549	-32.468	-1.96	-30.508	6.9
	C2	12.43	-6.689	-7.364	-23.271	-2.321	-20.95	7.5
	C3	21.3	-6.37	-9.559	-30.029	4.666	-34.695	6.2

B	Compound	$K_{\text{D,pred}}$ [μM]	ΔG [kcal mol^{-1}]	T. Energy [kcal mol^{-1}]	I. Energy [kcal mol^{-1}]	vdW Energy [kcal mol^{-1}]	Electrostatic Energy [kcal mol^{-1}]	Thr-1-Lactone distance [\AA]
$\beta 1i$	C1	7.959	-6.953	-19.898	-27.529	-13.506	-14.023	8.8
	C2	8.067	-6.945	-4.830	-21.318	-9.904	-11.414	6.1
	C3	22.87	-6.328	-5.438	-21.534	-0.924	-20.610	5.2
$\beta 2i$	C1	9.487	-6.849	-22.519	-29.889	-8.034	-21.855	8.6
	C2	16.84	-6.509	-8.364	-24.732	-3.414	-21.318	8.6
	C3	16.87	-6.508	-12.007	-33.114	-1.473	-31.641	5.3
$\beta 5i$	C1	5.973	-7.123	-25.270	-32.410	-12.876	-19.534	5.6
	C2	10.91	-6.766	-11.075	-28.657	-11.490	-17.167	5.9
	C3	10.99	-6.762	-13.963	-37.543	-8.997	-28.546	7.0

A, constitutive proteasome subunits; B, immunoproteasome subunits.

Structurally, these molecules were predicted to establish a variable number of H-bonds with amino acid residues in close proximity to the proteasome catalytic sites, with the carbonyl group of the lactone ring being always favorably positioned for a nucleophilic attack by the proteasome catalytic Thr-1 residue, resulting in the opening of the γ -lactone ring and acylation of the hydroxyl group, as expected for candidate proteasome

inhibitors carrying lactone moieties [224] (Figures 33 and 34), and as supported by covalent docking analysis (Fig. 35). Interestingly, the predicted distances between the hydroxyl group of Thr-1 and the carbonyl group of the lactone and the consequent different tendency to form a covalent bond (more than the calculated binding affinity values) were in agreement with the general higher inhibitory effect toward constitutive proteasome observed in the *in vitro* studies, in particular with T-L and BrAAP activities of constitutive and immuno-proteasomes, respectively.

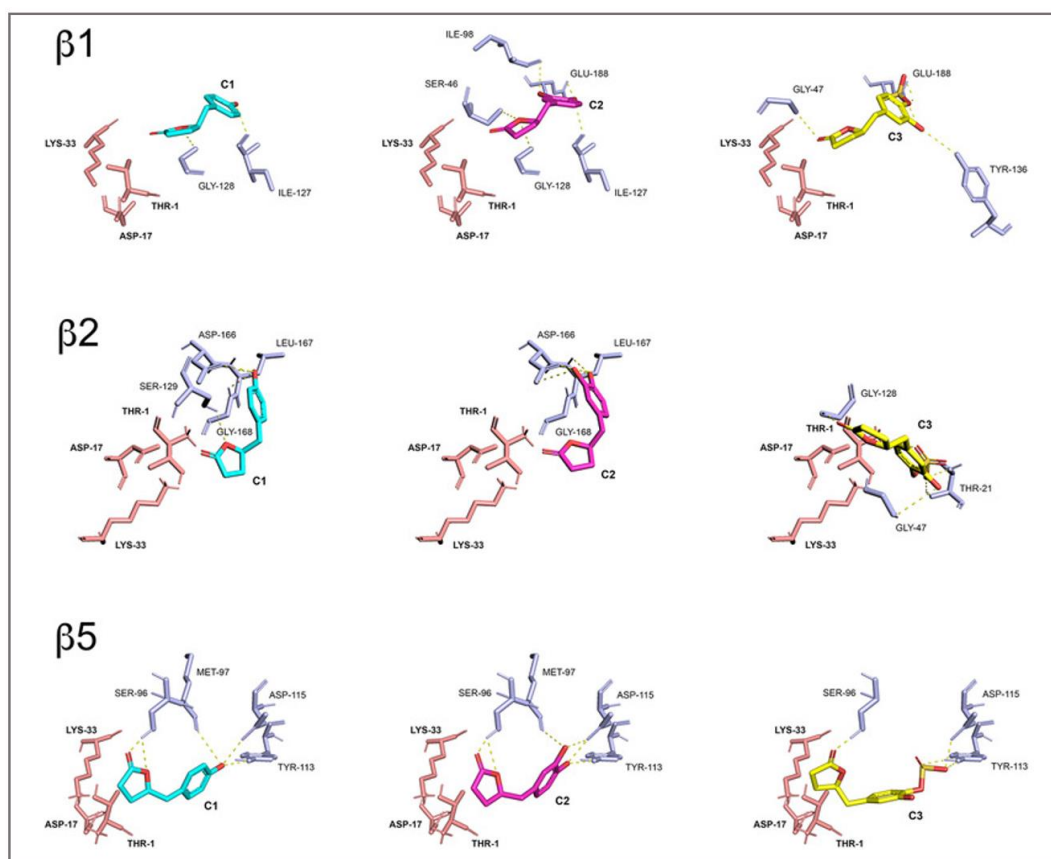


Figure 33. Comparative visualization of computed binding modes of PVLs C1, C2, and C3 to $\beta 1$, $\beta 2$, and $\beta 5$ subunits of human constitutive 20S proteasome (pdb ID: 6rgq). Only the catalytic residues (Thr-1, Asp-17 and Lys-33) and other residues in close proximity to the active site that are directly involved in the formation of H-bonds are displayed as pink and light blue sticks, respectively. H-bonds are indicated as yellow dashed solid lines.

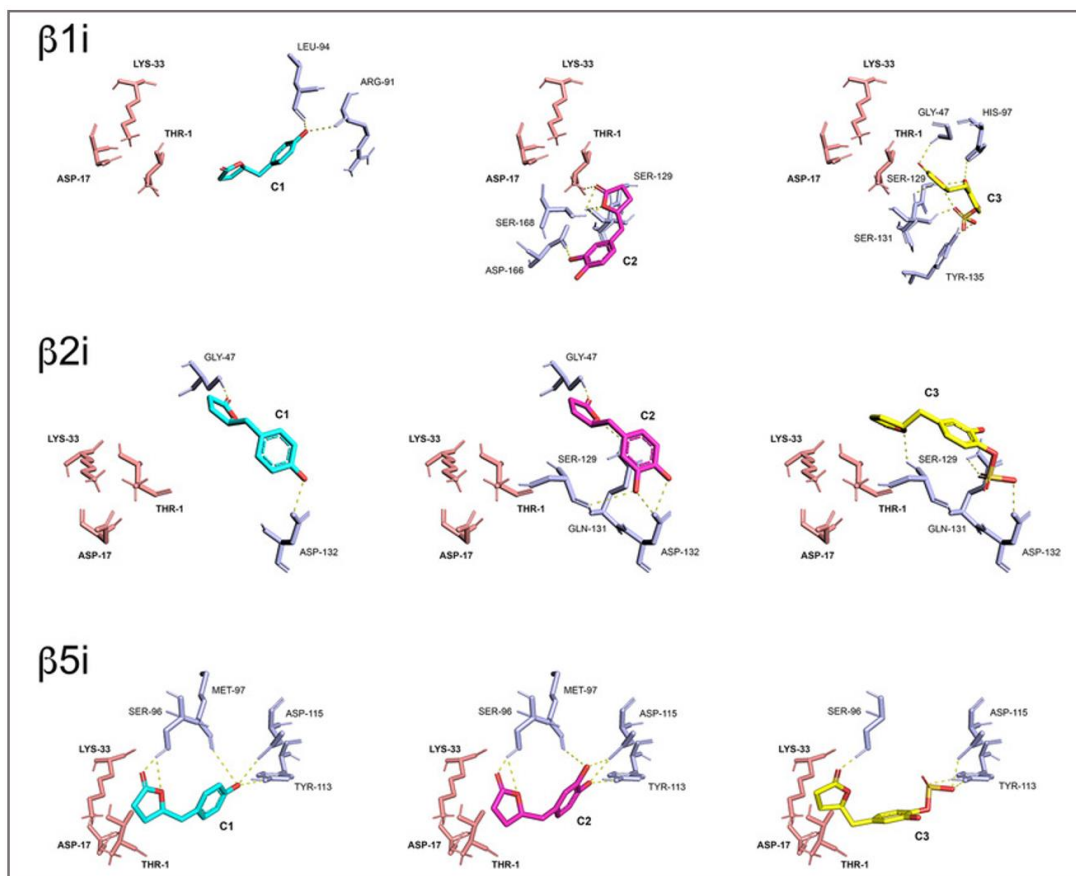


Figure 34. Comparative visualization of computed binding modes of PVLs C1, C2, and C3 to $\beta 1i$, $\beta 2i$, and $\beta 5i$ subunits of human immunoproteasome (pdb ID: 6e5b). Only the catalytic residues (Thr-1, Asp-17, and Lys-33) and other residues in close proximity to the active site that are directly involved in the formation of H-bonds are displayed as pink and light blue sticks, respectively. H-bonds are indicated as yellow dashed solid lines.

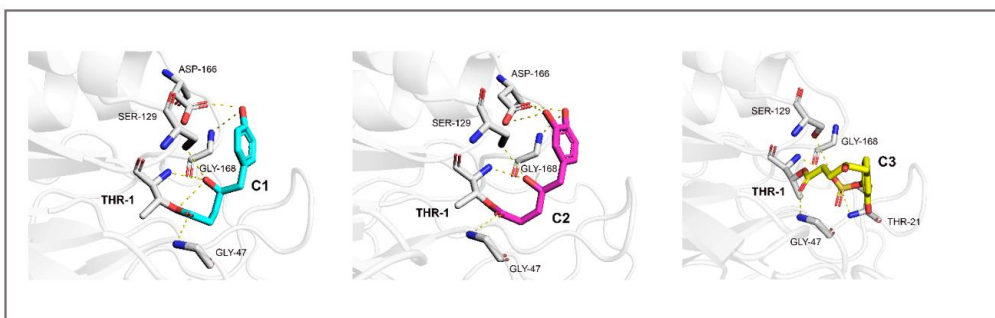


Figure 35. Binding models of C1, C2 and C3 bound to Thr-1 catalytic residue of constitutive 20S proteasome. Covalent docking was performed using Dockcovalent (Covalent docking of large libraries for the discovery of chemical probes. Nir London, Rand M Miller, Shyam Krishnan, Kenji Uchida, John J Irwin, Oliv Eidam, Lucie Gibold, Peter Cimermančič, Richard Bonnet, Brian K Shoichet & Jack Taunton *Nature Chemical Biology* volume 10, pages 1066–1072(2014)). Amino acids involved in the formation of covalent and H-bonds are highlighted as sticks.

4.2.3 Effects of PVLs on the Autophagic Pathway

Together with the proteasome, autophagy represents a major quality control system responsible for the maintenance of cellular homeostasis. The effect on autophagy of the three PVLs was evaluated measuring the expression of proteins involved in this pathway, such as LC3II, the lipidated form of LC3 that localizes in autophagosomal membranes, and p62, a substrate of autophagy that accumulates in cells when autophagy is inhibited [81]. Upon 6 h treatment with the three metabolites (1 and 5 μ M), SH-SY5Y control cells showed increased levels of LC3II but almost no change in the expression of the p62 protein, suggesting the activation of the early steps of the autophagic pathway in this cell line (Fig. 36). A minor effect was observed at this time point in the two transfected clones, as LC3II increased in APPwt and APPmut cells

upon exposure to C2 and C1, respectively and no variations in p62 amounts were detectable. Interestingly, the 24 h treatment markedly modified the levels of both proteins not only in untransfected cells but also in APPmut cells, demonstrating the complete activation of autophagy with a significant downregulation of the p62 protein (Fig. 37). APPwt cells were the least sensible to the action of the compounds. In details, upon long-term exposure to the three PVLs, this clone showed increased levels of LC3II but only 5-(3'-hydroxyphenyl)- γ -valerolactone-4'-sulfate (C3) favored p62 degradation, suggesting the complete activation of autophagy. To further confirm data on the activation of the autophagic pathway, we measured the amounts of autophagic vacuoles staining PVLs-treated cells with the autofluorescent dye MDC [225]. Figure 38. shows the increased number of autophagosomes in the three cell lines treated for a period of 24 h with the PVLs of interest. Increased numbers of autophagic vacuoles were detected in all the treated cell lines, but they were particularly evident in normal SH-SY5Y and APPmut cells.

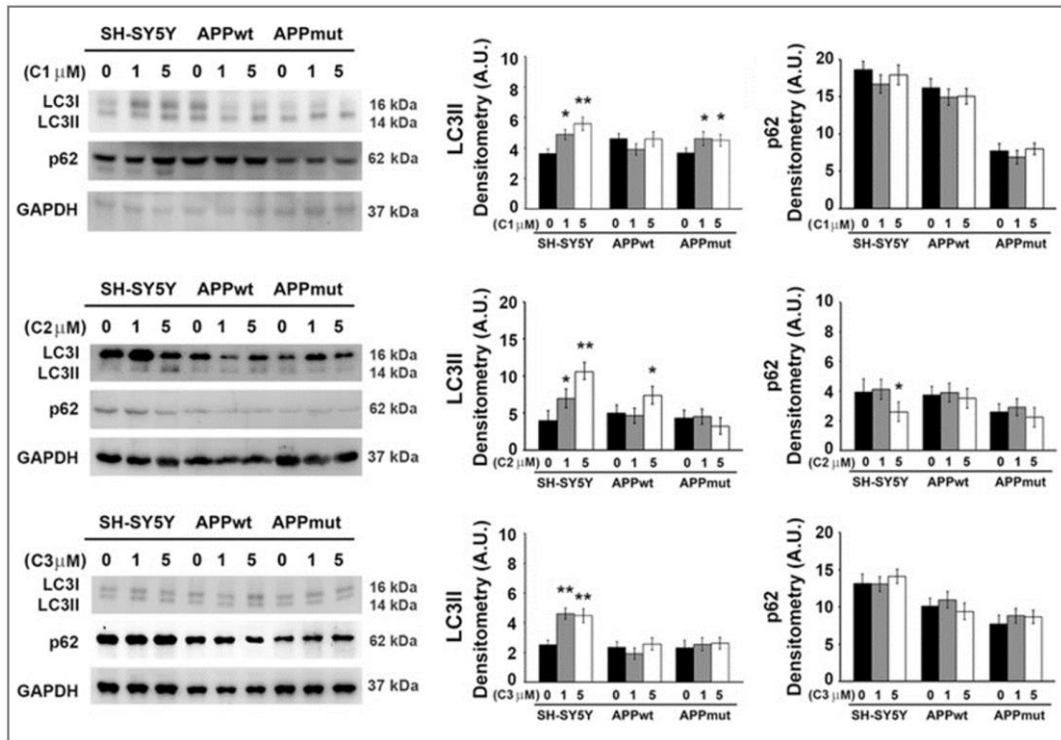


Figure 36. LC3II and p62 detected in SH-SY5Y control and transfected cells upon 6 h exposure to PVLs. Representative immunoblots and densitometric analyses obtained from five separate experiments are shown (A.U. arbitrary units). Equal protein loading was verified by using an anti-GAPDH antibody. Data points marked with an asterisk are statistically significant compared to the respective untreated cell line (* $p < 0.05$, ** $p < 0.01$).

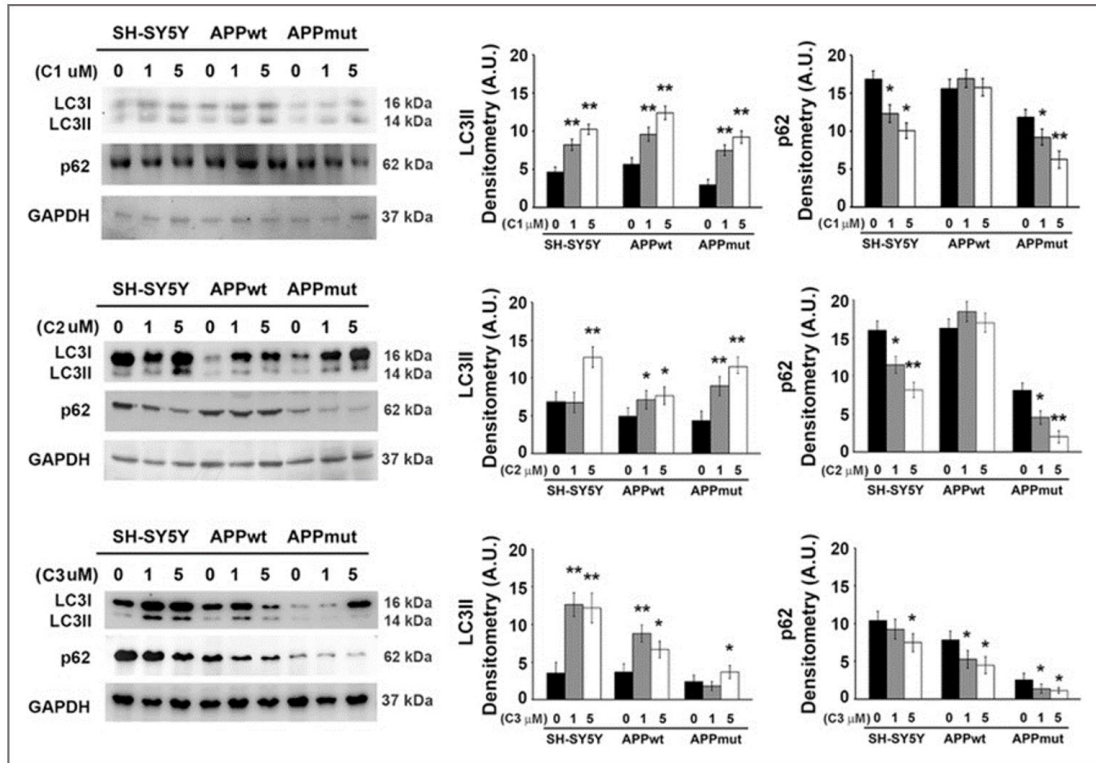


Figure 37. LC3II and p62 detected in SH-SY5Y control and transfected cells upon 24 h exposure to valerolactones. Representative immunoblots and densitometric analyses obtained from five separate experiments are shown (A.U. arbitrary units). Equal protein loading was verified by using an anti-GAPDH antibody. Data points marked with an asterisk are statistically significant compared to the respective untreated cell line (**p* < 0.05, ***p* < 0.01).

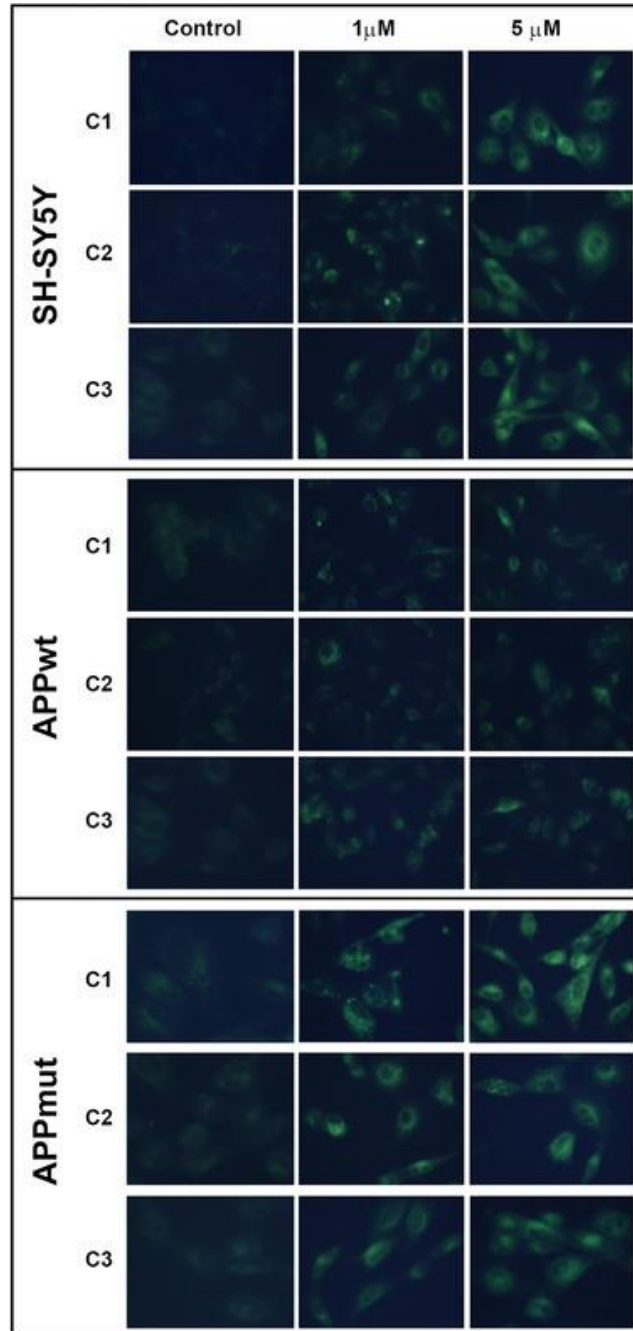


Figure 38. MDC staining of induced autophagic vacuoles in neuronal cells treated with C1, C2, and C3 (Control, 1 and 5 μ M). Cells were treated with PVLs for 24 h and then incubated with MDC dye as indicated in the Materials and methods section.

4.2.4 PVLs Effect on Cathepsin B Activity

Cathepsin B is a lysosomal cysteine protease that was shown to be upregulated in AD

subjects and to play a role in plaques formation and consequent behavioral deficits and neuropathology of AD [104]. We previously characterized the three cell lines in terms of cathepsin B activity, highlighting that it is strongly upregulated in APPmut cells, with no differences between APPwt cells and control neuronal cells [82]. Growing evidence suggests that cathepsin B inhibition is able to reduce A β levels [[105], [226], [227]]. Cathepsin B functionality was measured in cell lysates after the exposure to the three PVLs. Upon 6 h treatment, only APPmut cells showed an inhibited cathepsin B activity (20% inhibition upon 5 μ M C1 and C2 treatment and 30% inhibition upon 5 μ M C3 treatment), whereas after 24 h, a decreased functionality of the enzyme was observed also in control and APPwt cells (Figure 39, panel A). Similarly, a computational predictive study was conducted to characterize the interaction between C1, C2 and C3 and cathepsin B. This in silico analysis indicated interactions with moderate affinities (K_D in the range 1–5 μ M, with the same trend displayed for proteasome (Table 3)). Structurally, the valerolactones were predicted to establish H-bonds with amino acid residues of the active site cleft of the enzyme, the resulting binding pose being likely to prevent substrate access to the catalytic Cys-29 [228], consistently with our experimental evidence. Again, the lactone carbonyl was favorably positioned for a nucleophilic attack by the thiol group of Cys-29 (Figure 39, panel B), in line with the possible acylation of cysteine (Fig. 40) [229].

Table 3. Predictive affinities and energy contribution values for the complexes formed between human cathepsin B and C1, C2, and C3

Compound	$K_{D,pred}$ [μM]	ΔG [kcal mol ⁻¹]	T. Energy [kcal mol ⁻¹]	I. Energy [kcal mol ⁻¹]	vdW Energy [kcal mol ⁻¹]	Electrostatic Energy [kcal mol ⁻¹]	Cys-29-Lactone distance [\AA]
C1	1.61	-7.899	-10.161	-26.132	-20.005	-6.127	8.8
C2	4.26	-7.323	-11.223	-27.287	-12.506	-14.781	6.1
C3	5.53	-7.169	-25.500	-35.483	-15.572	-19.911	5.2

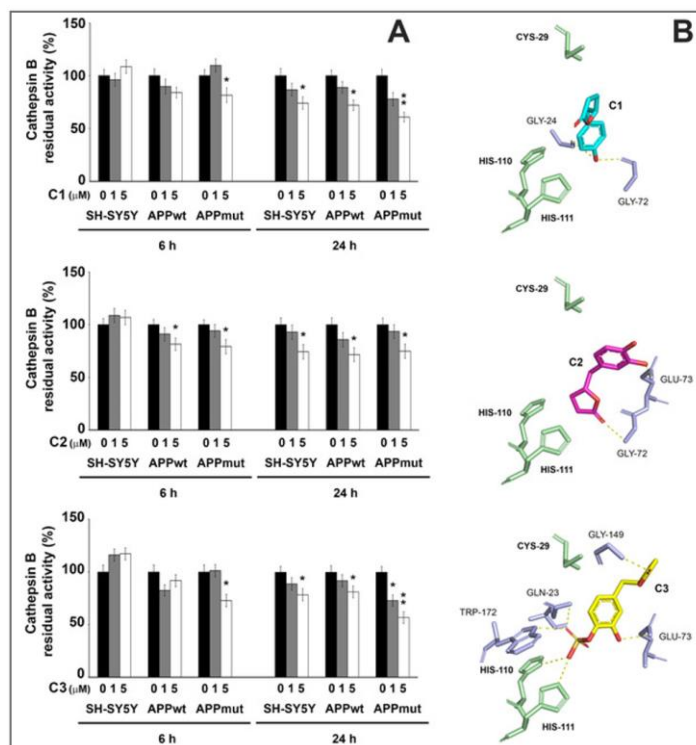


Figure 39. A) Cathepsin B activity measured in SH-SY5Y control and transfected cells upon 6 and 24-h exposure to PVLs. Activity was measured using a fluorogenic peptide as substrate as described in the Materials and Methods section. Data are indicated as percentage versus untreated control/transfected cells (* $p < 0.05$, ** $p < 0.01$). B) Comparative visualization of computed binding modes of valerolactones C1, C2, and C3 to human cathepsin B (pdb ID: 1csb). Only the residues involved in the catalysis (Cys-29, His-110, and His-111) and other residues in close proximity to the active site that are directly involved in the formation of H-bonds are displayed as light green and light blue sticks, respectively. H-bonds are indicated as yellow dashed solid lines.

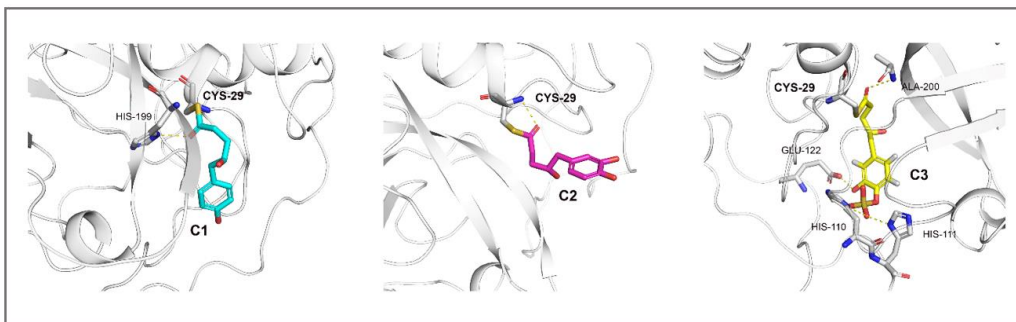


Figure 40. Binding models of C1, C2 and C3 bound to Cys-29 catalytic residue of cathepsin B. Covalent docking was performed using Dockcovalent (Covalent docking of large libraries for the discovery of chemical probes. Nir London, Rand M Miller, Shyam Krishnan, Kenji Uchida, John J Irwin, Oliv Eidam, Lucie Gibold, Peter Cimermančič, Richard Bonnet, Brian K Shoichet & Jack Taunton *Nature Chemical Biology* volume 10, pages 1066–1072(2014)). Amino acids involved in the formation of covalent and H-bonds are highlighted as sticks.

4.2.5 Amyloid- β (1-42) Levels Upon Exposure to PVLs

As previously reported, APPwt and APPmut clones show comparable APP expression levels, higher than control SH-SY5Y cells, and generate and release elevated amounts of A β (1-42) peptide in their culture media [82]. Furthermore, APPmut cells produced and released significant higher levels of A β (1-42) peptide than APPwt cells [230]. The levels of this peptide were detected both in the medium and cellular extracts of treated control and transfected SH-SY5Y cells using an ELISA kit.

PVLs treatment significantly reduced the amounts of intracellular and extracellular A β (1-42) with comparable final effects in the two tested samples. In detail, C3 was the most effective in reducing the amount of the toxic peptide in APPmut cells (35% reduction both in cell extracts and cell medium) (Fig. 41). The monohydroxylated

metabolite (C1) exerted similar effects on the three cell lines whereas C2, the less active among the three metabolites, did not induce any change in A β (1-42) levels in APPwt cells. Interestingly, these data on the amount of intracellular and released amyloid peptide reflect the activation of the autophagic pathway induced by the compounds with the exception of C1 and its effect on APPwt cells. In fact, although it was not able to completely activate autophagy in this cell line, it significantly reduced the amounts of A β (1-42) peptide.

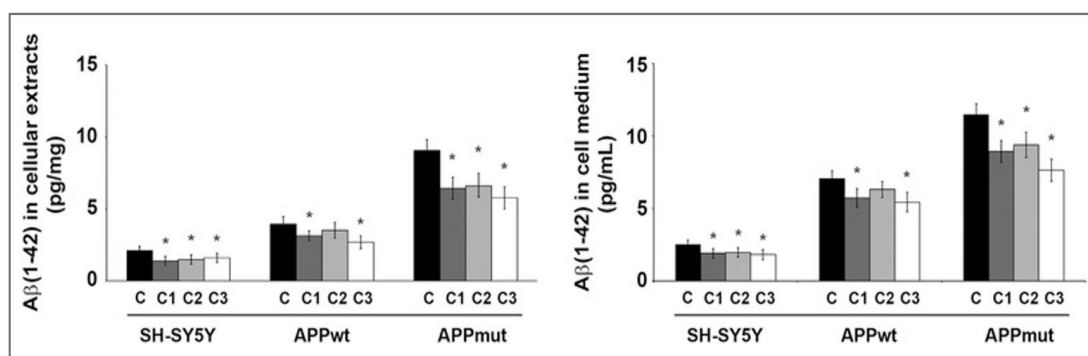


Figure 41. Levels of A β (1-42) measured in cellular extracts and cell medium upon 24 h treatment with C1, C2, and C3 (5 μ M). Protein levels were measured using an ELISA kit as described in the Materials and Methods section. Data are indicated as percentage versus untreated control/transfected cells (* p < 0.05, ** p < 0.01).

4.3 Discussion

Proteolytic systems principally responsible for protein quality control in neurons. Defective proteolytic pathways and accumulation of amyloid peptides in senile plaques characterize AD neuropathology. A proper modulation of intracellular proteolysis could therefore help in ameliorating AD pathology. On this regard, dietary polyphenols and their derivatives, besides the antioxidant and anti-inflammatory activity, were reported to regulate proteolysis and to act as anti-amyloid agents, making them interesting candidates in preventative strategies against AD [231]. An increasing number of studies is now dissecting the biological properties of PVLs, products of intestinal microbial metabolism of flavan-3-ols, that constitute a rich portion of phenolic metabolites in the circulation of subjects exposed to the widely spread dietary sources of this subclass of compounds [161].

In this study, we investigated the ability of three PVLs to modulate proteolysis in SH-SY5Y neuronal cells and to counteract the production and release of the toxic A β (1-42) peptide, at levels readily achievable in body fluids upon moderate consumption of flavonoid-rich foods or beverages [[232], [233]]. In details, two microbial metabolites with different hydroxylation patterns, the 5-(4'-hydroxyphenyl)- γ -valerolactone and the 5-(3',4'-dihydroxyphenyl)- γ -valerolactone, and the conjugated derivative 5-(3'-hydroxyphenyl)- γ -valerolactone-4'-sulfate, were tested.

The three compounds similarly affected the functionality of isolated 20S proteasomes,

both the constitutive and the immunoproteasome, inducing an almost complete inhibition at the highest doses. They were particularly effective in inhibiting the catalytic subunits of the constitutive complex, with the exception of the BrAAP subunit that showed the highest inhibition in the immunoproteasome (Table 1). *In silico* computational studies better clarified the mechanisms behind the observed inhibitory trend (Table 2), underlining the central role of the lactone moiety, produced by the action of intestinal bacteria that open the C-ring of the flavan-3-ol precursor and convert it into the PVL [[234], [235]]. This group is likely to undergo a nucleophilic attack by the N-terminal threonine of the active site of proteasomes and covalently inhibits the enzyme, like previously reported for proteasome inhibitors carrying the same functional group [224] (Figures 33 and 34). This newly generated lactone group strongly increases the inhibitory potency of PVLs with respect to parental catechins such as (-)-epicatechin and EGCG [236].

We then treated human SH-SY5Y neuroblastoma cells, control and APPwt/APPmut transfected cells, with the three metabolites and evaluated their effects on cellular proteolysis. Previous studies from our laboratory indicated the presence of a less functional proteasome in APP transfected cells, mainly the APPmut clone [82]. PVLs inhibited the 20S and 26S complexes in a time- and subunit-dependent manner (Figures 27, 28, 29, 30, 31 and 32), with the monohydroxylated form (C1, 5-(4'-hydroxyphenyl)- γ -valerolactone) and the sulfated derivative (C3, 5-(3'-hydroxyphenyl)- γ -valerolactone-4'-sulfate) resulting the most effective. APPmut cells showed the highest

degree of proteasome inhibition likely due to an already compromised enzymatic complex, as a consequence of the higher amounts of amyloid peptides released. These results indicate that PVLs can act like proteasome modulators as widely reported for their flavan-3-ol precursors and other polyphenols [[237]–[240]]. While comparisons with other compounds may be biased by the different experimental settings, the prospects of these PVLs have been demonstrated. Further works should be designed to understand the relationship among these microbial-derived phenolic metabolites and phase II-conjugated flavan-3-ols able to cross the BBB, identifying the most active metabolites upon flavan-3-ol consumption, and investigating their synergistic, additive, and/or antagonistic effects occurring in presence of multiple metabolites.

The coordinated action of proteolytic systems is fundamental for protein quality control and for the maintenance of cellular homeostasis, especially in conditions where protein aggregates easily tend to accumulate. Numerous studies described a marked alteration of both the proteasome and autophagy in neurodegenerative diseases, including Parkinson's disease, Huntington's disease, amyotrophic lateral sclerosis, frontotemporal dementia, and AD, with these defects favoring aggregates-mediated toxicity [[240]–[243]]. Considering the complex and the dynamic nature of the autophagic pathway [82], we monitored several markers associated with different steps of this process. Our data show that PVLs treatment upregulated autophagy in the three cell lines, mainly in untransfected and APPmut cells, as shown by the increase in autophagosomes formation and the simultaneous reduction of p62 levels (Figures 37 and 38). The

complete activation of the autophagic process in these two cell lines was observed upon 24 h exposure whereas only SH-SY5Y control cells showed an increased amount of LC3II upon the short time treatment, suggesting an earlier response of untransfected cells to the treatment (Fig. 36). These findings indicate that the presence of the wild-type or mutated sequence of the APP influences the final effect of the metabolites on this proteolytic pathway. Among the tested compounds, only 5-(3'-hydroxyphenyl)- γ -valerolactone-4'-sulfate (C3) was able to trigger complete autophagy in APPwt cells.

We then dissected the effects of the three metabolites on cathepsin B activity. This enzyme was associated with the amyloidogenic APP processing and the consequent release of amyloid peptides [105] and we previously found that the expression of the V717G mutated sequence of APP in SH-SY5Y cells strongly elevated the activity of the hydrolase [82]. Our *in silico* and experimental data indicate that these PVLs can effectively inhibit the activity of this enzyme preventing the substrate access to the catalytic Cys-29 residue. The slight differences observed in cathepsin B inhibition between control and transfected cells suggest that the presence of the wt or mut APP sequence does not significantly alter the final effect of these metabolites on the protease (Figures 39 and 40).

Considering the ability of PVLs to modulate cellular proteolytic systems involved in A β generation and processing, we investigated possible effects on the production and release of the A β (1-42) peptide. Autophagy activation in response to inhibition of the

proteasome is frequently observed in cells and it is considered as a compensatory protective mechanism to guarantee the elimination of protein aggregates and alleviate associated proteotoxic stress [[98], [244], [245]]. This crosstalk between protein degradative pathways assumes a central role in neurodegenerations, including AD, and it was demonstrated to help neurons getting rid of detrimental A β (1-42) peptides [226]. In addition, it was demonstrated that cathepsin B exhibits β -secretase activity in secretory vesicles of neuronal chromaffin cells and that its inhibitors can lower amyloid levels produced from APP in guinea pigs, suggesting that a reduction in cathepsin B functionality can ameliorate AD condition [[104], [105], [227]]. In line with these observations, the three tested PVLs diminished the amounts of A β (1-42) in the medium and lysates of neuronal cells with the only exception of C2 that did not modify the levels of the toxic peptide in APPwt cells (Fig. 41). On this regard, metabolites C1 and C2 exhibited a comparable effect in this cell line showing a limited activity in upregulating autophagy and inducing a significant inhibition of cathepsin B functionality. It is therefore reasonable to think that, beyond cathepsin B inhibition, 5-(4'-hydroxyphenyl)- γ -valerolactone (C1) exerts its effect against amyloid peptides through additional mechanisms, likely involving other enzymes responsible for APP processing and amyloid production.

These results on the anti-amyloid and neuroprotective effects of the considered metabolites are in line with previous findings on PVLs ability to detoxify amyloid- β oligomers and prevent memory impairment [166]. Also relevant in this context are data

showing that these metabolites can cross the blood-brain barrier, reach the brain parenchyma and promote neurogenesis in the brain [[164], [165]]. Together, these data further confirm the beneficial role of a diet rich in catechins and proanthocyanidins, whose metabolites can successfully reduce the presence of molecular markers associated with the onset and progression of neurodegeneration.

In conclusion, our findings provide, for the first time, evidence for the neuroprotective activity of PVLs, microbiota-derived metabolites of flavan-3-ols, associated with the modulation of intracellular proteolytic systems and suggest their use in preventative strategies against AD. Future experiments should be performed to enrich the evidence gathered so far. In this regard, a better understanding of the journey of flavan-3-ol metabolites into the brain, addressing transportation mechanisms through the BBB, and taking into account their effects in the framework of animal models of AD may serve to provide effective, tailored dietary recommendations.

Chapter 5: Role of Astrocytes' proteolytic systems in Alzheimer's disease

5.1 Materials and methods

5.1.1 Reagents and Chemicals

The substrates Suc-Leu-Leu-Val-Tyr-7-Amino-4-methylcoumarin (AMC), Z-Leu-Ser-Thr-Arg-AMC, Z-Leu-Leu-Glu-AMC for assaying the chymotrypsin-like (ChT-L), trypsin-like (T-L), and peptidyl glutamyl-peptide hydrolyzing (PGPH) proteasomal activities were purchased from Sigma-Aldrich S.r.L. (Milano, Italy). The substrate Z-Gly-Pro-Ala-Leu-Ala-MCA to test the branched chain amino acids preferring (BrAAP) activity was obtained from Biomatik (Cambridge, Ontario). Aminopeptidase N (EC 3.4.11.2) for the coupled assay utilized to detect BrAAP activity was purified from pig kidney as reported elsewhere [214]. Cathepsin B and cathepsin L substrates (Z-Arg-Arg-AMC and Z-Phe-Arg-7-amino-4-trifluoromethyl-coumarin (AFC) respectively) and inhibitors (CA074Me and N-(1-Naphthalenylsulfonyl)-Ile-Trp-aldehyde) were obtained from Sigma-Aldrich S.r.L. (Milano, Italy). Media and chemicals used for cell cultures were purchased from Enzo Life Sciences, Inc. The membranes for western blot analyses were purchased from Millipore (Milan, Italy). Proteins immobilized on polyvinylidene fluoride membranes were detected with the enhanced chemiluminescence (ECL) technique (Amersham Pharmacia Biotech, Milan, Italy) on a ChemiDoc MP, Chemiluminescence system (Biorad, Italy).

5.1.2 Cell lines

Generation of immortalized astrocytes from hippocampi of WT and 3xTg-AD mice (WT-iAstro and 3Tg-iAstro cells) was described elsewhere [246]. Immortalized astrocytes were kindly provided by Prof. Dmitry Lim (University of Piemonte Orientale). iAstro lines were maintained in complete culture media containing Dulbecco's modified Eagle's medium (DMEM; Sigma-Aldrich, Cat. No. D5671) supplemented with 10% fetal bovine serum (Gibco, Cat. No. 10270), 2 mM L-glutamine (Sigma-Aldrich), and 1% penicillin/streptomycin solution (Sigma-Aldrich). Cells were incubated with growth medium at 37 °C equilibrated with 95% air and 5% CO₂ in flasks or dishes. Cells were passaged once a week and used for experiments between passages 12 and 20 from establishment [246].

5.1.3 Cell treatment with 4-phenil-butirric-acid (4-PBA)

WT-iAstro and 3Tg-iAstro cells were treated with 4-PBA (Sant Cruz Biotechnology, Cat. sc-232961) [[247], [248]] at a concentration of 3 μM for 48 h.

5.1.4 Cell lysis

After removing the medium and washing with cold phosphate buffered saline (PBS), cells were harvested in PBS and centrifuged at 1600 ×g for 5 min. The pellet was resuspended in a lysis buffer (20 mM Tris, pH 7.4, 250 mM sucrose, 1 mM EDTA and 5 mM β-mercaptoethanol) and passed through a 29-gauge needle at least ten times. Lysates were centrifuged at 12,000 ×g for 15 min and the supernatants were stored at

– 80 °C. Protein concentration was estimated by the method of Bradford [167] using bovine serum albumin (BSA) as standard.

5.1.5 Proteasome activities

Proteasome activities were measured in cell lysates through fluorimetric assays, as previously reported [222], using the following synthetic substrates: Leu-Leu-Val-Tyr-AMC for ChT-L, Leu-Ser-Thr-Arg-AMC for T-L, Leu-Leu-Glu-AMC for PGPH, and Gly-Pro-Ala-Leu-Ala-AMC for BrAAP, whose test is performed with the addition of the aminopeptidase-N (AP-N). The incubation mixture contained 1 µg of cell lysate, the appropriate substrate, and 50 mM Tris/HCl pH 8.0, up to a final volume of 100 µL. Incubation was performed at 37 °C, and after 60 min, the fluorescence of the hydrolyzed 7-amino-4-methyl-coumarin (AMC) was recorded (AMC, $\lambda_{exc} = 365$ nm, $\lambda_{em} = 449$ nm) on a SpectraMax Gemini XPS microplate reader (Molecular Devices, Sunnyvale, CA, USA). The 26S proteasome ChT-L activity was tested using Suc-Leu-Leu-Val-Tyr-AMC as substrate and 50 mM Tris/HCl pH 8.0 buffer containing 10 mM MgCl₂, 1 mM dithiothreitol, and 2 mM ATP. The effective 20S proteasome contribution to short peptide cleavage was evaluated with control experiments performed using specific proteasome inhibitors, Z-Gly-Pro-Phe-Leu-CHO and lactacystin (5 µM in the reaction mixture), and then subtracting the obtained fluorescence values from the values obtained in cell lysates.

5.1.6 Cathepsins activities

Cathepsin B and L proteolytic activities were measured in cell lysates following the protocol described by Tchoupè *et al.* [249] using the fluorogenic peptides Z-Arg-Arg-AMC and Z-Phe-Arg-AFC respectively, at a final concentration of 5 μ M. The mixture for cathepsin B, containing 7 μ g of protein lysate, was pre-incubated in 100 mM phosphate buffer pH 6.0, 1 mM EDTA and 2 mM dithiothreitol for 5 min at 30 °C. Upon the addition of the substrate, the mixture was incubated for 15 min at 30 °C. Similarly, the mixture for cathepsin L, containing 7 μ g of protein lysate, was incubated in 100 mM sodium acetate buffer pH 5.5, 1 mM EDTA and 2 mM 37 dithiothreitol for 5 min at 30 °C and, upon the addition of the substrate, the mixture was incubated for 15 min at 30 °C. The fluorescence of the hydrolyzed 7-amino-4-methyl-coumarin (AMC, λ_{exc} = 365 nm, λ_{em} = 449 nm) and 7-amino-4- trifluoromethylcoumarin (AFC, λ_{exc} = 397 nm, λ_{em} = 500 nm) was detected on a SpectraMax Gemini XPS microplate reader. The effective cathepsin contribution to the proteolysis was evaluated through control experiments performed using the specific inhibitor CA074Me and subtracting these values from the fluorescence values obtained by analyzing cell lysates.

5.1.7 Western blotting analysis

Cell lysates (20 μ g of total proteins) were resolved by 12% or 15% SDS/PAGE and electroblotted onto PVDF membranes. Membranes with transferred proteins were incubated with the specific primary monoclonal antibody and successively with the proper peroxidase conjugated secondary antibody. Monoclonal antibodies against

ubiquitin, $\beta 5$, $\beta 2$, and $\beta 1$ proteasomal subunits, Beclin-1, Nrf2 and Histone Deacetylase 6 (HDAC6) were obtained from Santa Cruz Biotechnology, Inc. (Heidelberg, Germany). Anti- $\beta 5i$, anti- $\beta 2i$, and anti- $\beta 1i$ rabbit monoclonal antibodies were from AFFINITI Research Products Ltd, (Mamhead, United Kingdom). SQSTM1/p62 (sequestosome 1/p62) mouse monoclonal antibody was from Sigma-Aldrich S.r.L. (Milano, Italy), and the anti-LC3B antibody and cathepsin B were purchased from Cell Signaling Technology, Inc. The immunoblot detection was performed with ECL western blotting detection reagents using a Biorad ChemiDoc MP system. Each gel was loaded with molecular weight markers in the range of 12 to 225 kDa (GE Healthcare).

Glyceraldehyde-3-phosphate dehydrogenase (GAPDH) and β -actin were utilized as controls for equal protein loading: membranes were stripped and re-probed with anti-GAPDH or anti β -actin monoclonal antibodies (Santa Cruz Biotechnology, Heidelberg, Germany). Stripping buffer contained 200 mM glycine, 0.1% SDS, and 1% Tween 20. ChemiDoc acquired immunoblot images were processed through Image J software (NIH, USA) to calculate the background mean value and its standard deviation. The background-free image was obtained subtracting the background intensity mean value from the original digital data. The integrated densitometric value associated with each band was then calculated as the sum of the density values over all the pixels belonging to the considered band having a density value higher than the background standard deviation. Each band densitometric value was normalized to the relative GAPDH or β -actin signal intensity. The ratios of band intensities were calculated within the same

Western blot. All the calculations were carried out using the Matlab environment (The MathWorks Inc., Natick, MA, USA).

5.1.8 Monodansylcadaverine Assay

Autophagy induction was assayed in both WT and 3Tg-iAstro with monodansylcadaverine (MDC, Sigma-Aldrich S.r.L. Milano, Italy) staining, using a fluorescent lysosomotropic compound that is incorporated into multilamellar bodies as a probe for labeling of autophagic vacuoles in cultured cells by fluorescence microscopy [225]. In detail, 6×10^5 cells/well were seeded into 6-well culture plates. Following overnight growth, 1 μ M MDC was added to cell medium. After 10 min incubation at 37 °C, cells were washed three times with phosphate buffered solution (PBS) and immediately analyzed with an Olympus IX71 fluorescence microscope, equipped with a 380–420 nm filter. At least five areas were scanned for each sample and images are representative of three distinct subgroups for both cell lines.

5.1.9 Statistical Analysis

Biochemical data is expressed as mean values \pm S.D. Statistical analysis was performed using the student's t-test or one-way ANOVA, followed by the Bonferroni test. *P*-Values $p < 0.05$ (*) and $p < 0.01$ (**) were considered to be statistically significant.

5.2 Results

5.2.1 26S proteasome functionality is impaired in 3Tg-iAstro

Cell lysates from both WT- and 3Tg-iAstro hippocampal astrocytes immortalized cultures were analyzed through enzymatic assays and western blotting analysis in order to monitor the functionality of the 26S proteasome and the intracellular levels of ubiquitin conjugates.

A markedly reduced proteasomal 26S ChT-L activity was observed in 3Tg-iAstro compared to WT astrocytes (40% reduction, Fig. 42A). Accordingly, Western blotting results showed higher levels of ubiquitinated substrates in 3Tg-iAstro compared to WT astrocytes (Fig. 42B). The nature of Ub-conjugates has not been determined, yet such results are in agreement with previous studies in which increased levels of Ub-proteins were demonstrated to correlate with inhibited proteasomal activity [[83], [84]]. As UPS is able to degrade soluble misfolded proteins or small oligomers, large protein aggregates prevent degradation and inhibit UPS activity [[242], [250]]. Overall, our data proves and confirms the impaired proteasomal activity in the immortalized hippocampal astrocytes from 3xTg- AD mice.

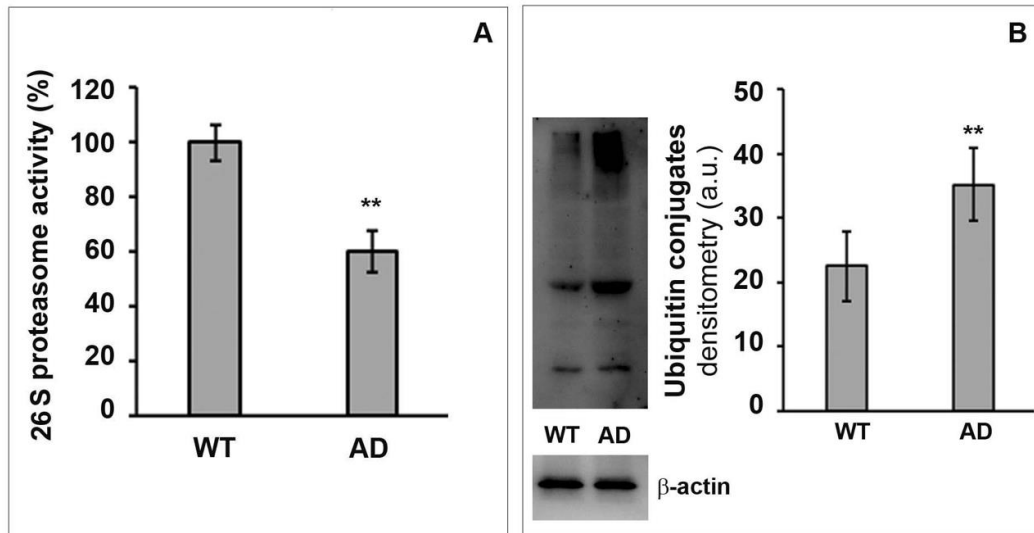


Figure 42. Deregulation of UPS in 3Tg-iAstro. 26S Proteasome activity in WT-iAstro (WT) and 3Tg-iAstro (AD) (panel A) and Ubiquitin conjugates quantization through western blotting (panel B). The densitometry from five separate blots and an immunoblot which is representative of three distinct cellular subgroups are reported. Equal protein loading was verified by using an anti- β -actin antibody and normalized expression of the target proteins is reported as arbitrary units (a.u.). Data points marked with asterisks are statistically significant compared to the WT counterpart (at the same passage number) (** $p < 0.01$) upon Student's t-test.

5.2.2 20S proteasome activities are down-regulated in hippocampal murine AD astrocytes

26S proteasome analysis provides an insight in the ATP-Ubiquitin-dependent protein degradation pathway, whereas 20S proteasome, lacking 19S regulatory subunits, is regulated by ubiquitin-independent mechanisms with a different target-specificity. Despite most of the research focusing on 26S proteasome, several works have demonstrated that the 20S proteasome is one of the cytoplasmic components that adapts to oxidative stress and promotes oxidized protein degradation [[251], [252]] preventing

the formation of protein aggregates. On this basis, the decreased activity trend we have observed suggest that AD cytoplasmic aggregates are able to block 26S proteasome but they can also block 20S proteasome independently from the ubiquitin post-translational modification.

20S proteasomal core catalytic activities were measured through enzymatic assays using specific synthetic fluorogenic substrates. In detail, 20S proteasomal chymotrypsin-like and trypsin-like activities, attributed to $\beta 5$ and $\beta 2$ respectively, were the most significantly decreased in 3Tg-iAstro compared to WT cells. The ability to cleave after branched-chain amino acids (BrAAP activity) showed a moderate decrease in AD astrocytes, whereas no significant difference was observed in PGPH activity, constitutively attributed to $\beta 1$ subunit (Fig. 43).

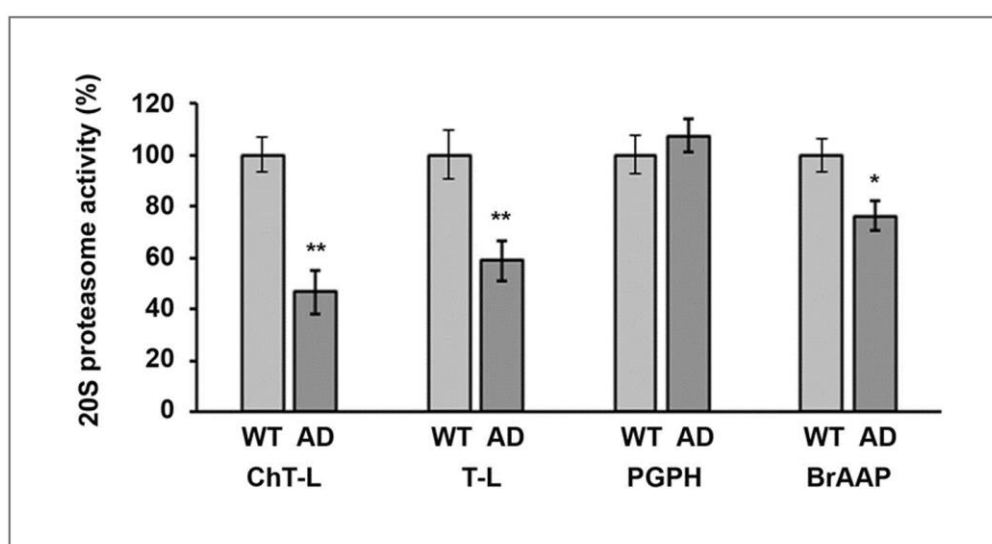


Figure 43. Decreased 20S proteasome activities in 3Tg-iAstro. 20S proteasomal activities were measured in WT-iAstro (WT) and 3Tg-iAstro (AD) immortalized hippocampal astrocytes through enzymatic assay as reported in Material and Methods section. From left to right chymotrypsin-like activity (ChT-L), trypsin-like activity (T-L), peptidyl-glutamyl peptide-hydrolyzing activity (PGPH) and branched-chain amino acid cleavage activity (BrAAP) of the 20S proteasome are reported. Activities are expressed as percentage of WT (data from three independent subgroups of both cell types at the same passage number). Data points marked with asterisks are statistically significant compared to the WT counterpart ($*p < 0.05$, $**p < 0.01$), upon Student's t-test.

5.2.3 Constitutive proteasome and immunoproteasome are differentially expressed in 3Tg-iAstro compared to WT-iAstro

After evaluating the activity levels of the 20S proteasome we performed a detailed analysis of the 20S proteasome subunits composition in the attempt to identify differently expresses constitutive and immune-proteasomes in the two cell types. Western blotting detection of constitutive and inducible proteasomal catalytic β subunits revealed a reduced expression of constitutive 20S β subunits, specifically $\beta 2$ and $\beta 5$, and increased protein levels of $\beta 2i$ and $\beta 5i$ subunits in 3Tg-iAstro compared to WT cells ($*p < 0.05$, Fig. 44), in agreement with data from enzymatic assays. Levels of $\beta 1$ and $\beta 1i$ subunits were equally expressed in hippocampal astrocytes from 3xTg-AD and WT mice, in line with the stable PGPH activity in the two cellular types.

Moreover, results are coherent with previous research data which demonstrated that, upon protein aggregates production during AD pathogenesis, in the attempt to cope

with the increased cytoplasmic burden, cells prioritize the expression of immunoproteasome subunits to clear protein aggregates or oxidized proteins [[88], [253]].

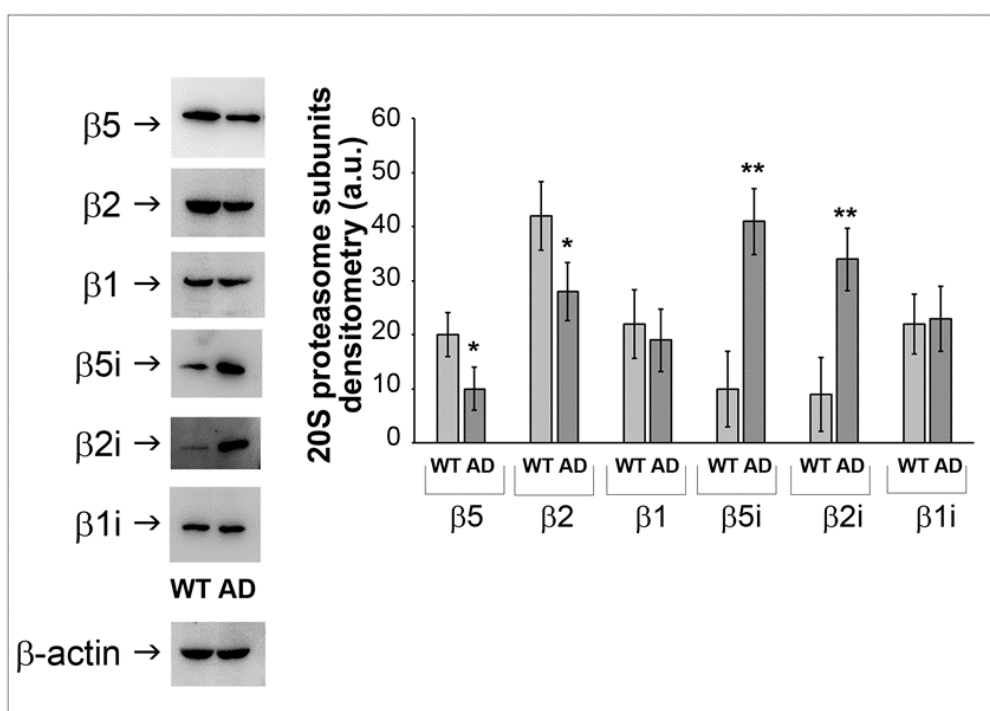


Figure 44. 20S proteasome subunits composition. Representative Western blots of 20S proteasome constitutive ($\beta 5$, $\beta 2$, $\beta 1$) and inducible ($\beta 5i$, $\beta 2i$, $\beta 1i$) subunits in WT-iAstro (WT) and 3Tg-iAstro (AD) immortalized murine astrocytes. Equal protein loading was verified by using an anti- β -actin antibody and normalized expression of the target protein is reported as arbitrary units (a.u.). The densitometric analyses obtained from five separate blots and three independent cell lines are shown. Data points marked with asterisks ($*p < 0.05$, $**p < 0.01$) are statistically significant compared to WT cells (at the same passage number) upon Student's t-test.

These results provide a panoramic overview on UPS deregulation in hippocampal astrocytes from transgenic AD mice with patterns already occurring in AD neural cells

from both mouse and human subjects [[82], [254]].

5.2.4 The autophagic proteolytic pathway is altered in 3Tg-iAstro

Key autophagy-related markers and the functionality of cathepsin B and cathepsin L lysosomal enzymes were analyzed in astrocytes lysates in order to investigate autophagy-mediated proteolysis in the two cell subgroups.

Cathepsins B and L are cysteine proteases present in lysosomes that were demonstrated to play a role in the amyloid precursor protein processing [103]. Cathepsin B activity was significantly higher in hippocampal AD astrocytes compared to WT-iAstro, whereas no significant differences were observed in cathepsin L activity (Fig. 45 panel A).

In addition, the expression levels of cathepsin B were detected through western blotting assay. Interestingly, AD astrocytes exhibited higher levels of cathepsin B with respect to WT cells (Fig. 45 panel B), consistently with the increased activity. It is known that upon UPS failure, the cell's attempt to remove protein aggregates exploits autophagy which is therefore up-regulated to cope with the extended demand [45].

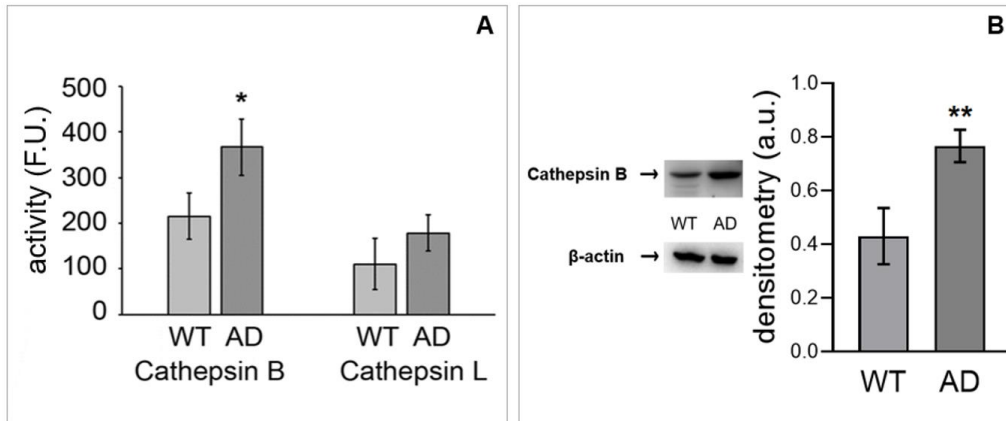


Figure 45. Cathepsin B and Cathepsin L in immortalized astrocytes. Panel A: Microplate activity assay results for activities of Cathepsin B and Cathepsin L from both WT-iAstro (WT) and 3Tg-iAstro (AD) cells. Results are expressed as fluorescence units (F.U.); Panel B: Cathepsin B expression levels in WT-iAstro (WT) and 3Tg-iAstro (AD) immortalized astrocytes. A representative blot is reported and the densitometric analyses obtained from five separate blots related to three independent cell lines is shown. Equal protein loading was verified by using an anti- β -actin antibody and normalized expression of the target protein is reported as arbitrary units (a.u.). Detection was executed by ECL. Data points marked with asterisks are statistically significant compared to their respective WT astrocytes at the same passage number (* $p < 0.05$, ** $p < 0.01$ upon Student's t-test).

We next evaluated the levels of the autophagy related proteins beclin-1, LC3-II and p62. Beclin-1 plays a key role in autophagy, being involved in the enrolment of membranes to form autophagosomes [93]. LC3-II is tightly bound to the autophagosomal membranes and is an established autophagic marker [255]. Interestingly, hippocampal 3Tg-iAstro displayed higher levels of both beclin-1 and LC3-II with respect to WT astrocytes, suggesting that autophagy was initiated (Figure 46, panels A, B).

Moreover, p62 is a scaffold protein and behaves like a signaling hub for multiple

pathways including protein turnover via the UPS and autophagy. It can interact with autophagosomes-associated LC3-II and ubiquitinated conjugates to engulf the aggregates in autophagosomes. It interacts with cytoplasmic histone deacetylase 6 (HDAC6) by inhibiting its deacetylase activity to maintain the levels of acetylated α -tubulin and stabilize microtubules to enhance autophagosome trafficking. Its synthesis is regulated by Nrf2 (NF-E2-related factor 2), which is a transcription factor [[98], [255], [256]].

Western blotting analyses revealed that the intracellular levels of p62 were markedly higher in 3Tg-iAstro, compared with WT astrocytes, suggesting an altered autophagic flux in AD possibly due to both an increased p62 synthesis and a decreased p62 proteolysis as indicated by the enhanced Nrf2 and the decreased HDAC6 intracellular levels in 3Tg-iAstro (Figure 46, panels A, B), in agreement with studies showing that p62 synthesis can be induced by an increase in Nrf2 expression upon UPS deficiency. Simultaneously, p62 accumulation can depend on an age-dependent deficient autophagic functionality [98].

Staining with monodansylcadaverine (MDC) was used to additionally monitor the autophagic cascade [225], measuring the amounts of autophagic vacuoles (AVs), the most abundant organelles contained within the dystrophic neurites that are associated with β -amyloid in senile plaques [257]. The analyses revealed an increased uptake of MDC into vacuoles in AD astrocytes with the classical punctate pattern of MDC-

labeled fluorescence (Fig. 46 panel C), indicating a failure of AVs transport and maturation (i.e. impaired AV/lysosome fusion), in agreement with increased LC3-II levels in 3Tg-iAstro cells (Figure 46, panels A, B). These results suggest that the autophagic cascade is altered in 3Tg-iAstro, accurately reproducing AD pathology.

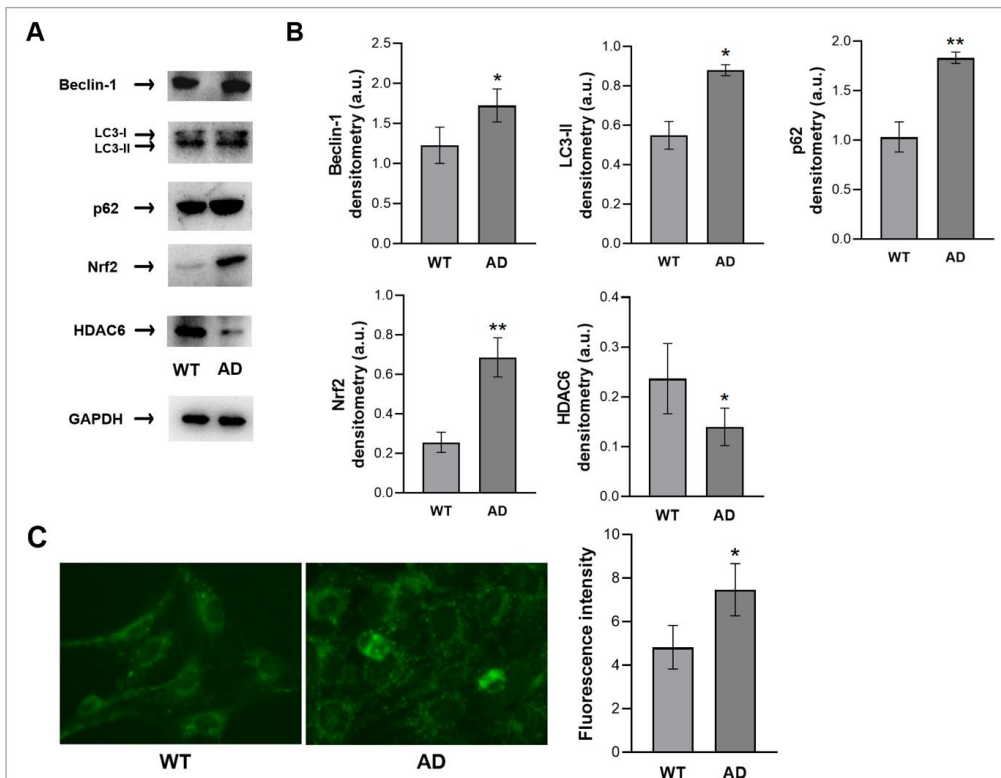


Figure 46. Autophagic markers. Panel A: Representative Western blots of Beclin-1, LC3-II, p62, Nrf2 and HDAC6 in WT-iAstro (WT) and 3Tg-iAstro (AD) immortalized astrocytes. Panels B: The densitometric analyses of Beclin-1, LC3-II, p62, Nrf2 and HDAC6 expression obtained from five separate blots and three independent cell lines are shown. Equal protein loading was verified by using an anti-GAPDH antibody and normalized expression of the target protein is reported as arbitrary units (a.u.). Detection was executed by ECL. Panel C: WT-iAstro (WT) and 3Tg-iAstro (AD) astrocytes were incubated with MDC and analyzed by fluorescence microscopy to visualize autophagic vacuoles. Data points marked with asterisks ($*p < 0.05$, $**p < 0.01$) are statistically significant compared to WT cells (at the same passage number) upon Student's t-test.

5.2.5 4-PBA restores both proteasomal and autophagic deficits of 3Tg-iAstro cells

Our data demonstrate that deregulation both proteasomal and autophagic proteolytic pathway in astrocytes during AD. A small molecule, 4-PBA (4-phenil butyric acid), approved by the FDA, has shown a neuroprotective effect on AD *in vivo* and *in vitro* models [[258], [259]]. Moreover, it has been proven that 4-PBA, due to its action as a chemical chaperone, can assist in protein trafficking and folding thus preventing protein aggregation [258]. Therefore, to validate whether the assistance in proper protein folding and trafficking may be beneficial for keeping functional proteolytic systems in 3Tg-iAstro cells. Upon 48h incubation with 3 μ M 4-PBA, a significantly increased chymotrypsin-like, trypsin-like, BrAAP and 26S chymotrypsin-like proteasome activity in 3Tg-iAstro cells can be observed (Fig. 47 panel A). As a consequence, reduced levels of ubiquitin conjugated proteins are detected (Fig. 47 panel D). 4-PBA didn't significantly affect the UPS mediated proteolysis in WT cells (Figure 47, panels

A, B, D). Interestingly, treatment with 4-PBA restored the expression levels of constitutive and inducible proteasome subunits (Figure 47, panels B, C). Altogether, these data indicate that the chemical chaperone prevented misfolded proteins accumulation observed in 3Tg-iAstro cells.

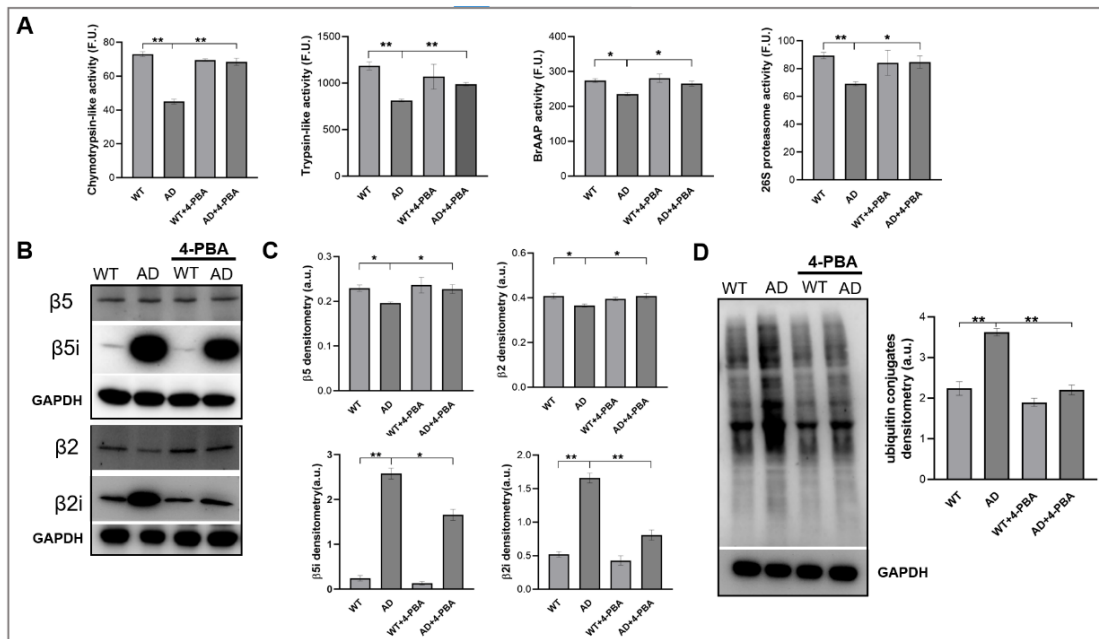


Figure 47. 4-PBA restores the functionality of UPS in 3Tg-iAstro. WT-iAstro (WT) and 3Tg-iAstro (AD) were treated or not with 4-PBA 3 μ M, for 48h respectively. Panel A: 20S Chymotrypsin-like, Trypsin-like, branched-chain amino acid cleavage (BrAAP) activity and 26S proteasome activity measured in WT, AD, WT treated with 4-PBA (WT+4-PBA) and AD treated with 4-PBA (AD+4-PBA) immortalized astrocytes. Values are expressed as fluorescence units (F.U.) and the asterisk (* $p < 0.05$ and ** $p < 0.01$) indicates significantly different values compared with untreated cells using one-way ANOVA, followed by the Bonferroni test. Panel B: Representative Western blots of β 5, β 5i, β 2, and β 2i in WT, AD, WT treated with 4-PBA (WT+4-PBA) and AD treated with 4-PBA (AD+4-PBA) immortalized astrocytes. Panel C: The densitometric analyses of β 5, β 5i, β 2, and β 2i expression obtained from five separate blots and three independent experiments are shown. Equal protein loading was verified by using an anti-GAPDH antibody and normalized expression of the target protein is reported as arbitrary units (a.u.). Detection was executed by ECL. Panel D: Representative western blots of ubiquitin and relative densitometry obtained from five separate blots and three independent experiments. Anti-GAPDH was used as equal loading control. Data points marked with asterisks (* $p < 0.05$, ** $p < 0.01$) are statistically significant compared to untreated cells using one-way ANOVA, followed by the Bonferroni test.

p62, LC3-II, beclin-1 and cathepsin B are crucial components of the autophagy system. A significantly downregulated p62, LC3-II, beclin-1 and cathepsin B levels (Figure 48, panels A, B) in 3Tg-iAstro cells treated with 4-PBA was observed, in agreement with previous data demonstrating that 4-PBA inhibited ER stress induced autophagy [260]. Taken together, our data indicate that proteolytic pathways alterations compromise protein quality control in AD astrocytes and the chaperone mediated assistance of astrocytic protein trafficking may correct these alterations.

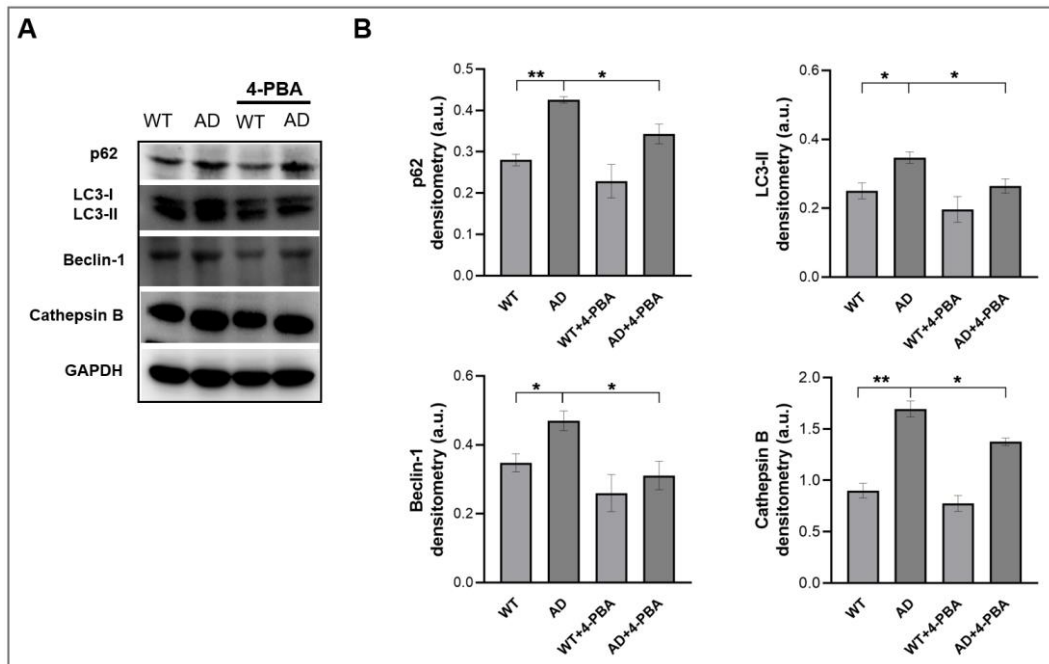


Figure 48. 4-PBA restores the defective autophagy in 3Tg-iAstro. WT-iAstro (WT) and 3Tg-iAstro (AD) were treated or not with 4-PBA 3 μ M, for 48h respectively. Panel A: Representative Western blots of p62, LC3-II, Beclin-1 and Cathepsin B in WT, AD, WT treated with 4-PBA (WT+4-PBA) and AD treated with 4-PBA (AD+4-PBA) immortalized astrocytes. Panels B: The densitometric analyses of p62, LC3-II, Beclin-1 and Cathepsin B expression obtained from five separate blots and three independent experiments are shown. Equal protein loading was verified by using an anti-GAPDH antibody and normalized expression of the target protein is reported as arbitrary units (a.u.). Detection was executed by ECL. Data points marked with asterisks ($*p < 0.05$, $**p < 0.01$) are statistically significant compared to untreated cells using one-way ANOVA, followed by the Bonferroni test.

5.3 Discussion

Alzheimer's disease (AD), the most common cause of dementia, is characterized by diminished cognitive function, specifically impairment of memory and judgement. With a rapidly ageing population, AD has become a major public health concern [[1], [4]]. Pathologically, AD is associated with protein misfolding and accumulation, chronic low-grade inflammation and cellular stress in CNS cells [[106], [261]]. So far, the major focus of research has been neural cells, considered the main contributor to the formation of protein aggregates, yet marginal importance has been given to how microglial cells and astrocytes intervene in AD pathogenic process not as solvers but as contributors to toxicity and tissue alterations present in AD brain. In this view, literature provides little information about the intracellular and molecular mechanism involved, despite the number of articles being increased in recent years. In the present work, we provide the characterization of the proteolytic systems of murine immortalized hippocampal astrocytes, obtained from 3xTg-AD mice and a wild type counterpart, to further understand the key pathways involved in protein degradation. Considering AD, a proteinopathy [14], it is of major importance to understand how cells try to deal with protein aggregates, and the specific contribution of all brain cell populations in AD pathogenesis.

In particular, the ubiquitin proteasome system (UPS) and the autophagy-lysosomal pathway are crucial for controlling proteostasis [262]. Thus, we focus on both UPS and autophagy to understand how their impairment contributes to the pathology. Significant

differences between WT and AD immortalized astrocytes were obtained, coherently with previous research on human and murine samples [[82], [106]].

Confirming the uniqueness of these immortalized astrocytes. These cells have been obtained as previously described based on the need to overcome all technical problems that result from analysis of primary cell lines. Currently human immortalized astrocytes are commercially available [263] but most of the information on the role of astrocytes in brain disease is obtained from primary astrocytes which show a series of technical and temporal limitations. Moreover, the majority of available cell lines is obtained from cortical regions and, even if cerebellum or midbrain astrocytes lines have also been reported [[264]–[266]], hippocampal astrocytes have yet to be exploited to their full potential. Being provided with immortalized hippocampal astrocytes is therefore a tremendous advantage to understand the specific molecular pathways behind their role in the disease. Furthermore, previous studies were more interested in having a general and macroscopic analysis of brain homogenates, rather than selecting, separating and differentially analyzing spatially distinct cell populations. In the present study we can provide data from single cell-type populations from both healthy hippocampus (WT) and 3xTg-AD mice hippocampus. The reliability of this model has been already proved, [[246], [267]] obtaining convincing results that encourage further investigation. As all *in vitro* single cell-type cultures, limitations are still present. The absence of microglial and neuronal cells in co-culture with astrocytes limits the number of investigations that can be carried out involving the way these cells interact and coordinate with each other.

In addition, immortalization of cells is a technique that is still not 100% efficient and effective and among manufactured cell batches not all displayed correct morphology and molecular markers [267]. As previously described in the methods section of this study, the three independent cell lines we analyzed all show astrocyte-like behavior in both WT and AD variants. Exploring the interplay between Ub-conjugates and 26S proteasome, we analyzed how Ub-conjugates protein levels vary, their increase reflecting a reduction of 26S proteasomal activity. Thus, the overall increased Ub-conjugate density obtained after western blotting analysis can be directly connected to the diminished 26S proteasomal activity when compared to WT, in accordance with previous studies demonstrating an impaired ATP synthesis in 3Tg-iAstro cells [267], since the degradation of ubiquitin conjugates by the 26S proteasome is coupled to ATP hydrolysis (Fig.42) [268]. Moreover, since the discovery of high levels of ubiquitin in senile plaques, correlation between amyloid polymers and 26S proteasome has been confirmed by evidence several times [[269], [270]].

Independently from ubiquitin conjugates, the 20S proteasome is able to degrade proteins which have not been ubiquitinated. We firstly investigated the intrinsic enzymatic activity of 20S proteasome. Despite the trend to decrease in activity, coherently with the 26S proteasome results, each activity showed a different pattern compared to WT. ChT-L and T-L activities come from $\beta 5$ and $\beta 2$ subunits respectively and were both decreased in AD samples, while PGPH activity was not down regulated by the exposure to intracellular protein aggregates. BrAAP functionality was also

slightly reduced in 3Tg-iAstro compared to WT counterpart (Fig. 43). This body of evidence highlights how ChT-L and T-L are preferentially impaired in AD astrocytes. This hints to a stronger involvement of $\beta 5$ and $\beta 2$ subunits in the attempt to remove intracellular protein aggregates, which are already known to halt the proteasome [[250], [271]–[273]]. Interestingly, our results confirmed the shift from 20S constitutive proteasome to immunoproteasome as $\beta 5i$ and $\beta 2i$ are increased and inversely correlated with constitutive $\beta 5$ and $\beta 2$ expression (Fig. 44) [274]. In addition, the increase in inducible subunits can be seen as a reaction to the inflammatory state promoting the production of immunopeptides that will be exposed on MHC surface molecules. The increase in $\beta 5i$ and $\beta 2i$ correlates with mRNA levels of β and βi subunits previously measured in human hippocampal astrocytes [275].

Autophagic flux alterations by amyloid peptides has been demonstrated in the brain of postmortem Alzheimer's disease patients, animal models and cell models [273]. Considering the complex and dynamic nature of the autophagy-lysosomal pathway, we monitored several markers associated with different steps of this process. Specifically, cathepsin B and cathepsin L lysosomal enzymes are differentially involved in AD development (Fig. 45). Cathepsin B is known to possess β -secretase-like activity and thus contribute to $A\beta$ production. Cathepsin L instead has shown the capability of increasing α -secretase activity. From literature [[276], [277]], when UPS is impaired, autophagy up-regulation occurs to enable clearance of larger aggregates.

In our study, much more autophagosomes and autolysosomes were observed in AD cells. Besides, the levels of Beclin-1 and LC3-II as well as the level of p62 were noticeable increased in AD astrocytes compared to WT, confirming a deficient autophagic function in AD (Fig. 46). p62 higher expression levels can be induced by an increased Nrf2 following UPS deficiency together with an inhibited autophagy reducing p62 degradation, in agreement with the accumulation of ubiquitin conjugates in 3Tg-iAstro and with previous studies [98]. Altogether, these results provide a clearer understanding of proteolytic machinery dysregulation of astroglial cells in AD pathology.

Moreover, treatment with the molecular chaperone 4-PBA restored proteolytic activities in 3Tg-iAstro cells (Figures 47 and 48). 4-PBA interacts with hydrophobic domains of misfolded proteins preventing their aggregation [278]. Thus, this chaperone shows the beneficial role on correcting protein folding and trafficking leading to the recovery of UPS and autophagy functionality in AD astrocytes.

Collectively, our data shed light on proteolytic systems alterations in these reliable immortalized hippocampal astrocytes and their role in AD. Furthermore, we propose a new mechanism involved in the beneficial effect of 4-PBA in neurodegenerative disorders.

6. Conclusions

Alterations in the composition of gut microbiota play an important role in the pathogenesis of Alzheimer's disease through the gut-brain axis. Recently, probiotics-based strategies have offered a number of potential health benefits for their ability to modulate gut microbial composition and the production of neuroprotective and anti-inflammatory metabolites.

Previous studies demonstrated that chronic, oral supplementation with SLAB51 probiotic formulation modified gut microbiota in 3xTg-AD mice, ameliorated glucose metabolism, inflammatory and oxidative status and partially recovered the impaired neuronal proteolysis, finally decreasing A β and tau aggregates and improving cognitive abilities, with consequent delay of AD progression [[19], [106], [153]].

Increasing evidence suggests that abnormal lipid metabolism can promote AD onset and development. Data here reported show that SLAB51 probiotic mixture exerted hypocholesterolemic effects in 3xTg-AD mice, qualitatively ameliorating plasma lipid composition, decreasing cholesterol biosynthesis and influencing alternative synthetic pathways of bile acids. Additionally, probiotic-induced variations in plasma fatty acid composition contribute to define a role for polyunsaturated fatty acids in the resolution of inflammation in AD [279].

Upon probiotics supplementation, restored HIF-1 α cerebral expression and decreased

levels of PHD2, together with reduced nitrite plasma concentration and iNOS cerebral levels confirmed the probiotic positive effect on oxidative status and immune function, but also indicate a beneficial effect on glucose metabolism, in agreement with previously published results [[19], [153]]. This paper describes another molecular mechanism through which SLAB51 probiotic formulation can counteract oxidation and inflammation and can improve energy metabolism in AD [280].

Future studies with different probiotic formulations should consider the importance to use living bacteria instead of inactivated bacterial strains. Multi-strains formulation may well have a higher chance to strategically shift gut microbiota composition with respect to single-strain approaches. Additionally, novel formulations with prebiotics could be considered in order to improve probiotics viability, stability and functionality [281].

The study on AD cellular model treated with dietary phenyl- γ -valerolactones clarified unexplored mechanisms of action of these antioxidant and anti-inflammatory compounds focusing on proteolysis. Specifically, the three tested PVLs inhibited UPS and activated autophagy in SHSY5Y stably transfected with mutated APP, consequently diminishing the amounts of A β (1-42) in cell lysates and in the growth medium. The resulting paper provides, for the first time, evidence for the neuroprotective activity of these microbiota-derived metabolites of flavan-3-ols, associated with the modulation of intracellular proteolytic systems and suggests their

potential use in preventative strategies against AD [282].

Furthermore, being impaired proteolysis critically involved in neurodegenerative conditions, we characterized the UPS and autophagy in both 3Tg-iAstro and WT-iAstro, which are newly generated immortalized hippocampal astrocytic cells from 3xTg-AD and wild type mice. Our data shed light on the impaired proteostasis in hippocampal Alzheimer's disease astrocytes with proteasome inhibition and autophagic compensatory activation, linked by increased p62 intracellular levels. Moreover, we demonstrated that 4-phenylbutyric acid, a neuroprotective aromatic short chain fatty acid approved by FDA, restored proteolysis in 3Tg-iAstro, proposing a new mechanism involved in the beneficial effect of 4-phenylbutyric acid in neurodegenerative disorders and providing additional validation to 3Tg-iAstro as *in vitro* model of Alzheimer's disease [283].

Collectively, our studies provide important contribution in the development of new therapeutic options for AD involving probiotics and/or bacterial metabolites. We have demonstrated that gut microbiota modulation can exert positive consequences on energy metabolism and brain oxidative and inflammatory status, by regulating plasma lipid profile, cholesterol biosynthesis, fatty acid composition and hypoxia inducible factor-1 α related pathways; in addition, we used *in silico* and *in vitro* cellular approaches to clarify the molecular mechanisms affected by microbiota-derived metabolites, with a focus on proteolytic pathways that are impaired in AD.

Published and unpublished data should be taken into account in future AD preventative and therapeutic protocols. Effectiveness of gut microbiota modulation will depend upon the proper combinations of bacterial strains or metabolites, time of treatment and disease stage.

Dietary interventions are generally safe and more advantageous than drug-based therapies and data here reported sustain oral bacteriotherapy as a promising therapeutic and preventative approach in neurodegenerative conditions and in AD.

7. Reference

- [1] J. Mendiola-Precoma, L. C. Berumen, K. Padilla, and G. Garcia-Alcocer, "Therapies for Prevention and Treatment of Alzheimer's Disease," *BioMed Research International*, vol. 2016. Hindawi Publishing Corporation, 2016. doi: 10.1155/2016/2589276.
- [2] S. Dan *et al.*, "Therapeutic and diagnostic applications of nanocomposites in the treatment Alzheimer's disease studies," *Biointerface Research in Applied Chemistry*, vol. 12, no. 1. 2022. doi: 10.33263/BRIAC121.940960.
- [3] S. Khan, K. H. Barve, and M. S. Kumar, "Recent Advancements in Pathogenesis, Diagnostics and Treatment of Alzheimer's Disease," *Curr Neuropharmacol*, vol. 18, no. 11, pp. 1106–1125, May 2020, doi: 10.2174/1570159x18666200528142429.
- [4] J. B. Toledo *et al.*, "Metabolic network failures in Alzheimer's disease: A biochemical road map," *Alzheimer's and Dementia*, vol. 13, no. 9, pp. 965–984, Sep. 2017, doi: 10.1016/j.jalz.2017.01.020.
- [5] M. Revi, "Alzheimer's Disease Therapeutic Approaches," in *Advances in experimental medicine and biology*, 1195, 105–116., 2020, pp. 105–116. doi: 10.1007/978-3-030-32633-3_15.
- [6] A. Serrano-Pozo and J. H. Growdon, "Is Alzheimer's Disease Risk Modifiable?," *Journal of Alzheimer's Disease*, vol. 67, no. 3. 2019. doi: 10.3233/JAD181028.
- [7] "2021 Alzheimer's disease facts and figures," *Alzheimer's and Dementia*, vol. 17, no. 3, pp. 327–406, Mar. 2021, doi: 10.1002/alz.12328.
- [8] C. Ballard, S. Gauthier, A. Corbett, C. Brayne, D. Aarsland, and E. Jones, "Alzheimer's disease," *The Lancet*, vol. 377, no. 9770. 2011. doi: 10.1016/S0140-6736(10)61349-9.
- [9] M. Giri, M. Zhang, and Y. Lü, "Genes associated with Alzheimer's disease: An overview and current status," *Clinical Interventions in Aging*, vol. 11. 2016. doi: 10.2147/CIA.S105769.
- [10] R. Cacace, K. Sleegers, and C. van Broeckhoven, "Molecular genetics of early-onset Alzheimer's disease revisited," *Alzheimer's and Dementia*, vol. 12, no. 6. 2016. doi: 10.1016/j.jalz.2016.01.012.
- [11] A. C. Naj *et al.*, "Effects of multiple genetic loci on age at onset in late-onset Alzheimer disease: A genome-wide association study," *JAMA Neurol*, vol. 71, no. 11, 2014, doi: 10.1001/jamaneurol.2014.1491.
- [12] B. Imtiaz, A. M. Tolppanen, M. Kivipelto, and H. Soininen, "Future directions in Alzheimer's disease from risk factors to prevention," *Biochemical Pharmacology*, vol. 88, no. 4. 2014. doi: 10.1016/j.bcp.2014.01.003.
- [13] D. S. Knopman *et al.*, "Alzheimer disease," *Nat Rev Dis Primers*, vol. 7, no. 1, Dec. 2021, doi: 10.1038/s41572-021-00269-y.
- [14] M. A. Deture and D. W. Dickson, "The neuropathological diagnosis of Alzheimer's disease," *Molecular Neurodegeneration*, vol. 14, no. 1. BioMed Central Ltd., Aug. 02, 2019. doi: 10.1186/s13024-019-0333-5.
- [15] E. P. Meyer, A. Ulmann-Schuler, M. Staufenbiel, and T. Krucker, "Altered morphology and 3D architecture of brain vasculature in a mouse model for Alzheimer's disease," 2008. [Online]. Available: www.pnas.org/cgi/content/full/
- [16] N. A. M. I. S. Y. Y Itoh 1, "Scanning electron microscopical study of the neurofibrillary tangles of Alzheimer's disease," *Acta Neuropathol*, Jul. 1997.

- [17] C. Ledig, A. Schuh, R. Guerrero, R. A. Heckemann, and D. Rueckert, "Structural brain imaging in Alzheimer's disease and mild cognitive impairment: biomarker analysis and shared morphometry database," *Sci Rep*, vol. 8, no. 1, Dec. 2018, doi: 10.1038/s41598-018-29295-9.
- [18] A. Metaxas and S. J. Kempf, "Neurofibrillary tangles in Alzheimer's disease: Elucidation of the molecular mechanism by immunohistochemistry and tau protein phospho-proteomics," *Neural Regen Res*, vol. 11, no. 10, pp. 1579–1581, Oct. 2016, doi: 10.4103/1673-5374.193234.
- [19] L. Bonfili *et al.*, "SLAB51 Probiotic Formulation Activates SIRT1 Pathway Promoting Antioxidant and Neuroprotective Effects in an AD Mouse Model," *Mol Neurobiol*, vol. 55, no. 10, pp. 7987–8000, Oct. 2018, doi: 10.1007/s12035-018-0973-4.
- [20] C. Haass, C. Kaether, G. Thinakaran, and S. Sisodia, "Trafficking and proteolytic processing of APP," *Cold Spring Harb Perspect Med*, vol. 2, no. 5, 2012, doi: 10.1101/cshperspect.a006270.
- [21] M. P. Kummer and M. T. Heneka, "Truncated and modified amyloid-beta species." [Online]. Available: <http://alzres.com/content/6/3/28>
- [22] S. García-Viñuales *et al.*, "The interplay between lipid and A β amyloid homeostasis in Alzheimer's Disease: risk factors and therapeutic opportunities," *Chem Phys Lipids*, vol. 236, May 2021, doi: 10.1016/j.chemphyslip.2021.105072.
- [23] G. F. Chen *et al.*, "Amyloid beta: Structure, biology and structure-based therapeutic development," *Acta Pharmacologica Sinica*, vol. 38, no. 9. Nature Publishing Group, pp. 1205–1235, Sep. 01, 2017. doi: 10.1038/aps.2017.28.
- [24] Z. Breijyeh and R. Karaman, "Comprehensive Review on Alzheimer's Disease: Causes and Treatment," *Molecules (Basel, Switzerland)*, vol. 25, no. 24. 2020. doi: 10.3390/molecules25245789.
- [25] Y. C. Kao, P. C. Ho, Y. K. Tu, I. M. Jou, and K. J. Tsai, "Lipids and alzheimer's disease," *International Journal of Molecular Sciences*, vol. 21, no. 4. MDPI AG, Feb. 02, 2020. doi: 10.3390/ijms21041505.
- [26] S. K. Byeon *et al.*, "Cerebrospinal fluid lipidomics for biomarkers of Alzheimer's disease," *Mol Omics*, vol. 17, no. 3, pp. 454–463, Jun. 2021, doi: 10.1039/d0mo00186d.
- [27] H. Su *et al.*, "Characterization of brain-derived extracellular vesicle lipids in Alzheimer's disease," *J Extracell Vesicles*, vol. 10, no. 7, May 2021, doi: 10.1002/jev2.12089.
- [28] M. Britschgi and T. Wyss-Coray, "Blood protein signature for the early diagnosis of alzheimer disease," *Archives of Neurology*, vol. 66, no. 2. 2009. doi: 10.1001/archneurol.2008.530.
- [29] M. Mapstone *et al.*, "Plasma phospholipids identify antecedent memory impairment in older adults," *Nat Med*, vol. 20, no. 4, pp. 415–418, 2014, doi: 10.1038/nm.3466.
- [30] Y. M. Kuo *et al.*, "Elevated low-density lipoprotein in Alzheimer's disease correlates with brain a β 1-42 levels," *Biochem Biophys Res Commun*, vol. 252, no. 3, 1998, doi: 10.1006/bbrc.1998.9652.
- [31] M. Agarwal and S. Khan, "Plasma Lipids as Biomarkers for Alzheimer's Disease: A Systematic Review," *Cureus*, 2020, doi: 10.7759/cureus.12008.
- [32] H. Yanai, "Effects of N-3 Polyunsaturated Fatty Acids on Dementia," *J Clin Med Res*, vol. 9, no. 1, 2017, doi: 10.14740/jocmr2815w.
- [33] R. K. McNamara, Y. Liu, R. Jandacek, T. Rider, and P. Tso, "The aging human orbitofrontal cortex: Decreasing polyunsaturated fatty acid composition and associated increases in lipogenic gene expression and stearoyl-CoA desaturase activity," *Prostaglandins Leukot Essent Fatty Acids*, vol. 78, no. 4–5, 2008, doi: 10.1016/j.plefa.2008.04.001.

- [34] Q. Yu *et al.*, “Lipidome alterations in human prefrontal cortex during development, aging, and cognitive disorders,” *Mol Psychiatry*, vol. 25, no. 11, 2020, doi: 10.1038/s41380-018-0200-8.
- [35] R. Bhawal, Q. Fu, E. T. Anderson, G. E. Gibson, and S. Zhang, “Serum metabolomic and lipidomic profiling reveals novel biomarkers of efficacy for benfotiamine in alzheimer’s disease,” *Int J Mol Sci*, vol. 22, no. 24, 2021, doi: 10.3390/ijms222413188.
- [36] J. M. Dietschy and S. D. Turley, “Cholesterol metabolism in the brain,” *Current Opinion in Lipidology*, vol. 12, no. 2. 2001. doi: 10.1097/00041433-200104000-00003.
- [37] P. Gamba, G. Testa, B. Sottero, S. Gargiulo, G. Poli, and G. Leonarduzzi, “The link between altered cholesterol metabolism and Alzheimer’s disease,” *Ann N Y Acad Sci*, vol. 1259, no. 1, 2012, doi: 10.1111/j.1749-6632.2012.06513.x.
- [38] M. Burns *et al.*, “Presenilin redistribution associated with aberrant cholesterol transport enhances β -amyloid production in vivo,” *Journal of Neuroscience*, vol. 23, no. 13, 2003, doi: 10.1523/jneurosci.23-13-05645.2003.
- [39] M. P. Burns *et al.*, “Co-localization of cholesterol, apolipoprotein E and fibrillar A β in amyloid plaques,” *Molecular Brain Research*, vol. 110, no. 1, 2003, doi: 10.1016/S0169-328X(02)00647-2.
- [40] Y. Sun, J. Yao, T. W. Kim, and A. R. Tall, “Expression of liver X receptor target genes decreases cellular amyloid β peptide secretion,” *Journal of Biological Chemistry*, vol. 278, no. 30, 2003, doi: 10.1074/jbc.M300760200.
- [41] R. Ricciarelli *et al.*, “Cholesterol and Alzheimer’s disease: A still poorly understood correlation,” *IUBMB Life*, vol. 64, no. 12. 2012. doi: 10.1002/iub.1091.
- [42] T. Hartmann, J. Kuchenbecker, and M. O. W. Grimm, “Alzheimer’s disease: the lipid connection,” *Journal of neurochemistry*, vol. 103 Suppl 1. 2007. doi: 10.1111/j.1471-4159.2007.04715.x.
- [43] B. Wolozin, W. Kellman, P. Russeau, G. G. Celesia, and G. Siegel, “Decreased prevalence of Alzheimer disease associated with 3-hydroxy-3-methylglutaryl coenzyme A reductase inhibitors,” *Arch Neurol*, vol. 57, no. 10, 2000, doi: 10.1001/archneur.57.10.1439.
- [44] X. mei Liu, X. min Zhao, C. Deng, Y. ping Zeng, and C. hua Hu, “Simvastatin improves olanzapine-induced dyslipidemia in rats through inhibiting hepatic mTOR signaling pathway,” *Acta Pharmacol Sin*, vol. 40, no. 8, 2019, doi: 10.1038/s41401-019-0212-1.
- [45] L. Agholme, M. Hallbeck, E. Benedikz, J. Marcusson, and K. Kgedal, “Amyloid- β secretion, generation, and lysosomal sequestration in response to proteasome inhibition: Involvement of autophagy,” *Journal of Alzheimer’s Disease*, vol. 31, no. 2, 2012, doi: 10.3233/JAD-2012-120001.
- [46] M. S. Brown and J. L. Goldstein, “The SREBP pathway: Regulation of cholesterol metabolism by proteolysis of a membrane-bound transcription factor,” *Cell*, vol. 89, no. 3. 1997. doi: 10.1016/S0092-8674(00)80213-5.
- [47] X. Hua, J. Wu, J. L. Goldstein, M. S. Brown, and H. H. Hobbs, “Structure of the human gene encoding sterol regulatory element binding protein-1 (SREBF1) and localization of SREBF1 and SREBF2 to chromosomes 17p11.2 and 22q13,” *Genomics*, vol. 25, no. 3, 1995, doi: 10.1016/0888-7543(95)80009-B.
- [48] X. Xu, J. S. So, J. G. Park, and A. H. Lee, “Transcriptional control of hepatic lipid metabolism by SREBP and ChREBP,” *Semin Liver Dis*, vol. 33, no. 4, 2013, doi: 10.1055/s-0033-1358523.
- [49] J. J. Repa *et al.*, “Regulation of mouse sterol regulatory element-binding protein-1c gene (SREBP-1c) by oxysterol receptors, LXR α and LXR β ,” *Genes Dev*, vol. 14, no. 22, 2000, doi: 10.1101/gad.844900.

- [50] J. Kang and S. Rivest, "Lipid metabolism and neuroinflammation in alzheimer's disease: A role for liver X receptors," *Endocrine Reviews*, vol. 33, no. 5. 2012. doi: 10.1210/er.2011-1049.
- [51] Z. Ma *et al.*, "Liver X receptors and their agonists: Targeting for cholesterol homeostasis and cardiovascular diseases," *Curr Issues Mol Biol*, vol. 22, 2017, doi: 10.21775/cimb.022.041.
- [52] M. v. Cannon, W. H. van Gilst, and R. A. de Boer, "Emerging role of liver X receptors in cardiac pathophysiology and heart failure," *Basic Research in Cardiology*, vol. 111, no. 1. 2016. doi: 10.1007/s00395-015-0520-7.
- [53] U. Panzenboeck *et al.*, "Liver-x receptor agonists modulate hdl and amyloid-beta metabolism in brain capillary endothelial cells forming the blood-brain barrier," *Atherosclerosis*, vol. 235, no. 2, 2014, doi: 10.1016/j.atherosclerosis.2014.05.509.
- [54] E. Scotti *et al.*, "Targeted Disruption of the Idol Gene Alters Cellular Regulation of the Low-Density Lipoprotein Receptor by Sterols and Liver X Receptor Agonists," *Mol Cell Biol*, vol. 31, no. 9, 2011, doi: 10.1128/mcb.01469-10.
- [55] J. Gao *et al.*, "The E3 ubiquitin ligase IDOL regulates synaptic ApoER2 levels and is important for plasticity and learning," *Elife*, vol. 6, 2017, doi: 10.7554/eLife.29178.
- [56] L. Zhang, K. Reue, L. G. Fong, S. G. Young, and P. Tontonoz, "Feedback regulation of cholesterol uptake by the LXR-IDOL-LDLR axis," *Arteriosclerosis, Thrombosis, and Vascular Biology*, vol. 32, no. 11. 2012. doi: 10.1161/ATVBAHA.112.250571.
- [57] A. C. Calkin *et al.*, "FERM-dependent E3 ligase recognition is a conserved mechanism for targeted degradation of lipoprotein receptors," *Proc Natl Acad Sci U S A*, vol. 108, no. 50, 2011, doi: 10.1073/pnas.1111589108.
- [58] J. E. van Lier, "New Therapeutic Targets for Brain Function and Disease," *Journal of Medicinal Chemistry*, vol. 63, no. 12. 2020. doi: 10.1021/acs.jmedchem.9b01947.
- [59] S. Maioli *et al.*, "Is It Possible to Improve Memory Function by Upregulation of the Cholesterol 24S-Hydroxylase (CYP46A1) in the Brain?," *PLoS One*, vol. 8, no. 7, 2013, doi: 10.1371/journal.pone.0068534.
- [60] E. Hudry *et al.*, "Adeno-associated virus gene therapy with cholesterol 24-hydroxylase reduces the amyloid pathology before or after the onset of amyloid plaques in mouse models of alzheimer's disease," *Molecular Therapy*, vol. 18, no. 1, 2010, doi: 10.1038/mt.2009.175.
- [61] M. Shafaati *et al.*, "Marked accumulation of 27-hydroxycholesterol in the brains of Alzheimer's patients with the Swedish APP 670/671 mutation," *J Lipid Res*, vol. 52, no. 5, 2011, doi: 10.1194/jlr.M014548.
- [62] Q. Liu *et al.*, "High-cholesterol diet results in elevated amyloid- β and oxysterols in rats," *Mol Med Rep*, vol. 17, no. 1, 2018, doi: 10.3892/mmr.2017.8003.
- [63] G. Testa *et al.*, "Changes in brain oxysterols at different stages of Alzheimer's disease: Their involvement in neuroinflammation," *Redox Biol*, vol. 10, 2016, doi: 10.1016/j.redox.2016.09.001.
- [64] O. O. Ogunshola and X. Antoniou, "Contribution of hypoxia to Alzheimer's disease: Is HIF-1 α a mediator of neurodegeneration?," *Cellular and Molecular Life Sciences*, vol. 66, no. 22. 2009. doi: 10.1007/s00018-009-0141-0.
- [65] A. Hambali *et al.*, "Hypoxia-Induced Neuroinflammation in Alzheimer's Disease: Potential Neuroprotective Effects of Centella asiatica," *Frontiers in Physiology*, vol. 12. 2021. doi: 10.3389/fphys.2021.712317.
- [66] R. Lall, R. Mohammed, and U. Ojha, "What are the links between hypoxia and alzheimer's disease?," *Neuropsychiatric Disease and Treatment*, vol. 15. 2019. doi: 10.2147/NDT.S203103.

- [67] V. Calsolaro and P. Edison, "Neuroinflammation in Alzheimer's disease: Current evidence and future directions," *Alzheimer's and Dementia*, vol. 12, no. 6. 2016. doi: 10.1016/j.jalz.2016.02.010.
- [68] H. Y. Zhu, F. F. Hong, and S. L. Yang, "The roles of nitric oxide synthase/nitric oxide pathway in the pathology of vascular dementia and related therapeutic approaches," *International Journal of Molecular Sciences*, vol. 22, no. 9. 2021. doi: 10.3390/ijms22094540.
- [69] S. B. A. Cau, F. S. Carneiro, and R. C. Tostes, "Differential modulation of nitric oxide synthases in aging: Therapeutic opportunities," *Frontiers in Physiology*, vol. 3 JUN. 2012. doi: 10.3389/fphys.2012.00218.
- [70] P. M. Liy, N. N. A. Puzi, S. Jose, and S. Vidyadaran, "Nitric oxide modulation in neuroinflammation and the role of mesenchymal stem cells," *Exp Biol Med*, vol. 246, no. 22, 2021, doi: 10.1177/1535370221997052.
- [71] N. Gresa-Arribas, C. Viéitez, G. Dentesano, J. Serratos, J. Saura, and C. Solà, "Modelling Neuroinflammation In Vitro: A Tool to Test the Potential Neuroprotective Effect of Anti-Inflammatory Agents," *PLoS One*, vol. 7, no. 9, 2012, doi: 10.1371/journal.pone.0045227.
- [72] A. Bal-Price and G. C. Brown, "Inflammatory neurodegeneration mediated by nitric oxide from activated glia-inhibiting neuronal respiration, causing glutamate release and excitotoxicity," *Journal of Neuroscience*, vol. 21, no. 17, 2001, doi: 10.1523/jneurosci.21-17-06480.2001.
- [73] R. Chen, U. H. Lai, L. Zhu, A. Singh, M. Ahmed, and N. R. Forsyth, "Reactive oxygen species formation in the brain at different oxygen levels: The role of hypoxia inducible factors," *Frontiers in Cell and Developmental Biology*, vol. 6, no. OCT. 2018. doi: 10.3389/fcell.2018.00132.
- [74] Z. N. Demidenko and M. v. Blagosklonny, "The purpose of the HIF-1/PHD feedback loop: To limit mTOR-induced HIF-1 α ," *Cell Cycle*, vol. 10, no. 10. 2011. doi: 10.4161/cc.10.10.15789.
- [75] H. Hassan and R. Chen, "Hypoxia in Alzheimer's disease: Effects of hypoxia inducible factors," *Neural Regeneration Research*, vol. 16, no. 2. 2021. doi: 10.4103/1673-5374.290898.
- [76] S. Baillieul, S. Chacaroun, S. Doutreleau, O. Detante, J. L. Pépin, and S. Verges, "Hypoxic conditioning and the central nervous system: A new therapeutic opportunity for brain and spinal cord injuries?," *Experimental Biology and Medicine*, vol. 242, no. 11. 2017. doi: 10.1177/1535370217712691.
- [77] S. Verges, S. Chacaroun, D. Godin-Ribuot, and S. Baillieul, "Hypoxic Conditioning as a New Therapeutic Modality," *Frontiers in Pediatrics*, vol. 3. 2015. doi: 10.3389/fped.2015.00058.
- [78] D. Chhangani and A. Mishra, "Protein quality control system in neurodegeneration: A healing company hard to beat but failure is fatal," *Molecular Neurobiology*, vol. 48, no. 1. 2013. doi: 10.1007/s12035-013-8411-0.
- [79] A. al Mamun *et al.*, "Exploring the Promise of Targeting Ubiquitin-Proteasome System to Combat Alzheimer's Disease," *Neurotoxicity Research*, vol. 38, no. 1. 2020. doi: 10.1007/s12640-020-00185-1.
- [80] R. Raynes, L. C. D. Pomatto, and K. J. A. Davies, "Degradation of oxidized proteins by the proteasome: Distinguishing between the 20S, 26S, and immunoproteasome proteolytic pathways," *Molecular Aspects of Medicine*, vol. 50. 2016. doi: 10.1016/j.mam.2016.05.001.
- [81] V. Cecarini *et al.*, "The fine-tuning of proteolytic pathways in Alzheimer's disease," *Cellular and Molecular Life Sciences*, vol. 73, no. 18. 2016. doi: 10.1007/s00018-016-2238-6.
- [82] V. Cecarini *et al.*, "Crosstalk between the ubiquitin-proteasome system and autophagy in a human cellular model of Alzheimer's disease," *Biochim Biophys Acta Mol Basis Dis*, vol. 1822, no. 11, 2012, doi: 10.1016/j.bbadis.2012.07.015.

- [83] L. Hong, H. C. Huang, and Z. F. Jiang, "Relationship between amyloid-beta and the ubiquitin-proteasome system in Alzheimer's disease," *Neurological Research*, vol. 36, no. 3. 2014. doi: 10.1179/1743132813Y.0000000288.
- [84] H. C. Tai, A. Serrano-Pozo, T. Hashimoto, M. P. Frosch, T. L. Spire-Jones, and B. T. Hyman, "The synaptic accumulation of hyperphosphorylated tau oligomers in Alzheimer disease is associated with dysfunction of the ubiquitin-proteasome system," *American Journal of Pathology*, vol. 181, no. 4, 2012, doi: 10.1016/j.ajpath.2012.06.033.
- [85] A. v. Gomes, "Genetics of Proteasome Diseases," *Scientifica (Cairo)*, vol. 2013, 2013, doi: 10.1155/2013/637629.
- [86] K. L. Rock and A. L. Goldberg, "Degradation of cell proteins and the generation of MHC class I-presented peptides," *Annual Review of Immunology*, vol. 17. 1999. doi: 10.1146/annurev.immunol.17.1.739.
- [87] L. K. Wagner *et al.*, "Immunoproteasome deficiency alters microglial cytokine response and improves cognitive deficits in Alzheimer's disease-like APPPS1 mice," *Acta Neuropathol Commun*, vol. 5, no. 1, 2017, doi: 10.1186/s40478-017-0453-5.
- [88] M. Mishto *et al.*, "Immunoproteasome and LMP2 polymorphism in aged and Alzheimer's disease brains," *Neurobiol Aging*, vol. 27, no. 1, 2006, doi: 10.1016/j.neurobiolaging.2004.12.004.
- [89] S. Song, J. Tan, Y. Miao, and Q. Zhang, "Crosstalk of ER stress-mediated autophagy and ER-phagy: Involvement of UPR and the core autophagy machinery," *Journal of Cellular Physiology*, vol. 233, no. 5. 2018. doi: 10.1002/jcp.26137.
- [90] K. Jing and K. Lim, "Why is autophagy important in human diseases?," *Exp Mol Med*, vol. 44, no. 2, 2012, doi: 10.3858/emmm.2012.44.2.028.
- [91] X. Zhang *et al.*, "Ischemia-induced upregulation of autophagy precludes dysfunctional lysosomal storage and associated synaptic impairments in neurons," *Autophagy*, vol. 17, no. 6, 2021, doi: 10.1080/15548627.2020.1840796.
- [92] S. C. Correia, R. Resende, P. I. Moreira, and C. M. Pereira, "Alzheimer's disease-related misfolded proteins and dysfunctional organelles on autophagy menu," *DNA Cell Biol*, vol. 34, no. 4, 2015, doi: 10.1089/dna.2014.2757.
- [93] L. G. Friedman, Y. H. Qureshi, and W. H. Yu, "Promoting Autophagic Clearance: Viable Therapeutic Targets in Alzheimer's Disease," *Neurotherapeutics*, vol. 12, no. 1. 2015. doi: 10.1007/s13311-014-0320-z.
- [94] P. A. Jaeger, F. Pickford, C. H. Sun, K. M. Lucin, E. Masliah, and T. Wyss-Coray, "Regulation of amyloid precursor protein processing by the beclin 1 complex," *PLoS One*, vol. 5, no. 6, 2010, doi: 10.1371/journal.pone.0011102.
- [95] F. Pickford *et al.*, "The autophagy-related protein beclin 1 shows reduced expression in early Alzheimer disease and regulates amyloid β accumulation in mice," *Journal of Clinical Investigation*, vol. 118, no. 6, 2008, doi: 10.1172/JCI33585.
- [96] L. Crews *et al.*, "Selective molecular alterations in the autophagy pathway in patients with Lewy body disease and in models of α -synucleinopathy," *PLoS One*, vol. 5, no. 2, 2010, doi: 10.1371/journal.pone.0009313.
- [97] Y. Liu *et al.*, "Impaired autophagic function in rat islets with aging," *Age (Omaha)*, vol. 35, no. 5, 2013, doi: 10.1007/s11357-012-9456-0.
- [98] W. J. Liu *et al.*, "p62 links the autophagy pathway and the ubiquitin-proteasome system upon ubiquitinated protein degradation," *Cellular and Molecular Biology Letters*, vol. 21, no. 1. 2016. doi: 10.1186/s11658-016-0031-z.
- [99] T. Xu *et al.*, "Cpl/cathepsin L is required for autolysosomal clearance in *Drosophila*," *Autophagy*, vol. 17, no. 10, 2021, doi: 10.1080/15548627.2020.1838105.

- [100] H. Iwama *et al.*, “Cathepsin B and D deficiency in the mouse pancreas induces impaired autophagy and chronic pancreatitis,” *Sci Rep*, vol. 11, no. 1, 2021, doi: 10.1038/s41598-021-85898-9.
- [101] A. Wille *et al.*, “Cathepsin L is involved in cathepsin D processing and regulation of apoptosis in A549 human lung epithelial cells,” *Biol Chem*, vol. 385, no. 7, 2004, doi: 10.1515/BC.2004.082.
- [102] J. Dennemärker *et al.*, “Impaired turnover of autophagolysosomes in cathepsin L deficiency,” in *Biological Chemistry*, 2010, vol. 391, no. 8. doi: 10.1515/BC.2010.097.
- [103] D. M. Klein, K. M. Felsenstein, and D. E. Brenneman, “Cathepsins B and L differentially regulate amyloid precursor protein processing,” *Journal of Pharmacology and Experimental Therapeutics*, vol. 328, no. 3, 2009, doi: 10.1124/jpet.108.147082.
- [104] V. Hook, L. Funkelstein, J. Wegrzyn, S. Bark, M. Kindy, and G. Hook, “Cysteine Cathepsins in the secretory vesicle produce active peptides: Cathepsin L generates peptide neurotransmitters and cathepsin B produces beta-amyloid of Alzheimer’s disease,” *Biochimica et Biophysica Acta - Proteins and Proteomics*, vol. 1824, no. 1. 2012. doi: 10.1016/j.bbapap.2011.08.015.
- [105] V. Hook *et al.*, “Inhibition of cathepsin B reduces β -amyloid production in regulated secretory vesicles of neuronal chromaffin cells: Evidence for cathepsin B as a candidate β -secretase of Alzheimer’s disease,” *Biol Chem*, vol. 386, no. 9, 2005, doi: 10.1515/BC.2005.108.
- [106] L. Bonfili *et al.*, “Microbiota modulation counteracts Alzheimer’s disease progression influencing neuronal proteolysis and gut hormones plasma levels,” *Sci Rep*, vol. 7, no. 1, 2017, doi: 10.1038/s41598-017-02587-2.
- [107] V. de J.R. De-Paula, A. S. Forlenza, and O. v. Forlenza, “Relevance of gutmicrobiota in cognition, behaviour and Alzheimer’s disease,” *Pharmacological Research*, vol. 136. 2018. doi: 10.1016/j.phrs.2018.07.007.
- [108] R. F. Villarán *et al.*, “Ulcerative colitis exacerbates lipopolysaccharide-induced damage to the nigral dopaminergic system: Potential risk factor in Parkinson’s disease,” *J Neurochem*, vol. 114, no. 6, 2010, doi: 10.1111/j.1471-4159.2010.06879.x.
- [109] Y.-K. Kim and C. Shin, “The Microbiota-Gut-Brain Axis in Neuropsychiatric Disorders: Pathophysiological Mechanisms and Novel Treatments,” *Curr Neuropharmacol*, vol. 15, 2018, doi: 10.2174/1570159x15666170915141036.
- [110] A. M. Valdes, J. Walter, E. Segal, and T. D. Spector, “Role of the gut microbiota in nutrition and health,” *BMJ (Online)*, vol. 361, 2018, doi: 10.1136/bmj.k2179.
- [111] J. A. Hawrelak and S. P. Myers, “The causes of intestinal dysbiosis: A review,” *Alternative Medicine Review*, vol. 9, no. 2. 2004.
- [112] M. Koszewicz *et al.*, “Dysbiosis is one of the risk factor for stroke and cognitive impairment and potential target for treatment,” *Pharmacological Research*, vol. 164. 2021. doi: 10.1016/j.phrs.2020.105277.
- [113] U. Shabbir, M. S. Arshad, A. Sameen, and D. H. Oh, “Crosstalk between gut and brain in alzheimer’s disease: The role of gut microbiota modulation strategies,” *Nutrients*, vol. 13, no. 2. 2021. doi: 10.3390/nu13020690.
- [114] A. Cattaneo *et al.*, “Association of brain amyloidosis with pro-inflammatory gut bacterial taxa and peripheral inflammation markers in cognitively impaired elderly,” *Neurobiol Aging*, vol. 49, 2017, doi: 10.1016/j.neurobiolaging.2016.08.019.
- [115] S. S. Cao, “Cellular stress responses and gut microbiota in inflammatory bowel disease,” *Gastroenterology Research and Practice*, vol. 2018. 2018. doi: 10.1155/2018/7192646.
- [116] V. K. Sharma *et al.*, “Dysbiosis and alzheimer’s disease: A role for chronic stress?,” *Biomolecules*, vol. 11, no. 5. 2021. doi: 10.3390/biom11050678.

- [117] J. Garthwaite, S. L. Charles, and R. Chess-Williams, "Endothelium-derived relaxing factor release on activation of NMDA receptors suggests role as intercellular messenger in the brain," *Nature*, vol. 336, no. 6197, 1988, doi: 10.1038/336385a0.
- [118] N. Asimwe, S. G. Yeo, M. S. Kim, J. Jung, and N. Y. Jeong, "Nitric oxide: Exploring the contextual link with Alzheimer's disease," *Oxidative Medicine and Cellular Longevity*, vol. 2016, 2016, doi: 10.1155/2016/7205747.
- [119] D. A. Butterfield, J. Drake, C. Pocernich, and A. Castegna, "Evidence of oxidative damage in Alzheimer's disease brain: Central role for amyloid β -peptide," *Trends in Molecular Medicine*, vol. 7, no. 12, 2001, doi: 10.1016/S1471-4914(01)02173-6.
- [120] D. A. Butterfield and C. M. Lauderback, "Lipid peroxidation and protein oxidation in Alzheimer's disease brain: Potential causes and consequences involving amyloid β -peptide-associated free radical oxidative stress," *Free Radic Biol Med*, vol. 32, no. 11, 2002, doi: 10.1016/S0891-5849(02)00794-3.
- [121] M. Moszak, M. Szulińska, and P. Bogdański, "You are what you eat—the relationship between diet, microbiota, and metabolic disorders— A review," *Nutrients*, vol. 12, no. 4, 2020, doi: 10.3390/nu12041096.
- [122] A. Cotillard *et al.*, "Dietary intervention impact on gut microbial gene richness," *Nature*, vol. 500, no. 7464, 2013, doi: 10.1038/nature12480.
- [123] E. le Chatelier *et al.*, "Richness of human gut microbiome correlates with metabolic markers," *Nature*, vol. 500, no. 7464, 2013, doi: 10.1038/nature12506.
- [124] J. Hardy, "Alzheimer's disease: The amyloid cascade hypothesis - An update and reappraisal," *Journal of Alzheimer's Disease*, vol. 9, no. SUPPL. 3, 2006, doi: 10.3233/jad-2006-9s317.
- [125] Y. Wang *et al.*, "27-Hydroxycholesterol contributes to cognitive deficits in APP/PS1 transgenic mice through microbiota dysbiosis and intestinal barrier dysfunction," *J Neuroinflammation*, vol. 17, no. 1, 2020, doi: 10.1186/s12974-020-01873-7.
- [126] L. F. Iannone *et al.*, "Microbiota-gut brain axis involvement in neuropsychiatric disorders," *Expert Review of Neurotherapeutics*, vol. 19, no. 10, 2019, doi: 10.1080/14737175.2019.1638763.
- [127] M. Marizzoni *et al.*, "Short-Chain Fatty Acids and Lipopolysaccharide as Mediators between Gut Dysbiosis and Amyloid Pathology in Alzheimer's Disease," *Journal of Alzheimer's Disease*, vol. 78, no. 2, 2020, doi: 10.3233/JAD-200306.
- [128] R. J. A. Cámara, R. Ziegler, S. Begré, A. M. Schoepfer, and R. von Känel, "The role of psychological stress in inflammatory bowel disease: Quality assessment of methods of 18 prospective studies and suggestions for future research," *Digestion*, vol. 80, no. 2, 2009, doi: 10.1159/000226087.
- [129] G. de Lartigue, C. B. de La Serre, and H. E. Raybould, "Vagal afferent neurons in high fat diet-induced obesity; intestinal microflora, gut inflammation and cholecystokinin," *Physiol Behav*, vol. 105, no. 1, 2011, doi: 10.1016/j.physbeh.2011.02.040.
- [130] E. Grasset *et al.*, "A Specific Gut Microbiota Dysbiosis of Type 2 Diabetic Mice Induces GLP-1 Resistance through an Enteric NO-Dependent and Gut-Brain Axis Mechanism," *Cell Metab*, vol. 25, no. 5, 2017, doi: 10.1016/j.cmet.2017.04.013.
- [131] E. M. M. Quigley, "Microbiota-Brain-Gut Axis and Neurodegenerative Diseases," *Current Neurology and Neuroscience Reports*, vol. 17, no. 12, 2017, doi: 10.1007/s11910-017-0802-6.
- [132] C. Jiang, G. Li, P. Huang, Z. Liu, and B. Zhao, "The Gut Microbiota and Alzheimer's Disease," *Journal of Alzheimer's Disease*, vol. 58, no. 1, 2017, doi: 10.3233/JAD-161141.

- [133] C. Pellegrini, L. Antonioli, V. Calderone, R. Colucci, M. Fornai, and C. Blandizzi, "Microbiota-gut-brain axis in health and disease: Is NLRP3 inflammasome at the crossroads of microbiota-gut-brain communications?," *Prog Neurobiol*, vol. 191, 2020, doi: 10.1016/j.pneurobio.2020.101806.
- [134] E. Distrutti *et al.*, "Modulation of intestinal microbiota by the probiotic VSL#3 resets brain gene expression and ameliorates the age-related deficit in LTP," *PLoS One*, vol. 9, no. 9, 2014, doi: 10.1371/journal.pone.0106503.
- [135] S. Oddo *et al.*, "Triple-transgenic model of Alzheimer's Disease with plaques and tangles: Intracellular A β and synaptic dysfunction," *Neuron*, vol. 39, no. 3, 2003, doi: 10.1016/S0896-6273(03)00434-3.
- [136] V. D'Argenio, I. Veneruso, C. Gong, V. Cecarini, L. Bonfili, and A. M. Eleuteri, "Gut Microbiome and Mycobiome Alterations in an In Vivo Model of Alzheimer's Disease," *Genes (Basel)*, vol. 13, no. 9, p. 1564, Aug. 2022, doi: 10.3390/genes13091564.
- [137] Y. Wang and L. H. Kasper, "The role of microbiome in central nervous system disorders," *Brain, Behavior, and Immunity*, vol. 38, 2014. doi: 10.1016/j.bbi.2013.12.015.
- [138] S. S. Kang *et al.*, "Diet and exercise orthogonally alter the gut microbiome and reveal independent associations with anxiety and cognition," *Mol Neurodegener*, vol. 9, no. 1, 2014, doi: 10.1186/1750-1326-9-36.
- [139] J. L. P. Fieldhouse *et al.*, "A suboptimal diet is associated with poorer cognition: The NUDAD project," *Nutrients*, vol. 12, no. 3, 2020, doi: 10.3390/nu12030703.
- [140] R. A. C. Penha Filho, S. J. A. Díaz, F. S. Fernando, Y. F. Chang, R. L. Andreatti Filho, and A. Berchieri Junior, "Immunomodulatory activity and control of Salmonella Enteritidis colonization in the intestinal tract of chickens by Lactobacillus based probiotic," *Vet Immunol Immunopathol*, vol. 167, no. 1–2, 2015, doi: 10.1016/j.vetimm.2015.06.006.
- [141] R. N. Fedorak *et al.*, "The probiotic vsl#3 has anti-inflammatory effects and could reduce endoscopic recurrence after surgery for crohn's disease," *Clinical Gastroenterology and Hepatology*, vol. 13, no. 5, 2015, doi: 10.1016/j.cgh.2014.10.031.
- [142] G. Rossi *et al.*, "Comparison of microbiological, histological, and immunomodulatory parameters in response to treatment with either combination therapy with prednisone and metronidazole or probiotic VSL#3 strains in dogs with idiopathic inflammatory bowel disease," *PLoS One*, vol. 9, no. 4, 2014, doi: 10.1371/journal.pone.0094699.
- [143] N. D. Chu, M. B. Smith, A. R. Perrotta, Z. Kassam, and E. J. Alm, "Profiling living bacteria informs preparation of fecal microbiota transplantations," *PLoS One*, vol. 12, no. 1, 2017, doi: 10.1371/journal.pone.0170922.
- [144] J. Sun *et al.*, "Fecal microbiota transplantation alleviated Alzheimer's disease-like pathogenesis in APP/PS1 transgenic mice," *Transl Psychiatry*, vol. 9, no. 1, 2019, doi: 10.1038/s41398-019-0525-3.
- [145] M. S. Kim *et al.*, "Transfer of a healthy microbiota reduces amyloid and tau pathology in an Alzheimer's disease animal model," *Gut*, vol. 69, no. 2, 2020, doi: 10.1136/gutjnl-2018-317431.
- [146] B. H. Mullish *et al.*, "The use of faecal microbiota transplant as treatment for recurrent or refractory Clostridium difficile infection and other potential indications: Joint British Society of Gastroenterology (BSG) and Healthcare Infection Society (HIS) guidelines," *Gut*, vol. 67, no. 11, 2018, doi: 10.1136/gutjnl-2018-316818.
- [147] S. Liu, J. Gao, M. Zhu, K. Liu, and H. L. Zhang, "Gut Microbiota and Dysbiosis in Alzheimer's Disease: Implications for Pathogenesis and Treatment," *Molecular Neurobiology*, vol. 57, no. 12, 2020. doi: 10.1007/s12035-020-02073-3.

- [148] J. Sun *et al.*, “Fructooligosaccharides Ameliorating Cognitive Deficits and Neurodegeneration in APP/PS1 Transgenic Mice through Modulating Gut Microbiota,” *J Agric Food Chem*, vol. 67, no. 10, 2019, doi: 10.1021/acs.jafc.8b07313.
- [149] Z. A. Bendiks, K. E. B. Knudsen, M. J. Keenan, and M. L. Marco, “Conserved and variable responses of the gut microbiome to resistant starch type 2,” *Nutrition Research*, vol. 77. 2020. doi: 10.1016/j.nutres.2020.02.009.
- [150] J. D. Hoffman *et al.*, “Dietary inulin alters the gut microbiome, enhances systemic metabolism and reduces neuroinflammation in an APOE4 mouse model,” *PLoS One*, vol. 14, no. 8, 2019, doi: 10.1371/journal.pone.0221828.
- [151] P. Shokryazdan, M. Faseleh Jahromi, B. Navidshad, and J. B. Liang, “Effects of prebiotics on immune system and cytokine expression,” *Medical Microbiology and Immunology*, vol. 206, no. 1. 2017. doi: 10.1007/s00430-016-0481-y.
- [152] R. Naomi, H. Embong, F. Othman, H. F. Ghazi, N. Maruthey, and H. Bahari, “Probiotics for alzheimer’s disease: A systematic review,” *Nutrients*, vol. 14, no. 1. 2022. doi: 10.3390/nu14010020.
- [153] L. Bonfili *et al.*, “Gut microbiota manipulation through probiotics oral administration restores glucose homeostasis in a mouse model of Alzheimer’s disease,” *Neurobiol Aging*, vol. 87, 2020, doi: 10.1016/j.neurobiolaging.2019.11.004.
- [154] X. Yang, D. Yu, L. Xue, H. Li, and J. Du, “Probiotics modulate the microbiota–gut–brain axis and improve memory deficits in aged SAMP8 mice,” *Acta Pharm Sin B*, vol. 10, no. 3, 2020, doi: 10.1016/j.apsb.2019.07.001.
- [155] D. Abraham *et al.*, “Exercise and probiotics attenuate the development of Alzheimer’s disease in transgenic mice: Role of microbiome,” *Exp Gerontol*, vol. 115, 2019, doi: 10.1016/j.exger.2018.12.005.
- [156] E. Akbari *et al.*, “Effect of probiotic supplementation on cognitive function and metabolic status in Alzheimer’s disease: A randomized, double-blind and controlled trial,” *Front Aging Neurosci*, vol. 8, no. NOV, 2016, doi: 10.3389/fnagi.2016.00256.
- [157] S. N. A. Bukhari, “Dietary Polyphenols as Therapeutic Intervention for Alzheimer’s Disease: A Mechanistic Insight,” *Antioxidants*, vol. 11, no. 3. 2022. doi: 10.3390/antiox11030554.
- [158] M. Leclerc, S. Dudonné, and F. Calon, “Can natural products exert neuroprotection without crossing the blood–brain barrier?,” *International Journal of Molecular Sciences*, vol. 22, no. 7. 2021. doi: 10.3390/ijms22073356.
- [159] J. Bensalem *et al.*, “Dietary polyphenol supplementation prevents alterations of spatial navigation in middle-aged mice,” *Front Behav Neurosci*, vol. 10, no. FEB, 2016, doi: 10.3389/fnbeh.2016.00009.
- [160] P. Philip *et al.*, “Acute intake of a grape and blueberry polyphenol-rich extract ameliorates cognitive performance in healthy young adults during a sustained cognitive effort,” *Antioxidants*, vol. 8, no. 12, 2019, doi: 10.3390/antiox8120650.
- [161] P. Mena *et al.*, “Phenyl- γ -valerolactones and phenylvaleric acids, the main colonic metabolites of flavan-3-ols: Synthesis, analysis, bioavailability, and bioactivity,” *Natural Product Reports*, vol. 36, no. 5. 2019. doi: 10.1039/c8np00062j.
- [162] L. Mele *et al.*, “Phenyl- γ -valerolactones, flavan-3-ol colonic metabolites, protect brown adipocytes from oxidative stress without affecting their differentiation or function,” *Mol Nutr Food Res*, vol. 61, no. 9, 2017, doi: 10.1002/mnfr.201700074.
- [163] G. Borges, J. I. Ottaviani, J. J. J. van der Hoof, H. Schroeter, and A. Crozier, “Absorption, metabolism, distribution and excretion of (–)-epicatechin: A review of recent findings,” *Molecular Aspects of Medicine*, vol. 61. 2018. doi: 10.1016/j.mam.2017.11.002.

- [164] K. Unno *et al.*, “Blood–Brain Barrier Permeability of Green Tea Catechin Metabolites and their Neuritogenic Activity in Human Neuroblastoma SH-SY5Y Cells,” *Mol Nutr Food Res*, vol. 61, no. 12, 2017, doi: 10.1002/mnfr.201700294.
- [165] D. Angelino *et al.*, “5-(Hydroxyphenyl)- γ -valerolactone-sulfate, a key microbial metabolite of flavan-3-ols, is able to reach the brain: Evidence from different in silico, in vitro and in vivo experimental models,” *Nutrients*, vol. 11, no. 11, 2019, doi: 10.3390/nu11112678.
- [166] R. Ruotolo *et al.*, “Flavonoid-Derived Human Phenyl- γ -Valerolactone Metabolites Selectively Detoxify Amyloid- β Oligomers and Prevent Memory Impairment in a Mouse Model of Alzheimer’s Disease,” *Mol Nutr Food Res*, vol. 64, no. 5, 2020, doi: 10.1002/mnfr.201900890.
- [167] M. M. Bradford, “A Rapid and Sensitive Method for the Quantitation of Microgram Quantities of Protein Utilizing the Principle of Protein-Dye Binding,” *Anal Biochem*, vol. 72, 1976.
- [168] M. Cuccioloni *et al.*, “Epigallocatechin-3-gallate potently inhibits the in vitro activity of hydroxy-3-methyl-glutaryl-CoA reductase,” *J Lipid Res*, vol. 52, no. 5, 2011, doi: 10.1194/jlr.M011817.
- [169] M. M. Bradford, “A rapid and sensitive method for the quantitation of microgram quantities of protein utilizing the principle of protein-dye binding,” *Anal Biochem*, vol. 72, no. 1, pp. 248–254, 1976, doi: [https://doi.org/10.1016/0003-2697\(76\)90527-3](https://doi.org/10.1016/0003-2697(76)90527-3).
- [170] M. Mozzicafreddo, M. Cuccioloni, A. M. Eleuteri, and M. Angeletti, “Rapid reverse phase-HPLC assay of HMG-CoA reductase activity,” *J Lipid Res*, vol. 51, no. 8, 2010, doi: 10.1194/jlr.D006155.
- [171] L. Bonfili *et al.*, “Wheat sprout extract-induced apoptosis in human cancer cells by proteasomes modulation,” *Biochimie*, vol. 91, no. 9, 2009, doi: 10.1016/j.biochi.2009.06.001.
- [172] C. Glaser, H. Demmelmair, and B. Koletzko, “High-throughput analysis of fatty acid composition of plasma glycerophospholipids,” *J Lipid Res*, vol. 51, no. 1, 2010, doi: 10.1194/jlr.D000547.
- [173] A. B. Reiss, “Cholesterol and apolipoprotein E in Alzheimer’s disease,” *Am J Alzheimers Dis Other Demen*, vol. 20, no. 2, 2005, doi: 10.1177/153331750502000208.
- [174] B. Wang and P. Tontonoz, “Liver X receptors in lipid signalling and membrane homeostasis,” *Nature Reviews Endocrinology*, vol. 14, no. 8, 2018, doi: 10.1038/s41574-018-0037-x.
- [175] A. P. Simopoulos, “The importance of the ratio of omega-6/omega-3 essential fatty acids,” *Biomedicine and Pharmacotherapy*, vol. 56, no. 8, 2002, doi: 10.1016/S0753-3322(02)00253-6.
- [176] J. J. Dinicolantonio and J. H. O’Keefe, “Importance of maintaining a low omega-6/omega-3 ratio for reducing inflammation,” *Open Heart*, vol. 5, no. 2, 2018, doi: 10.1136/openhrt-2018-000946.
- [177] H. Meng *et al.*, “Comparison of diets enriched in stearic, oleic, and palmitic acids on inflammation, immune response, cardiometabolic risk factors, and fecal bile acid concentrations in mildly hypercholesterolemic postmenopausal women - Randomized crossover trial,” *American Journal of Clinical Nutrition*, vol. 110, no. 2, 2019, doi: 10.1093/ajcn/nqz095.
- [178] N. G. Forouhi *et al.*, “Differences in the prospective association between individual plasma phospholipid saturated fatty acids and incident type 2 diabetes: The EPIC-InterAct case-cohort study,” *Lancet Diabetes Endocrinol*, vol. 2, no. 10, 2014, doi: 10.1016/S2213-8587(14)70146-9.
- [179] D. W. Russell, R. W. Halford, D. M. O. Ramirez, R. Shah, and T. Kotti, “Cholesterol 24-hydroxylase: An enzyme of cholesterol turnover in the brain,” *Annual Review of Biochemistry*, vol. 78, 2009, doi: 10.1146/annurev.biochem.78.072407.103859.

- [180] J. Kim *et al.*, “Alterations in Gut Microbiota by Statin Therapy and Possible Intermediate Effects on Hyperglycemia and Hyperlipidemia,” *Front Microbiol*, vol. 10, 2019, doi: 10.3389/fmicb.2019.01947.
- [181] J. Xia *et al.*, “Modulation of the immune response and metabolism in germ-free rats colonized by the probiotic *Lactobacillus salivarius* LI01,” *Appl Microbiol Biotechnol*, vol. 105, no. 4, 2021, doi: 10.1007/s00253-021-11099-z.
- [182] C. Reitz, M. X. Tang, J. Luchsinger, and R. Mayeux, “Relation of Plasma Lipids to Alzheimer Disease and Vascular Dementia,” *Arch Neurol*, vol. 61, no. 5, 2004, doi: 10.1001/archneur.61.5.705.
- [183] S. Park *et al.*, “Cholesterol-lowering effect of *Lactobacillus rhamnosus* BFE5264 and its influence on the gut microbiome and propionate level in a murine model,” *PLoS One*, vol. 13, no. 8, 2018, doi: 10.1371/journal.pone.0203150.
- [184] L. Wang *et al.*, “Combined lowering effects of rosuvastatin and *L. acidophilus* on cholesterol levels in rat,” *J Microbiol Biotechnol*, vol. 29, no. 3, 2019, doi: 10.4014/JMB.1806.06004.
- [185] K. Weitkunat *et al.*, “Importance of propionate for the repression of hepatic lipogenesis and improvement of insulin sensitivity in high-fat diet-induced obesity,” *Mol Nutr Food Res*, vol. 60, no. 12, 2016, doi: 10.1002/mnfr.201600305.
- [186] M. T. Bengoechea-Alonso and J. Ericsson, “SREBP in signal transduction: cholesterol metabolism and beyond,” *Current Opinion in Cell Biology*, vol. 19, no. 2, 2007. doi: 10.1016/j.ceb.2007.02.004.
- [187] I. Shimomura, Y. Bashmakov, S. Ikemoto, J. D. Horton, M. S. Brown, and J. L. Goldstein, “Insulin selectively increases SREBP-1C mRNA in the livers of rats with streptozotocin-induced diabetes,” *Proc Natl Acad Sci U S A*, vol. 96, no. 24, 1999, doi: 10.1073/pnas.96.24.13656.
- [188] J. Vaya and H. M. Schipper, “Oxysterols, cholesterol homeostasis, and Alzheimer disease,” *Journal of Neurochemistry*, vol. 102, no. 6, 2007. doi: 10.1111/j.1471-4159.2007.04689.x.
- [189] D. Mongan, C. Healy, H. J. Jones, S. Zammit, M. Cannon, and D. R. Cotter, “Plasma polyunsaturated fatty acids and mental disorders in adolescence and early adulthood: cross-sectional and longitudinal associations in a general population cohort,” *Transl Psychiatry*, vol. 11, no. 1, 2021, doi: 10.1038/s41398-021-01425-4.
- [190] J. H. Liu *et al.*, “Acute EPA-induced learning and memory impairment in mice is prevented by DHA,” *Nat Commun*, vol. 11, no. 1, 2020, doi: 10.1038/s41467-020-19255-1.
- [191] A. Pal, A. H. Metherel, L. Fiabane, N. Buddenbaum, R. P. Bazinet, and S. R. Shaikh, “Do eicosapentaenoic acid and docosahexaenoic acid have the potential to compete against each other?,” *Nutrients*, vol. 12, no. 12, 2020. doi: 10.3390/nu12123718.
- [192] V. Samba, F. Echeverria, A. Valenzuela, R. Chouinard-Watkins, and R. Valenzuela, “Docosahexaenoic and arachidonic acids as neuroprotective nutrients throughout the life cycle,” *Nutrients*, vol. 13, no. 3, 2021. doi: 10.3390/nu13030986.
- [193] H. Tallima and R. el Ridi, “Arachidonic acid: Physiological roles and potential health benefits – A review,” *Journal of Advanced Research*, vol. 11, 2018. doi: 10.1016/j.jare.2017.11.004.
- [194] U. N. Das, “Arachidonic acid and lipoxin A4 as possible endogenous anti-diabetic molecules,” *Prostaglandins Leukot Essent Fatty Acids*, vol. 88, no. 3, 2013, doi: 10.1016/j.plefa.2012.11.009.
- [195] J. Y. L. Chiang, “Regulation of bile acid synthesis: Pathways, nuclear receptors, and mechanisms,” *Journal of Hepatology*, vol. 40, no. 3, 2004. doi: 10.1016/j.jhep.2003.11.006.

- [196] P. Gamba, E. Staurengi, G. Testa, S. Giannelli, B. Sottero, and G. Leonarduzzi, "A crosstalk between brain cholesterol oxidation and glucose metabolism in Alzheimer's disease," *Front Neurosci*, vol. 13, no. MAY, 2019, doi: 10.3389/fnins.2019.00556.
- [197] J. D. CRAWFORD, M. E. TERRY, and G. M. ROURKE, "Simplification of drug dosage calculation by application of the surface area principle.," *Pediatrics*, vol. 5, no. 5, 1950, doi: 10.1542/peds.5.5.783.
- [198] H. Tohgi, T. Abe, K. Yamazaki, T. Murata, C. Isobe, and E. Ishizaki, "The cerebrospinal fluid oxidized NO metabolites, nitrite and nitrate, in Alzheimer's disease and vascular dementia of Binswanger type and multiple small infarct type," *J Neural Transm*, vol. 105, no. 10–12, 1998, doi: 10.1007/s007020050131.
- [199] Y. Liu, F. Liu, K. Iqbal, I. Grundke-Iqbal, and C. X. Gong, "Decreased glucose transporters correlate to abnormal hyperphosphorylation of tau in Alzheimer disease," *FEBS Lett*, vol. 582, no. 2, 2008, doi: 10.1016/j.febslet.2007.12.035.
- [200] M. C. Chan, J. P. Holt-Martyn, C. J. Schofield, and P. J. Ratcliffe, "Pharmacological targeting of the HIF hydroxylases - A new field in medicine development," *Molecular Aspects of Medicine*, vol. 47–48. 2016. doi: 10.1016/j.mam.2016.01.001.
- [201] K. Shaw *et al.*, "Neurovascular coupling and oxygenation are decreased in hippocampus compared to neocortex because of microvascular differences," *Nat Commun*, vol. 12, no. 1, 2021, doi: 10.1038/s41467-021-23508-y.
- [202] Y. Pan *et al.*, "Multiple Factors Affecting Cellular Redox Status and Energy Metabolism Modulate Hypoxia-Inducible Factor Prolyl Hydroxylase Activity In Vivo and In Vitro," *Mol Cell Biol*, vol. 27, no. 3, 2007, doi: 10.1128/mcb.01223-06.
- [203] E. Metzen, J. Zhou, W. Jelkmann, J. Fandrey, and B. Brüne, "Nitric oxide impairs normoxic degradation of HIF-1 α by inhibition of prolyl hydroxylases," *Mol Biol Cell*, vol. 14, no. 8, 2003, doi: 10.1091/mbc.E02-12-0791.
- [204] G. Ceccarelli *et al.*, "Oxygen sparing effect of bacteriotherapy in covid-19," *Nutrients*, vol. 13, no. 8, 2021, doi: 10.3390/nu13082898.
- [205] S. M. T. Islam, J. Won, M. Khan, M. D. Mannie, and I. Singh, "Hypoxia-inducible factor-1 drives divergent immunomodulatory functions in the pathogenesis of autoimmune diseases," *Immunology*, vol. 164, no. 1. 2021. doi: 10.1111/imm.13335.
- [206] M. Hayashi *et al.*, "Induction of glucose transporter 1 expression through hypoxia-inducible factor 1 α under hypoxic conditions in trophoblast-derived cells," *Journal of Endocrinology*, vol. 183, no. 1, 2004, doi: 10.1677/joe.1.05599.
- [207] H. J. Lüth, M. Holzer, U. Gärtner, M. Staufenbiel, and T. Arendt, "Expression of endothelial and inducible NOS-isoforms is increased in Alzheimer's disease, in APP23 transgenic mice and after experimental brain lesion in rat: Evidence for an induction by amyloid pathology," *Brain Res*, vol. 913, no. 1, 2001, doi: 10.1016/S0006-8993(01)02758-5.
- [208] H. J. Lüth, G. Münch, and T. Arendt, "Aberrant expression of NOS isoforms in Alzheimer's disease is structurally related to nitrotyrosine formation," *Brain Res*, vol. 953, no. 1–2, 2002, doi: 10.1016/S0006-8993(02)03280-8.
- [209] S. S. C. Rao, A. Rehman, S. Yu, and N. M. de Andino, "Brain fogginess, gas and bloating: A link between SIBO, probiotics and metabolic acidosis article," in *Clinical and Translational Gastroenterology*, 2018, vol. 9, no. 6. doi: 10.1038/s41424-018-0030-7.
- [210] M. Mitić and T. Lazarević-Pašti, "Does the application of acetylcholinesterase inhibitors in the treatment of Alzheimer's disease lead to depression?," *Expert Opinion on Drug Metabolism and Toxicology*, vol. 17, no. 7. 2021. doi: 10.1080/17425255.2021.1931681.

- [211] M. Lozupone *et al.*, “The relationship between epigenetics and microbiota in neuropsychiatric diseases,” *Epigenomics*, vol. 12, no. 17. 2020. doi: 10.2217/epi-2020-0053.
- [212] N. Brindani *et al.*, “Synthetic and analytical strategies for the quantification of phenyl- γ -valerolactone conjugated metabolites in human urine,” *Mol Nutr Food Res*, vol. 61, no. 9, 2017, doi: 10.1002/mnfr.201700077.
- [213] C. Curti *et al.*, “Catalytic, Enantioselective Vinylogous Mukaiyama Aldol Reaction of Furan-Based Dienoxy Silanes: A Chemodivergent Approach to γ -Valerolactone Flavan-3-ol Metabolites and δ -Lactone Analogues,” *Advanced Synthesis and Catalysis*, vol. 357, no. 18. 2015. doi: 10.1002/adsc.201500705.
- [214] C. P. I. E. A. A. N. PFLEIDERER G, “ISOLATION OF AN AMINOPEPTIDASE FROM KIDNEY PARTICLES,” *Biochem Z*, Dec. 1963.
- [215] G. M. Morris *et al.*, “Software news and updates AutoDock4 and AutoDockTools4: Automated docking with selective receptor flexibility,” *J Comput Chem*, vol. 30, no. 16, 2009, doi: 10.1002/jcc.21256.
- [216] M. D. Hanwell, D. E. Curtis, D. C. Lonie, T. Vandermeersch, E. Zurek, and G. R. Hutchison, “Avogadro: An advanced semantic chemical editor, visualization, and analysis platform,” *J Cheminform*, vol. 4, no. 8, 2012, doi: 10.1186/1758-2946-4-17.
- [217] A. Toste Rêgo and P. C. A. da Fonseca, “Characterization of Fully Recombinant Human 20S and 20S-PA200 Proteasome Complexes,” *Mol Cell*, vol. 76, no. 1, 2019, doi: 10.1016/j.molcel.2019.07.014.
- [218] H. M. Berman *et al.*, “The Protein Data Bank,” *Nucleic Acids Research*, vol. 28, no. 1. 2000. doi: 10.1093/nar/28.1.235.
- [219] D. Turk *et al.*, “Crystal Structure of Cathepsin B Inhibited with CA030 at 2.0-Å resolution: A Basis for the Design of Specific Epoxysuccinyl Inhibitors,” *Biochemistry*, vol. 34, no. 14, 1995, doi: 10.1021/bi00014a037.
- [220] A. M. Eleuteri, M. Angeletti, G. Lupidi, R. Tacconi, L. Bini, and E. Fioretti, “Isolation and characterization of bovine thymus multicatalytic proteinase complex,” *Protein Expr Purif*, vol. 18, no. 2, 2000, doi: 10.1006/prep.1999.1187.
- [221] T. Mosmann, “Rapid colorimetric assay for cellular growth and survival: Application to proliferation and cytotoxicity assays,” *J Immunol Methods*, vol. 65, no. 1–2, 1983, doi: 10.1016/0022-1759(83)90303-4.
- [222] L. Bonfili *et al.*, “Essential amino acid mixtures drive cancer cells to apoptosis through proteasome inhibition and autophagy activation,” *FEBS Journal*, vol. 284, no. 11, 2017, doi: 10.1111/febs.14081.
- [223] M. Groll *et al.*, “Structure of 20S proteasome from yeast at 2.4 Å resolution,” *Nature*, vol. 386, no. 6624, 1997, doi: 10.1038/386463a0.
- [224] M. Groll, E. P. Balskus, and E. N. Jacobsen, “Structural analysis of spiro β -lactone proteasome inhibitors,” *J Am Chem Soc*, vol. 130, no. 45, 2008, doi: 10.1021/ja806059t.
- [225] A. Biederbick, H. F. Kern, and H. P. Elsasser, “Monodansylcadaverine (MDC) is a specific in vivo marker for autophagic vacuoles,” *Eur J Cell Biol*, vol. 66, no. 1, 1995.
- [226] V. Cecarini *et al.*, “Neuroprotective effects of p62(SQSTM1)-engineered lactic acid bacteria in Alzheimer’s disease: A pre-clinical study,” *Aging*, vol. 12, no. 16, 2020, doi: 10.18632/aging.103900.
- [227] V. Hook, M. Kindy, and G. Hook, “Cysteine protease inhibitors effectively reduce in vivo levels of brain β -amyloid related to Alzheimer’s disease,” *Biol Chem*, vol. 388, no. 2, 2007, doi: 10.1515/BC.2007.027.
- [228] J. Schmitz, E. Gilberg, R. Löser, J. Bajorath, U. Bartz, and M. Gütschow, “Cathepsin B: Active site mapping with peptidic substrates and inhibitors,” *Bioorganic and Medicinal Chemistry*, vol. 27, no. 1. 2019. doi: 10.1016/j.bmc.2018.10.017.


- [229] T. Schirmeister and A. Klockow, "Cysteine Protease Inhibitors Containing Small Rings," *Mini-Reviews in Medicinal Chemistry*, vol. 3, no. 6, 2005, doi: 10.2174/1389557033487935.
- [230] M. Zampagni *et al.*, "Lipid rafts are primary mediators of amyloid oxidative attack on plasma membrane," *J Mol Med*, vol. 88, no. 6, 2010, doi: 10.1007/s00109-010-0603-8.
- [231] S. Dhakal, N. Kushairi, C. W. Phan, B. Adhikari, V. Sabaratnam, and I. Macreadie, "Dietary polyphenols: A multifactorial strategy to target alzheimer's disease," *International Journal of Molecular Sciences*, vol. 20, no. 20, 2019, doi: 10.3390/ijms20205090.
- [232] P. Mena *et al.*, "5-(3',4'-Dihydroxyphenyl)- γ -valerolactone and its sulphate conjugates, representative circulating metabolites of flavan-3-ols, exhibit anti-adhesive activity against uropathogenic *Escherichia coli* in bladder epithelial cells," *J Funct Foods*, vol. 29, 2017, doi: 10.1016/j.jff.2016.12.035.
- [233] F. Castello *et al.*, "Bioavailability and pharmacokinetic profile of grape pomace phenolic compounds in humans," *Arch Biochem Biophys*, vol. 646, 2018, doi: 10.1016/j.abb.2018.03.021.
- [234] M. v. Selma, J. C. Espín, and F. A. Tomás-Barberán, "Interaction between phenolics and gut microbiota: Role in human health," *Journal of Agricultural and Food Chemistry*, vol. 57, no. 15, 2009, doi: 10.1021/jf902107d.
- [235] A. Braune and M. Blaut, "Bacterial species involved in the conversion of dietary flavonoids in the human gut," *Gut Microbes*, vol. 7, no. 3, 2016, doi: 10.1080/19490976.2016.1158395.
- [236] A. Pettinari, M. Amici, M. Cuccioloni, M. Angeletti, E. Fioretti, and A. M. Eleuteri, "Effect of polyphenolic compounds on the proteolytic activities of constitutive and immuno-proteasomes," *Antioxid Redox Signal*, vol. 8, no. 1–2, 2006, doi: 10.1089/ars.2006.8.121.
- [237] L. Bonfili *et al.*, "Natural polyphenols as proteasome modulators and their role as anti-cancer compounds," *FEBS Journal*, vol. 275, no. 22, 2008, doi: 10.1111/j.1742-4658.2008.06696.x.
- [238] K. Osanai, K. R. Landis-Piowar, Q. P. Dou, and T. H. Chan, "A para-amino substituent on the D-ring of green tea polyphenol epigallocatechin-3-gallate as a novel proteasome inhibitor and cancer cell apoptosis inducer," *Bioorg Med Chem*, vol. 15, no. 15, 2007, doi: 10.1016/j.bmc.2007.05.041.
- [239] L. Bonfili, M. Cuccioloni, M. Mozzicafreddo, V. Cekarini, M. Angeletti, and A. M. Eleuteri, "Identification of an EGCG oxidation derivative with proteasome modulatory activity," *Biochimie*, vol. 93, no. 5, 2011, doi: 10.1016/j.biochi.2011.02.003.
- [240] M. Cuccioloni *et al.*, "Mangiferin blocks proliferation and induces apoptosis of breast cancer cells: Via suppression of the mevalonate pathway and by proteasome inhibition," *Food Funct*, vol. 7, no. 10, 2016, doi: 10.1039/c6fo01037g.
- [241] F. Limanaqi, F. Biagioni, S. Gambardella, P. Familiari, A. Frati, and F. Fornai, "Promiscuous roles of autophagy and proteasome in neurodegenerative proteinopathies," *International Journal of Molecular Sciences*, vol. 21, no. 8, 2020, doi: 10.3390/ijms21083028.
- [242] T. A. Thibaudeau, R. T. Anderson, and D. M. Smith, "A common mechanism of proteasome impairment by neurodegenerative disease-associated oligomers," *Nat Commun*, vol. 9, no. 1, 2018, doi: 10.1038/s41467-018-03509-0.
- [243] T. Hara *et al.*, "Suppression of basal autophagy in neural cells causes neurodegenerative disease in mice," *Nature*, vol. 441, no. 7095, 2006, doi: 10.1038/nature04724.
- [244] C. Li *et al.*, "Proteasome Inhibition Activates Autophagy-Lysosome Pathway Associated With TFEB Dephosphorylation and Nuclear Translocation," *Front Cell Dev Biol*, vol. 7, 2019, doi: 10.3389/fcell.2019.00170.

- [245] K. Zhu, K. Dunner, and D. J. McConkey, "Proteasome inhibitors activate autophagy as a cytoprotective response in human prostate cancer cells," *Oncogene*, vol. 29, no. 3, 2010, doi: 10.1038/onc.2009.343.
- [246] F. Rocchio *et al.*, "Gene expression, proteome and calcium signaling alterations in immortalized hippocampal astrocytes from an Alzheimer's disease mouse model," *Cell Death Dis*, vol. 10, no. 1, 2019, doi: 10.1038/s41419-018-1264-8.
- [247] U. Özcan *et al.*, "Chemical chaperones reduce ER stress and restore glucose homeostasis in a mouse model of type 2 diabetes," *Science (1979)*, vol. 313, no. 5790, 2006, doi: 10.1126/science.1128294.
- [248] M. Corazzari *et al.*, "Oncogenic BRAF induces chronic ER stress condition resulting in increased basal autophagy and apoptotic resistance of cutaneous melanoma," *Cell Death Differ*, vol. 22, no. 6, 2015, doi: 10.1038/cdd.2014.183.
- [249] J. R. Tchoupé, T. Moreau, F. Gauthier, and J. G. Bieth, "Photometric or fluorometric assay of cathepsin B, L and H and papain using substrates with an aminotrifluoromethylcoumarin leaving group," *Biochimica et Biophysica Acta (BBA)/Protein Structure and Molecular*, vol. 1076, no. 1, 1991, doi: 10.1016/0167-4838(91)90232-O.
- [250] S. Keck, R. Nitsch, T. Grune, and O. Ullrich, "Proteasome inhibition by paired helical filament-tau in brains of patients with Alzheimer's disease," *J Neurochem*, vol. 85, no. 1, 2003, doi: 10.1046/j.1471-4159.2003.01642.x.
- [251] A. M. Pickering and K. J. A. Davies, "Degradation of damaged proteins: The main function of the 20S proteasome," in *Progress in Molecular Biology and Translational Science*, vol. 109, 2012. doi: 10.1016/B978-0-12-397863-9.00006-7.
- [252] C. T. Aiken, R. M. Kaake, X. Wang, and L. Huang, "Oxidative Stress-Mediated Regulation of Proteasome Complexes," *Molecular & Cellular Proteomics*, vol. 10, no. 5, 2011, doi: 10.1074/mcp.m110.006924.
- [253] A. H. P. Jansen, E. A. J. Reits, and E. M. Hol, "The ubiquitin proteasome system in glia and its role in neurodegenerative diseases," *Frontiers in Molecular Neuroscience*, vol. 7, no. AUG. 2014. doi: 10.3389/fnmol.2014.00073.
- [254] M. Olabarria, H. N. Noristani, A. Verkhratsky, and J. J. Rodríguez, "Concomitant astroglial atrophy and astrogliosis in a triple transgenic animal model of Alzheimer's disease," *Glia*, vol. 58, no. 7, 2010, doi: 10.1002/glia.20967.
- [255] X. Jiang *et al.*, "Metastatic prostate cancer-associated P62 inhibits autophagy flux and promotes epithelial to mesenchymal transition by sustaining the level of HDAC6," *Prostate*, vol. 78, no. 6, 2018, doi: 10.1002/pros.23487.
- [256] P. Sánchez-Martin and M. Komatsu, "p62/SQSTM1 – Steering the cell through health and disease," *Journal of Cell Science*, vol. 131, no. 21. 2018. doi: 10.1242/jcs.222836.
- [257] W. H. Yu *et al.*, "Autophagic vacuoles are enriched in amyloid precursor protein-secretase activities: Implications for β -amyloid peptide over-production and localization in Alzheimer's disease," *International Journal of Biochemistry and Cell Biology*, vol. 36, no. 12, 2004, doi: 10.1016/j.biocel.2004.05.010.
- [258] J. C. Wiley *et al.*, "Phenylbutyric acid rescues endoplasmic reticulum stress-induced suppression of APP proteolysis and prevents apoptosis in neuronal cells," *PLoS One*, vol. 5, no. 2, 2010, doi: 10.1371/journal.pone.0009135.
- [259] J. C. Wiley, C. Pettan-Brewer, and W. C. Ladiges, "Phenylbutyric acid reduces amyloid plaques and rescues cognitive behavior in AD transgenic mice," *Aging Cell*, vol. 10, no. 3, 2011, doi: 10.1111/j.1474-9726.2011.00680.x.
- [260] D. S. Kim *et al.*, "The regulatory mechanism of 4-phenylbutyric acid against ER stress-induced autophagy in human gingival fibroblasts," *Arch Pharm Res*, vol. 35, no. 7, 2012, doi: 10.1007/s12272-012-0718-2.

- [261] K. Volgyi, G. Juhász, Z. Kovacs, and B. Penke, “Dysfunction of Endoplasmic Reticulum (ER) and Mitochondria (MT) in Alzheimer’s Disease: The Role of the ER-MT Cross-Talk,” *Curr Alzheimer Res*, vol. 12, no. 7, 2015, doi: 10.2174/1567205012666150710095035.
- [262] W. X. Ding *et al.*, “Linking of autophagy to ubiquitin-proteasome system is important for the regulation of endoplasmic reticulum stress and cell viability,” *American Journal of Pathology*, vol. 171, no. 2, 2007, doi: 10.2353/ajpath.2007.070188.
- [263] D. E. Eigenmann, G. Xue, K. S. Kim, A. v. Moses, M. Hamburger, and M. Oufir, “Comparative study of four immortalized human brain capillary endothelial cell lines, hCMEC/D3, hBMEC, TY10, and BB19, and optimization of culture conditions, for an in vitro blood-brain barrier model for drug permeability studies,” *Fluids Barriers CNS*, vol. 10, no. 1, 2013, doi: 10.1186/2045-8118-10-33.
- [264] K. An, Y. Xu, H. Yang, H. hua Shu, H. bing Xiang, and Y. ke Tian, “Subarachnoid transplantation of immortalized galanin-overexpressing astrocytes attenuates chronic neuropathic pain,” *European Journal of Pain*, vol. 14, no. 6, 2010, doi: 10.1016/j.ejpain.2009.10.015.
- [265] N. S. Roy, C. Cleren, S. K. Singh, L. Yang, M. F. Beal, and S. A. Goldman, “Functional engraftment of human ES cell-derived dopaminergic neurons enriched by coculture with telomerase-immortalized midbrain astrocytes,” *Nat Med*, vol. 12, no. 11, 2006, doi: 10.1038/nm1495.
- [266] F. Alliot and B. Pessac, “Astrocytic cell clones derived from established cultures of 8-day postnatal mouse cerebella,” *Brain Res*, vol. 306, no. 1–2, 1984, doi: 10.1016/0006-8993(84)90377-9.
- [267] G. Dematteis *et al.*, “Proteomic analysis links alterations of bioenergetics, mitochondria-ER interactions and proteostasis in hippocampal astrocytes from 3xTg-AD mice,” *Cell Death Dis*, vol. 11, no. 8, 2020, doi: 10.1038/s41419-020-02911-1.
- [268] N. Myeku *et al.*, “Tau-driven 26S proteasome impairment and cognitive dysfunction can be prevented early in disease by activating cAMP-PKA signaling,” *Nat Med*, vol. 22, no. 1, 2016, doi: 10.1038/nm.4011.
- [269] G. Perry, R. Friedman, G. Shaw, and V. Chau, “Ubiquitin is detected in neurofibrillary tangles and senile plaque neurites of Alzheimer disease brains,” *Proc Natl Acad Sci U S A*, vol. 84, no. 9, 1987, doi: 10.1073/pnas.84.9.3033.
- [270] M. Lopez Salon, L. Pasquini, M. Besio Moreno, J. M. Pasquini, and E. Soto, “Relationship between β -amyloid degradation and the 26S proteasome in neural cells,” *Exp Neurol*, vol. 180, no. 2, 2003, doi: 10.1016/S0014-4886(02)00060-2.
- [271] D. Poppek *et al.*, “Phosphorylation inhibits turnover of the tau protein by the proteasome: Influence of RCAN1 and oxidative stress,” *Biochemical Journal*, vol. 400, no. 3, 2006, doi: 10.1042/BJ20060463.
- [272] T. Grune *et al.*, “Tau protein degradation is catalyzed by the ATP/ubiquitin-independent 20S proteasome under normal cell conditions,” *Arch Biochem Biophys*, vol. 500, no. 2, 2010, doi: 10.1016/j.abb.2010.05.008.
- [273] Z. Long *et al.*, “Dynamic changes of autophagic flux induced by Abeta in the brain of postmortem Alzheimer’s disease patients, animal models and cell models,” *Aging*, vol. 12, no. 11, 2020, doi: 10.18632/aging.103305.
- [274] A. M. Pickering, A. L. Koop, C. Y. Teoh, G. Ermak, T. Grune, and K. J. A. Davies, “The immunoproteasome, the 20S proteasome and the PA28 $\alpha\beta$ proteasome regulator are oxidative-stress-adaptive proteolytic complexes,” *Biochemical Journal*, vol. 432, no. 3, 2010, doi: 10.1042/BJ20100878.
- [275] M. Orre *et al.*, “Reactive glia show increased immunoproteasome activity in Alzheimer’s disease,” *Brain*, vol. 136, no. 5, 2013, doi: 10.1093/brain/awt083.

- [276] S. Kageyama *et al.*, “Proteasome dysfunction activates autophagy and the Keap1-Nrf2 pathway,” *Journal of Biological Chemistry*, vol. 289, no. 36, 2014, doi: 10.1074/jbc.M114.580357.
- [277] D. Lan, W. Wang, J. Zhuang, and Z. Zhao, “Proteasome inhibitor-induced autophagy in PC12 cells overexpressing A53T mutant α -synuclein,” *Mol Med Rep*, vol. 11, no. 3, 2015, doi: 10.3892/mmr.2014.3011.
- [278] L. Cortez and V. Sim, “The therapeutic potential of chemical chaperones in protein folding diseases,” *Prion*, vol. 8, no. 2, 2014. doi: 10.4161/pri.28938.
- [279] L. Bonfili *et al.*, “Gut microbiota modulation in Alzheimer’s disease: Focus on lipid metabolism,” *Clinical Nutrition*, vol. 41, no. 3, 2022, doi: 10.1016/j.clnu.2022.01.025.
- [280] L. Bonfili, C. Gong, F. Lombardi, M. G. Cifone, and A. M. Eleuteri, “Strategic modification of gut microbiota through oral bacteriotherapy influences hypoxia inducible factor-1 α : Therapeutic implication in Alzheimer’s disease,” *Int J Mol Sci*, vol. 23, no. 1, 2022, doi: 10.3390/ijms23010357.
- [281] L. Bonfili *et al.*, “Reply – Letter to the editor “Comment on ‘Gut microbiota modulation in Alzheimer’s disease: Focus on lipid metabolism Clinical nutrition 2022,’” *Clinical Nutrition*, Oct. 2022, doi: 10.1016/j.clnu.2022.06.029.
- [282] V. Cekarini *et al.*, “Flavan-3-ol Microbial Metabolites Modulate Proteolysis in Neuronal Cells Reducing Amyloid-beta (1-42) Levels,” *Mol Nutr Food Res*, vol. 65, no. 18, Sep. 2021, doi: 10.1002/mnfr.202100380.
- [283] Chunmei Gong *et al.*, “Immortalized Alzheimer’s disease astrocytes: characterization of their proteolytic systems,” *submitted to Molecular Neurobiology*, 2022.

REVIEW ARTICLE

Microbiota modulation as preventative and therapeutic approach in Alzheimer's diseaseLaura Bonfili, Valentina Cekarini, Olee Gogoi, Chunmei Gong, Massimiliano Cuccioloni, Mauro Angeletti, Giacomo Rossi and Anna Maria Eleuteri 

School of Biosciences and Veterinary Medicine, University of Camerino, Camerino, Italy

Keywords

Alzheimer's disease; dysbiosis; gut–brain axis; inflammation; microbiota modulation; oxidative stress; prebiotics; probiotics; proteolysis; therapeutic approaches

CorrespondenceA. M. Eleuteri, School of Biosciences and Veterinary Medicine, University of Camerino, Via Gentile III da Varano, 62032 Camerino (MC), Italy
Tel: +390737403267
E-mail: annamaria.eleuteri@unicam.it

(Received 8 June 2020, revised 27 August 2020, accepted 17 September 2020)

doi:10.1111/febs.15571

The gut microbiota coevolves with its host, and numerous factors like diet, lifestyle, drug intake and geographical location continuously modify its composition, deeply influencing host health. Recent studies demonstrated that gut dysbiosis can alter normal brain function through the so-called gut–brain axis, a bidirectional communication network between the central nervous system and the gastrointestinal tract, thus playing a key role in the pathogenesis of neurodegenerative disorders, such as Alzheimer's disease (AD). In this perspective, in the constant search for novel treatments in AD, the rational modulation of gut microbiota composition could represent a promising approach to prevent or delay AD onset or to counteract its progression. Preclinical and human studies on microbiota modulation through oral bacteriotherapy and faecal transplantation showed anti-inflammatory and antioxidant effects, upregulation of plasma concentration of neuroprotective hormones, restoration of impaired proteolytic pathways, amelioration of energy homeostasis with consequent decrease of AD molecular hallmarks and improvement of behavioural and cognitive performances. In this review, we dissect the role of gut microbiota in AD and highlight recent advances in the development of new multitarget strategies for microbiota modulation to be used as possible preventative and therapeutic approaches in AD.

Introduction

Microbiota is a community of symbiotic microorganisms that can be neutral, beneficial or detrimental to the host, with important regulatory functions in health and disease. The human body hosts trillions of microorganisms (bacteria, archaea, fungi and viruses) that colonize the skin surface, the respiratory tract, genitourinary organs and, most importantly, the gastrointestinal tract. Approximately 95% of the symbiotic organisms of the human microbiome can be found in the gut (gut microbiota) [1]. Gut microbial

ecosystem consists mainly of bacteria, mostly obligate anaerobes, fungi and viruses [2]. These diverse groups of microorganisms play multiple roles in humans, such as the fermentation of undigested carbohydrates, the production of short-chain fatty acids (SCFAs) and other metabolites, the synthesis of vitamins B and K, the metabolism of important substances (bile acids, sterols and drugs), and the protection against exogenous pathogens [3]. *Bacteroidetes* (~ 48%), *Firmicutes* (~ 51%), *Proteobacteria* and *Actinobacteria* (1%) are

Abbreviations

AD, Alzheimer's disease; APP, amyloid precursor protein; A β , amyloid beta; BBB, blood–brain barrier; BDNF, brain-derived neurotrophic factor; CNS, central nervous system; FMT, faecal microbiota transplantation; GABA, γ -aminobutyric acid; GIP, glucose-dependent insulinotropic polypeptide; GLP1, glucagon-like peptide-1; LPS, lipopolysaccharide; MCI, mild cognitive impairment; NFT, neurofibrillary tangles; SCFAs, short-chain fatty acids; TLRs, Toll-like receptors; UPS, ubiquitin–proteasome system.

Communication

Strategic Modification of Gut Microbiota through Oral Bacteriotherapy Influences Hypoxia Inducible Factor-1 α : Therapeutic Implication in Alzheimer's Disease

Laura Bonfili ^{1,*}, Chunmei Gong ¹, Francesca Lombardi ², Maria Grazia Cifone ²
and Anna Maria Eleuteri ^{1,*}

¹ School of Biosciences and Veterinary Medicine, University of Camerino, 62032 Camerino, Italy; chunmei.gong@unicam.it

² Department of Life, Health and Environmental Sciences, University of L'Aquila, 67010 L'Aquila, Italy; francesca.lombardi@univaq.it (F.L.); mariagrazia.cifone@univaq.it (M.G.C.)

* Correspondence: laura.bonfili@unicam.it (L.B.); annamaria.eleuteri@unicam.it (A.M.E.); Tel.: +39-0737-403247 (L.B.); +39-0737-403267 (A.M.E.)

Abstract: Dysbiosis contributes to Alzheimer's disease (AD) pathogenesis, and oral bacteriotherapy represents a promising preventative and therapeutic opportunity to remodel gut microbiota and to delay AD onset and progression by reducing neuroinflammation and amyloid and tau proteins aggregation. Specifically, SLAB51 multi-strain probiotic formulation positively influences multiple neuro-chemical pathways, but exact links between probiotics oral consumption and cerebral beneficial effects remain a gap of knowledge. Considering that cerebral blood oxygenation is particularly reduced in AD and that the decreased neurovascular function contributes to AD damages, hypoxia conditioning represents an encouraging strategy to cure diseases of the central nervous system. In this work, 8-week-old 3xTg-AD and wild-type mice were chronically supplemented with SLAB51 to evaluate effects on hypoxia-inducible factor-1 α (HIF-1 α), a key molecule regulating host-microbial crosstalk and a potential target in neurodegenerative pathologies. We report evidence that chronic supplementation with SLAB51 enhanced cerebral expression of HIF-1 α and decreased levels of prolyl hydroxylase 2 (PHD2), an oxygen dependent regulator of HIF-1 α degradation; moreover, it successfully counteracted the increase of inducible nitric oxide synthase (iNOS) brain expression and nitric oxide plasma levels in AD mice. Altogether, the results demonstrate an additional mechanism through which SLAB51 exerts neuroprotective and anti-inflammatory effects in this model of AD.

Keywords: hypoxia-inducible factor-1 α ; Alzheimer's disease; probiotics; microbiota; nitric oxide; prolyl hydroxylase 2



Citation: Bonfili, L.; Gong, C.; Lombardi, F.; Cifone, M.G.;

Eleuteri, A.M. Strategic Modification of Gut Microbiota through Oral Bacteriotherapy Influences Hypoxia Inducible Factor-1 α : Therapeutic Implication in Alzheimer's Disease. *Int. J. Mol. Sci.* **2022**, *23*, 357. <https://doi.org/10.3390/ijms23010357>

Academic Editor: Andreas Schwiertz

Received: 1 December 2021

Accepted: 27 December 2021

Published: 29 December 2021

Publisher's Note: MDPI stays neutral with regard to jurisdictional claims in published maps and institutional affiliations.



Copyright: © 2021 by the authors. Licensee MDPI, Basel, Switzerland. This article is an open access article distributed under the terms and conditions of the Creative Commons Attribution (CC BY) license (<https://creativecommons.org/licenses/by/4.0/>).

1. Introduction

Gut dysbiosis is an established key player in the pathogenesis of Alzheimer's diseases (AD) and, more generally, in age-related neurodegenerations. In fact, an increased concentration of proinflammatory bacteria in the gut is responsible for the enhanced secretion of lipopolysaccharides and amyloid peptides that can alter the intestinal permeability and the blood–brain barrier (BBB), consequently promoting neuroinflammation, oxidation, amyloid beta deposition, insulin resistance, and neuronal degeneration [1,2]. In AD, cerebral oxygen supply is impaired, contributing to neuroinflammation, plaque formation, neuronal death, and cognitive deficits with molecular mechanisms not well defined [3]. Neuroinflammation is associated to the overactivation of microglia, the resident innate immune cells that can trigger inflammatory signals and release proinflammatory cytokines, chemokines, and neurotoxic substances, such as matrix metalloproteinases, reactive oxygen species (ROS), and nitric oxide (NO).



Original article

Gut microbiota modulation in Alzheimer's disease: Focus on lipid metabolism



Laura Bonfli ^{a,*}, Massimiliano Cuccioloni ^a, Chunmei Gong ^a, Valentina Cecarini ^a, Michele Spina ^b, Yadong Zheng ^a, Mauro Angeletti ^a, Anna Maria Eleuteri ^a

^a School of Biosciences and Veterinary Medicine, University of Camerino, Via Gentile III da Varano, 62032 Camerino MC, Italy

^b Laboratorio Analisi Dr. Fioroni, Viale A. de Gasperi, 19, 63074, San Benedetto Del Tronto AP, Italy

ARTICLE INFO

Article history:

Received 24 May 2021

Accepted 26 January 2022

Keywords:

Alzheimer's disease
Microbiota modulation
Probiotics
Lipid metabolism
Cholesterol

SUMMARY

Background & aims: Alzheimer's disease (AD) and age-related dementias represent a major and increasing global health challenge. Unhealthy diet and lifestyle can unbalance the intestinal microbiota composition and, consequently energy metabolism, contributing to AD pathogenesis. Impairment of cerebral cholesterol metabolism occurs in both aging and AD, and lipid-lowering agents have been associated to a lower risk of neurodegenerative diseases, but the link between blood lipid profile and AD remains a matter of debate. Recently, probiotics have emerged as a promising and safe strategy to manipulate gut microbiota composition and increase the host health status through a multi-level mechanism that is currently under investigation. Specifically, oral supplementation with a multi-strain probiotic formulation (SLAB51) reduced amyloid beta aggregates and brain damages in a triple transgenic mouse model of AD (3xTg-AD). Treated mice showed improved cognitive functions in response to an enrichment of gut anti-inflammatory metabolites, increased plasma concentrations of neuro-protective gut hormones, and ameliorated glucose uptake and metabolism.

Methods: This work focuses on the evaluation of the effects of SLAB51 chronic administration on lipid metabolism in 3xTg-AD mice and the respective wild-type counterpart. On this purpose, 8 weeks old mice were orally administered with SLAB51 for 4 and 12 months to analyze the plasma lipid profile (using lipidomic analyses and enzymatic colorimetric assays), along with the cerebral and hepatic expression levels of key regulators of cholesterol metabolism (through Western blotting and ELISA).

Results: Upon probiotics administration, cholesterol biosynthesis was inhibited in AD mice with a process involving sterol regulatory element binding protein 1c and liver X receptors mediated pathways. Decreased plasma and brain concentration of 27-hydroxycholesterol and increased brain expression of cholesterol 24S-hydroxylase indicated that alternative pathways of bile acid synthesis are influenced. The plasmatic increase of arachidonic acid in treated AD mice reflects dynamic interactions among several actors of a complex inflammatory response, in which polyunsaturated fatty acids can compete each other and simultaneously co-operate in the resolution of inflammation.

Conclusions: These evidence, together with the hypocholesterolemic effects, the ameliorated fatty acids profile and the decreased omega 6/omega 3 ratio successfully demonstrated that microbiota modulation through probiotics can positively change lipid composition in AD mice, with arachidonic acid representing one important hub metabolite in the interactions among probiotic-induced lipid profile changes, insulin sensitivity, and inflammation.

© 2022 The Author(s). Published by Elsevier Ltd. This is an open access article under the CC BY license (<http://creativecommons.org/licenses/by/4.0/>).

1. Background

Alzheimer's disease (AD) is a debilitating neurodegenerative disorder that afflicts millions of adults worldwide and represents the main cause of late-life dementia. AD is characterized by neuronal cell loss associated with memory and cognitive decline,

* Corresponding author.

E-mail address: laura.bonfli@unicam.it (L. Bonfli).

<https://doi.org/10.1016/j.clnu.2022.01.025>

0261-5614/© 2022 The Author(s). Published by Elsevier Ltd. This is an open access article under the CC BY license (<http://creativecommons.org/licenses/by/4.0/>).



Contents lists available at ScienceDirect

Clinical Nutrition

journal homepage: <http://www.elsevier.com/locate/clnu>

Letter to the Editor

Reply – Letter to the editor “Comment on “Gut microbiota modulation in Alzheimer's disease: Focus on lipid metabolism Clinical nutrition 2022”

Dear Editor,

We sincerely thank Debora Eduarda da Silva Fidellis and colleagues for their positive comments on our recent article entitled “Gut microbiota modulation in Alzheimer's disease: focus on lipid metabolism” and for the constructive suggestion of considering different probiotic formulations in future studies.

We take this opportunity to stress the peculiarity of the multi-strain probiotic formulation used in our preclinical study. De Simone formulation, also named SLAB51, is a commercially available mixture of eight distinct living bacterial strains, mainly Lactobacilli and Bifidobacteria, that safely and positively affect human health [1,2]. Our preclinical studies demonstrated the SLAB51 multi-level mechanisms. Specifically, this formulation reduced am-

loid beta aggregates and brain damages in a triple transgenic mouse model of AD (3xTg-AD). Treated 3xTg-AD mice showed improved cognitive functions in response to an enrichment of gut anti-inflammatory metabolites, increased plasma concentrations of neuroprotective gut hormones, and ameliorated glucose and lipid (Fig. 1) metabolism [3–8].

Based on these evidences, future studies with different probiotic formulations should consider the importance to use living bacteria instead of inactivated bacterial strains. Moreover, multi-strains formulation may well have a higher chance to strategically shift gut microbiota composition with respect to single-strain approaches. Additionally, novel formulations with prebiotics could be considered in order to improve probiotics viability, stability and functionality.

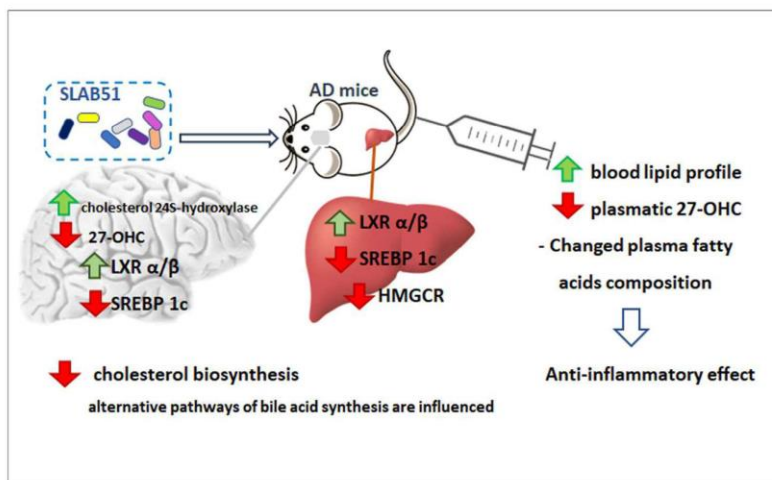


Fig. 1. Microbiota modulation through probiotics can positively change lipid composition and distribution in AD mice. Upon chronic administration with probiotics, cholesterol biosynthesis was inhibited in 3xTg-AD mice with a process involving sterol regulatory element binding protein 1c (SREBP1c) and liver X receptors (LXR α/β) mediated pathways. Decreased plasma and brain concentration of 27-hydroxycholesterol (27-OHC) and increased brain expression of cholesterol 24S-hydroxylase indicated that alternative pathways of bile acid synthesis are influenced.

<https://doi.org/10.1016/j.clnu.2022.06.029>

0261-5614/© 2022 Elsevier Ltd and European Society for Clinical Nutrition and Metabolism. All rights reserved.

Please cite this article as: L. Bonfili, M. Cuccioloni, C. Gong *et al.*, Reply – Letter to the editor “Comment on “Gut microbiota modulation in Alzheimer's disease: Focus on lipid metabolism Clinical nutrition 2022”, Clinical Nutrition, <https://doi.org/10.1016/j.clnu.2022.06.029>

Flavan-3-ol Microbial Metabolites Modulate Proteolysis in Neuronal Cells Reducing Amyloid-beta (1-42) Levels

Valentina Cecarini,* Massimiliano Cuccioloni, Yadong Zheng, Laura Bonfili, Chunmei Gong, Mauro Angeletti, Pedro Mena, Daniele Del Rio, and Anna Maria Eleuteri

Introduction: Alzheimer's disease (AD) is a progressive neurodegeneration characterized by extensive protein aggregation and deposition in the brain, associated with defective proteasomal and autophagic-lysosomal proteolytic pathways. Since current drugs can only reduce specific symptoms, the identification of novel treatments is a major concern in AD research. Among natural compounds, (poly)phenols and their derivatives/metabolites are emerging as candidates in AD prevention due to their multiple beneficial effects. This study aims to investigate the ability of a selection of phenyl- γ -valerolactones, gut microbiota-derived metabolites of flavan-3-ols, to modulate the functionality of cellular proteolytic pathways.

Methods and Results: Neuronal SH-SY5Y cells transfected with either the wild-type or the 717 valine-to-glycine amyloid precursor protein mutated gene are used as an AD model and treated with 5-(4'-hydroxyphenyl)- γ -valerolactone, 5-(3',4'-dihydroxyphenyl)- γ -valerolactone and 5-(3'-hydroxyphenyl)- γ -valerolactone-4'-sulfate. Combining *in vitro* and *in silico* studies, it is observed that the phenyl- γ -valerolactones of interest modulated cellular proteolysis via proteasome inhibition and consequent autophagy upregulation and inhibited cathepsin B activity, eventually reducing the amount of intra- and extracellular amyloid-beta (1-42) peptides.

Conclusion: The findings of this study establish, for the first time, that these metabolites exert a neuroprotective activity by regulating intracellular proteolysis and confirm the role of autophagy and cathepsin B as possible targets of AD preventive/therapeutic strategies.

amyloid-beta deposition in senile plaques and tau aggregation in neurofibrillary tangles. The sequential cleavage of the amyloid precursor protein (APP) through the so-called amyloidogenic pathway is responsible for the release of amyloid-beta ($A\beta$) peptides. A large part of these proteins are fragments of 40 amino acid residues in length, $A\beta$ (1-40), whereas a remaining portion is a 42-residues protein, $A\beta$ (1-42), known as the most toxic and particularly prone to aggregation.^[1] Defective proteolytic pathways, oxidative and inflammatory processes further exacerbate AD pathology.^[2,3] The ubiquitin proteasome system (UPS) and the autophagy-lysosomal pathway are the two major catabolic pathways in eukaryotic cells. The UPS is in charge of the degradation of cytosolic and nuclear proteins, including short-lived proteins, whereas autophagy is responsible for the clearance of protein aggregates and damaged organelles. Due to an age-dependent decline in their activity, aberrant proteins accumulate, contributing to the onset and development of age-related disorders, such as AD.^[4]

A growing number of studies has associated the intake of foods rich in (poly)phenols with a reduced risk of developing neurodegenerative diseases, including AD. Dietary products such as green tea, apples, berries, cocoa, and chocolate are extremely rich in

1. Introduction

Alzheimer's disease (AD) is a neurodegenerative condition mostly characterized by extensive protein aggregation with

in (poly)phenols with a reduced risk of developing neurodegenerative diseases, including AD. Dietary products such as green tea, apples, berries, cocoa, and chocolate are extremely rich in

V. Cecarini, M. Cuccioloni, Y. Zheng, L. Bonfili, C. Gong, M. Angeletti, A. M. Eleuteri
School of Biosciences and Veterinary Medicine
University of Camerino
Camerino Italy
E-mail: valentina.cecarini@unicam.it

P. Mena, D. Del Rio
Human Nutrition Unit
Department of Food and Drugs
University of Parma
Parma, Italy
P. Mena, D. Del Rio
Microbiome Research Hub
University of Parma
Parma, Italy

 The ORCID identification number(s) for the author(s) of this article can be found under <https://doi.org/10.1002/mnfr.202100380>

© 2021 The Authors. Molecular Nutrition & Food Research published by Wiley-VCH GmbH. This is an open access article under the terms of the Creative Commons Attribution License, which permits use, distribution and reproduction in any medium, provided the original work is properly cited.

DOI: 10.1002/mnfr.202100380

Article

Gut Microbiome and Mycobiome Alterations in an In Vivo Model of Alzheimer's Disease

Valeria D'Argenio ^{1,2,*}, Iolanda Veneruso ^{2,3}, Chunmei Gong ⁴, Valentina Cecarini ⁴, Laura Bonfilii ⁴ and Anna Maria Eleuteri ⁴

¹ Department of Human Sciences and Quality of Life Promotion, San Raffaele Open University, Via di Val Cannuta 247, 00166 Roma, Italy

² CEINGE-Biotecnologie Avanzate, Via G. Salvatore 486, 80145 Napoli, Italy

³ Department of Molecular Medicine and Medical Biotechnologies, Federico II University, Via Sergio Pansini 5, 80131 Napoli, Italy

⁴ School of Biosciences and Veterinary Medicine, University of Camerino, Via Gentile III da Varano, 62032 Camerino, Italy

* Correspondence: dargenio@ceinge.unina.it

Abstract: Gut microbiota has emerged as an important key regulator of health and disease status. Indeed, gut microbial dysbiosis has been identified in an increasing number of diseases, including neurodegenerative disorders. Accordingly, microbial alterations have been reported also in Alzheimer's disease (AD), suggesting possible pathogenetic mechanisms contributing to the development of specific AD hallmarks and exacerbating metabolic alterations and neuroinflammation. The identification of these mechanisms is crucial to develop novel, targeted therapies and identify potential biomarkers for diagnostic purposes. Thus, the possibility to have AD in vivo models to study this microbial ecosystem represents a great opportunity for translational applications. Here, we characterized both gut microbiome and mycobiome of 3xTg-AD mice, one of the most widely used AD models, to identify specific microbial alterations with respect to the wild-type counterpart. Interestingly, we found a significant reduction of the *Coprococcus* and an increased abundance of *Escherichia_Shigella* and *Barnesiella* genera in the AD mice compatible with a pro-inflammatory status and the development of AD-related pathogenetic features. Moreover, the fungal *Dipodascaceae* family was significantly increased, thus suggesting a possible contribution to the metabolic alterations found in AD. Our data point out the strict connection between bacterial dysbiosis and AD and, even if further studies are required to clarify the underlining mechanisms, it clearly indicates the need for extensive metagenomic studies over the bacterial counterpart.

Keywords: Alzheimer's disease; microbiome; mycobiome; metagenomic studies; 3xTg-AD mice



Citation: D'Argenio, V.; Veneruso, I.; Gong, C.; Cecarini, V.; Bonfilii, L.; Eleuteri, A.M. Gut Microbiome and Mycobiome Alterations in an In Vivo Model of Alzheimer's Disease. *Genes* **2022**, *13*, 1564. <https://doi.org/10.3390/genes13091564>

Academic Editor: Silvia Turrone

Received: 2 August 2022

Accepted: 27 August 2022

Published: 31 August 2022

Publisher's Note: MDPI stays neutral with regard to jurisdictional claims in published maps and institutional affiliations.



Copyright: © 2022 by the authors. Licensee MDPI, Basel, Switzerland. This article is an open access article distributed under the terms and conditions of the Creative Commons Attribution (CC BY) license (<https://creativecommons.org/licenses/by/4.0/>).

1. Introduction

It has been well established that the gut microbiota plays an important role in health status acquisition and maintenance, and, consequently, its alterations can be associated with several diseases [1]. This statement is true not only for intestinal diseases but can be extended also to extra-intestinal disorders [1]. In particular, it is well known that a stable and complex communication system exists between gut and brain, and the gut microbiota has been claimed as a factor able to influence the gut–brain axis [2–4]. As a consequence, it has been proposed that a microbial dysbiosis at the gut level, by acting through different mechanisms such as membrane permeability modifications, inflammatory response induction or toxic metabolite production, may play a role also in neurodegenerative disorders such as Alzheimer's disease (AD) [5]. Accordingly, several studies have shown a correlation between gut microbiota alterations and cognitive impairment and/or specific AD features [5–7]. These studies, even if often observatory and at a preliminary stage, have the overall merit of having highlighted an additional molecular mechanism involved in